Computational and Statistical Fitting of Particle Tracking Simulation on Oseen Vortex

Isabelle Lee

A thesis submitted in partial fulfillment of the
requirements for the degree of

Master of Science

University of Washington

2017

Committee:

Dana Dabiri, Chair

James Hermanson

Program Authorized to Offer Degree:
Aeronautics and Astronautics

University of Washington

Abstract

Computational and Statistical Fitting of
Particle Tracking Simulation
on Oseen Vortex

Isabelle Lee

Chair of the Supervisory Committee:
Associate Professor Dana Dabiri
Aeronautics and Astronautics

Visualization methods of fluid data are crucial for studying flows and turbulence, and one of the most common methods of simulation is particle tracking velocimetry (PTV). In this project, the visualization of flow is studied using PTV simulation of an Oseen vortex. For statistically fitting the fluid data, two main methods were used: regressive fitting and spline fitting. Final fits of data were done using Kriging, which is a sophisticated regression method, and thin plate spline fitting. Then, comparisons of the two methods were drawn using statistical methods. Kriging yielded lower mean squared error overall, but thin plate spline fitting method takes smoothness of fit into account.

TABLE OF CONTENTS

LIST OF FIGURES

LIST OF TABLES

GLOSSARY

PTV: Particle tracking velocimetry, a method for measuring velocity distributions in a flow

PIV: Particle image velocimetry, a method for measuring velocity distributions in a flow

TPAPS: Thin-plate smoothing spline function found in Matlab's Curve Fitting Toolbox

DACE: Surface fitting method using linear regression in Matlab's Kriging Toolbox

ACKNOWLEDGMENTS

The author would like to thank the University of Washington and the Department of Aeronautics and Astronautics for giving her the opportunity to explore a fascinating subject and collaborate with imaginative and motivated peers. She expresses her appreciation to her professors, Professor Dana Dabiri and Professor James Hermanson, as well as Charles Pecora and Professor Guang Lin of Purdue University for their indispensable collaboration.

DEDICATION

To new experiences, people, and friends that continue to help me become.

Chapter 1
INTRODUCTION

1.1 Background

1.1.1 Imaging Particles in Flow

The visualization of fluid motions is crucial to the field of fluid mechanics and turbulence, as it is the main method from which we analyze fluid motions from experimentally generated data. The two widespread, non-intrusive methods are Particle Image Velocimetry (PIV) and Particle Tracking Velocimetry (PTV). The shared purpose, distinctions and limitations of each method motivate this study. Thus, we further define and examine the two techniques.

1.1.2 Particle Image Velocimetry

In Particle Image Velocimetry (PIV), light scattering particles, or tracer particles, are added to the flow. Then, a pulsed laser beam setup illuminates the tracer particles. This setup is drawn out in 1.1. This scattered light is captured by high-resolution digital cameras. Through digital image processing and data analysis, the displacements of the particles are measured, and the particle velocities are indirectly measured from the displacements. There are various ways of interpolating the flow of a particle, and one common way of interpolation is through cross correlation, described in 1.2. With time-lapsed image data, the cross correlation or interpolation determines the direction of the displacements and velocities.

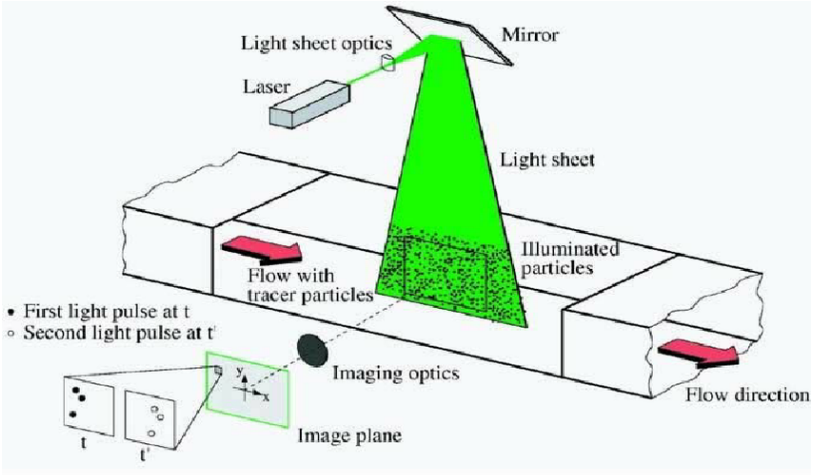

Figure 1.1: Setup for PTV and PTV

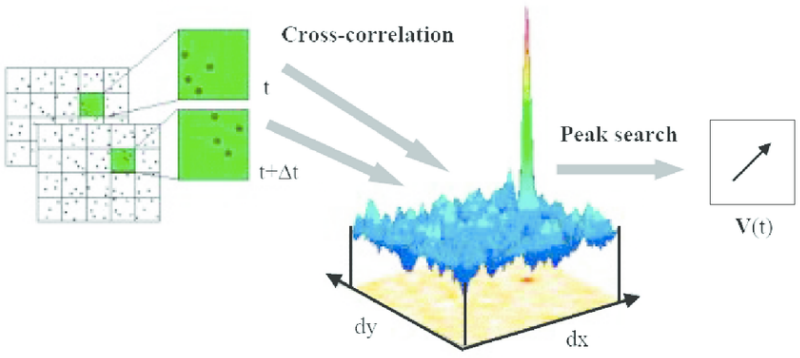

Figure 1.2: Correlation and Interpolation from PIV

1.1.3 Particle Tracking Velocimetry

On the other hand, Particle Tracking Velocimetry (PTV) aims to measure particle velocities directly. The setup of the PTV is similar to that of PIV: a laser beam illuminates the fluid in motion with tracer particles seeded. The experimental setup of the imaging is similar to that of PIV, as shown in 1.1. Then, there are two methods to extract the displacements and velocities of the particles: Lagrangian and Eulerian formulations. In the Lagrangian formulation, the camera takes multi-frame pictures (or videos) at intervals of time, and then, the individual particles are tracked. In Eulerian formulations, the velocity field of the fluid on a grid is measured.

Then, from these velocity field measurements, one may numerically calculate the spatial derivatives to determine the vorticities and the shear stresses of the fluids. This allows for richer insights about the evolution of flow, dynamic properties, as well as turbulence statistics.

1.1.4 Comparison of PTV and PIV

The two different approaches the visualization yield different limitations and advantages. The most pronounced advantage for PTV is that the algorithm provides more information about the flow than PIV. The direct particle trajectory is measured for PTV, whereas, the most probable trajectory of a particle within the interrogation region is measured for PIV. The cross correlation of the two images for PIV may become a source of error. Moreover, PTV provides more reliable results for multiphase flows, since the bubbles and obstructing fluid structures hinder cross correlations in PIV. Thus, PTV proves to be a competitive measurement and visualization technique for fluid simulations. However, PIV provides us with more number of vectors, which in turn, is advantageous to measure derivative quantities such as vorticities and the rate of strain tensor. For PTV, the spacing between the vectors would be too large

due to relatively small number of vectors in a given flow. One way of overcoming this obstacle is to increase the number of tracer particles or reducing the observation volume.

1.2 Oseen Vortex

1.2.1 Theory and Calculations

The Oseen-Lamb vortex is an initial single point vortex in a viscous, infinite flow.[8] Studying the Oseen vortex is essential for large eddy simulations and their initialization for turbulene applications, as well as lidar matched fiter designs for more practical applications. The Oseen-Lamb vortex can be thought of as a single point vortex in idealized flow. For a single point vortex, the system is axisymmetric, and therefore, there is no preferred direction of movement for the vortex. Then, the vorticity does not induce the velocity onto the vortex, and we are concerned with a purely diffusive flow. With this motivation and background, the Oseen-Lamb vortex is derived.

The Oseen-Lamb vortex is an alaytical solution to the Navier-Stokes equation.[8] Beginning with Navier-Stokes equation and the continuity equation,

$$\frac{\partial u}{\partial t} + u \cdot \nabla u = \frac{1}{\rho}\nabla p + \nu \triangle u \tag{1.1}$$

and

$$\nabla \cdot u = 0, \tag{1.2}$$

we may derive the equation of motion for vorticity ω. u is the velocity, ρ is the density of fluid, p is pressure, and ν is viscosity. Since the vorticity is defined as the curl of velocity, $\omega = \nabla \times u$, the curl of the Navier-Stokes equation becomes

$$\frac{\partial \omega}{\partial t} + u \cdot \nabla \omega = \omega \cdot \nabla u + \nu \triangle \omega, \tag{1.3}$$

and the continuity equation becomes

$$\nabla \cdot \omega = 0. \tag{1.4}$$

From the vorticity solution, we may also solve for the velocity by using Biot-Savart Law,

$$u(x) = -\frac{1}{4\pi}\int_{R^3}\frac{(x-x')\times\omega(x')}{||x-x'||^3}dx'. \tag{1.5}$$

The circulation theorem states

$$\Gamma = \oint_C u\cdot ds = \int_A \omega\cdot\hat{n}da, \tag{1.6}$$

where Γ is the circulation, which is physically a flux of vorticity through a unit surface. For a 2D incompressible flow, the vorticity equation simplifies further,

$$\frac{\partial\omega}{\partial t} + u\cdot\nabla\omega = \nu\triangle\omega. \tag{1.7}$$

In the case of the Oseen-Lamb Vortex which is a purely diffusive flow, the vorticity equation then becomes

$$\frac{\partial\omega}{\partial t} = \nu\triangle\omega. \tag{1.8}$$

The analytical solution to the vorticity equation for the Oseen-Lamb vortex is

$$\omega(r,t) = \frac{\Gamma}{4\pi\nu t}\exp\left(-\frac{r^2}{4\nu t}\right). \tag{1.9}$$

From this analytical expression of vorticity, we may also calculate the velocities. Due to symmetry, the radial velocity is 0, $v_r = 0$. The tangential velocity can be calculated using the Biot-Savart Law. The analytical expression of tangential velocity then becomes

$$v_\theta(r,t) = \frac{\Gamma}{2\pi r}\left[1-\exp\left(-\frac{r^2}{4\nu t}\right)\right]. \tag{1.10}$$

The datasets of interests are various rotation methods and vorticities of the Oseen vortex, and two methods of curve fitting were done on the datasets: a linear regression based method and a spline fitting based method.

Chapter 2

CURVE FITTING

2.1 Background on Regression Models

2.1.1 Linear Regression

Since both regressive splines and Kriging are rooted in linear regression, it is vital to establish basic parameters and understanding of linear regression before building on sophisticated models. Linear regression is one of the most fundamental methods of supervised learning in which we predict quantitative responses, or "targets", to data points. For the datasets concerned, the "inputs" of data, X, are positions of the strain rates and vorticity, and the "outputs" or "targets", Y, are stain rates and vorticities.

Setting the list of inputs as a vector, we define $X^T = (X_1, X_2, X_3, ..., X_N)$ for the dataset. Then, X^T becomes the vector of all positions for N data input, X_1, ... ,X_N. Assuming that the data has a linear shape ($E(Y|X)$ is linear), we find a linear fit to the dataset. Then, the linear regression model has the form

$$f(X) = \beta_0 + \sum_{j=1}^{N} X_j \beta_j. \tag{2.1}$$

where $f(X)$ is the linear regression approximation of the output Y, and β_js are the linear regression coefficients, which succinctly writes as $\beta = (\beta_0, \beta_1, ..., \beta_N)$. To find the best fit using linear regression, the β coefficients that best scale linear regression

is sufficient. This is typically done using the residual sum of squared errors, RSS,

$$RSS(\beta) = \sum_{i=1}^{N}(y_i - f(x_i))^2 = \sum_{i=1}^{N}(y_i - \beta_0 - \sum_{j=1}^{N} X_j\beta_j)^2 = (y - X\beta)^T(y - X\beta). \quad (2.2)$$

In order to find the minimum of the residuals,

$$\frac{\partial RSS}{\partial \beta} = -2X^T(y - X\beta) = 0. \quad (2.3)$$

Solving the above for β,

$$\hat{\beta} = (X^T X)^{-1} X^T y, \quad (2.4)$$

where the β parameters that yields best fit is approximated as $\hat{\beta}$. Similarly, best approximated output from linear regression becomes

$$\hat{y} = X\hat{\beta} = X(X^T X)^{-1} y, \quad (2.5)$$

where $\hat{y}_i = \hat{f}(x_i)$ is the best estimator of output.

The β parameters could be statistically interpreted with equation 2.4. Equation 2.4 can be re-written as

$$\hat{\beta} = (X^T X)^{-1} X^T y = \frac{\sum_{i=1}^{n}(y_i - \bar{y})(x_i - \bar{x})}{\sum_{i=1}^{n}(x_i - \bar{x})^2} = \frac{Cov(x, y)}{Var(x)}. \quad (2.6)$$

Covariance signifies how much two variables vary jointly; if one variable increases, the other variable would likely increase. Variance signifies how much the data deviates from the mean. Then, β parameter signifies how much the output varies according to input scaled by standardization.

2.1.2 Kriging

Building on linear regression, Kriging is a more sophisticated model that includes the randomness in predictive fit of data.[11] Matlab's Kriging package "DACE" developed at Technical University of Denmark uses Kriging model from supervised machine

learning to be applied for physical system models and particularly for fluid modeling, so establishing fundamentals of Kriging techniques and discussing hyperparameters of the model are essential.[1] Kriging is often called "Gaussian process regression," for it uses gaussian process prior. A Gaussian process is a specific kind of machine learning models that assumes the observations occur in a continuous domain.

In Kriging, the design sites are analogous to data inputs of linear regression. Then, we define $S = [s_1, ..., s_N]^T$ as design sites that correspond to positions of each data point. The "responses" in Kriging are analogous to output of data in linear regression. Then, we define $Y = [y_1, ..., Y_m]^T$. The normalizing assumption specifically for DACE package used for this project is

$$\mu[S_{:,j}] = 0, V[S_{:,j}, S_{:,j}] = 1, \tag{2.7}$$

$$\mu[Y_{:,j}] = 0, V[Y_{:,j}, Y_{:,j}] = 1, \tag{2.8}$$

where μ is the mean and V is the covariances. The prediction of the model is defined as

$$\hat{y_l}(x) = F(\beta_{:,l}, x) + z_l(x), \tag{2.9}$$

where $\hat{y_l}$ is the estimator for l^{th} component of the outcome, $F(\beta_{:,l}, x)$ is the estimator prediction of linear regression, and $z_l(x)$ is the "random function" that introduces noise. This prediction estimator statement indicates that Kriging is a departure from regression to include stochasticity. This model, then, can be thought of as a deterministic response combined with stochastic path. The model assumes that the random process, z_l, obeys

$$E[z_l(s)z_l(x)] = \sigma_l^2 R(\theta, s, x), \tag{2.10}$$

where $R(\theta, s, x)$ is correlation between x and s with a scalable parameter θ.

2.1.3 Kriging Estimator

With the theoretical parameters defined and described, the Kriging estimator of the "DACE" package is discussed. In this section, the Kriging estimator and the mean squared error are defined.

First, we recognize that the parameters and variables can be written in matrix form. The regression estimator is an ensemble of all estimators at all design sites, and can be written as a vector,

$$F = [f(s_1), ..., f(s_N)]^T. \tag{2.11}$$

Then, the stochastic processes can also be written as a matrix of all noise correlation functions shown below,

$$R_{ij} = R(\theta, s_i, s_j), \tag{2.12}$$

and in matrix form,

$$r(x) = [R(\theta, s_1, x), ..., R(\theta, s_N, x)]^T, \tag{2.13}$$

where s_i represents the design site and x is an untried point at fit. Similarly, the Kriging estimator can be written as

$$\hat{y}(x) = c^T Y, \tag{2.14}$$

where $c = c(x)$ is a real valued function, and Y is the outputs. Then, the Kriging estimator is determined by deriving an appropriate expression for c. As in linear regression, we start by examining the minimization quantity for the fit. For the Kriging fits, the minimizing quantity is the mean squared error, analogous to the linear regression.

$$\hat{y} - y = c^T Y - y \tag{2.15}$$
$$= c^T(F\beta + Z) - (f^T\beta + z) \tag{2.16}$$
$$= c^T Z - z + (F^T c - f)^T \beta, \tag{2.17}$$

where Z is the error at the design sites.

Moreover, the estimator is assumed to be unbiased. This would ensure that the estimating statistics and our parameter matches the true values at sampling sites eventually. More precisely, the expected value of the estimators to equal the parameter. Mathematically, this is shown as (2.18) in our context.

$$F^T c = f. \tag{2.18}$$

Then, the minimizing quantity can be expressed in terms of ϕ:

$$\phi(x) = E[(\hat{y} - y)^2] \tag{2.19}$$
$$= E[(c^T Z - z)^2] \tag{2.20}$$
$$= E[z^2 + c^T Z Z^T c - 2c^T Z z] \tag{2.21}$$
$$= \sigma^2(1 + c^T R c - 2c^T r), \tag{2.22}$$

where $Z = [z_1, ..., z_m]^T$ is error, so the standard deviation $\sigma^2 = z^2$.

Then, so far we have the minimization quantity and the minimizing constraint defined: $F^T c - f = 0$ as the minimization constraint and $\phi(x) = \sigma^2(1 + c^T R c - 2c^T r)$ as the minimization quantity. The curve fitting to minimize with respect to the unbiased constraint can be cast as a lagrangian multiplier problem. The Lagrangian of the system then becomes:

$$L = \sigma^2(1 + c^T R c - 2c^T r) - \lambda^T(F^T c - f), \tag{2.23}$$

where λ is the lagrangian multiplier. In the lagrangian multiplier problem, the system would hit the minima at the zero point in the derivative, so we take the derivative and set it equal to 0. Then, we could solve for the optimal λ,

$$\hat{\lambda} = (F^T R^{-1} F)^{-1}(F^T R^{-1} r - f), \tag{2.24}$$

and

$$c = R^{-1}(r - F\hat{\lambda}). \tag{2.25}$$

From linear regression, we have the optimal β^* values, as shown in (2.5). Then, plugging this in, we can solve for the Kriging estimator:

$$\hat{y} = f^T \beta^* + r^T \gamma^*, \tag{2.26}$$

where γ^* is found by the residuals: $R\gamma^* = Y - F\beta^*$. The minmization quantity, MSE, is

$$\psi = \sigma^2(1 + c^T(Rc - 2r)) = \sigma^2(1 + u^T(F^T R^{-1} F)^{-1} u - r^T R^{-1} r), \tag{2.27}$$

where $u = F^T R^{-1} r - f$ and σ^2 is the standard deviation of the fit.

2.1.4 Kriging Parameters, and Model Evaluation

With the model defined, the statistics and parameters are discussed. With Dace's toolbox, there are three main parameters, which are levels of linear regression, correlation models, and correlation hyperparameter. The table 2.1 summarizes these choices and options. Then, each of the parameters are discussed, and the next section explains the choices of the parameters.

First, the level of regression of the model discribes the order of regression polynomials. The 0th order corresponds to constants, 1st order corresponds to a linear model, and the 2nd order corresponds to a quadratic model. Since the shape of the

Table 2.1: Parameters for Kriging

Level of Linear Regression
'regpoly0', 'regpoly1', 'regpoly2'
Correlation Models
Gaussian, Exponential, Linear, Cubic, Spherical, Spline
Hyperparameters
Θ parameter for Correlation Models

datasets is bowl-shaped, the 2nd parabolic shape of quadratic order regression is perhaps most appropriate. All three orders of linear regression were applied, and the complete results are shown in Appendix A.

The correlation models are the mathematical expressions of the random processes. In simple terms, it could be thought of as how the errors were modeled. The figure 2.1 shows the correlating function for DACE. All correlation models decrease as the distance increases, and the larger values of θ expediates the tapering. The correlation model is chosen based on the nature of the datasets, and the underlying physics behind the generation of the data.

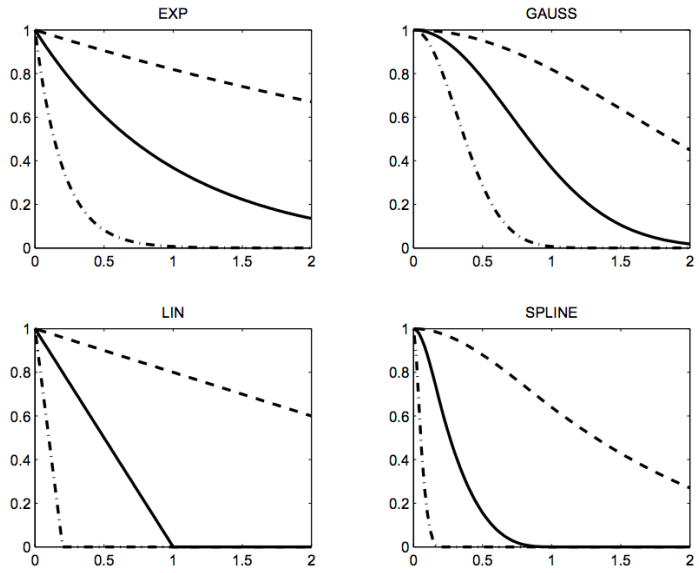

Figure 2.1: Examples of Kriging correlation functions

2.2 Statistical Fitting using Dace

The choices of the parameters for the datasets are summarized as shown in the table 2.2. First, the second level of regression is chosen, since the scatter plot of the raw data is "bowl-shaped" Oseen vortex. For the correlation function, the Gaussian was chosen, since the vorticity and rotation are continuously differentiable and the correlation is likely to show a parabolic behavior near the origin.[1] For the hyperparameter of correlation models, the initial choice was set to 1, and DACE model autocorrects parameters for lower mean squared error values.

Table 2.2: The chosen parameters for Kriging

Level of Linear Regression
'regpoly2'
Correlation Models
Gaussian
Hyperparameters
Θ parameter for Correlation Models

2.3 Spline Fitting using Matlab's Curve Fitting Toolbox and tpaps

Regression-based models provide a fit by including all data points. This statistical fitting allows for general trendlines of data, but the local variations from the fit could largely affect the fit at a global scale. To correct for this weakness in statistical regression, the smoothing spline fits would allow for local abberations to be represented with a local fitting function without affecting the general fit. This section describes the spline fitting method, and how the local fits are combined to give a general fit.

2.3.1 Advantages of Spline Fitting

Spline functions are continuous segmented functions that form elements for a complete fit. First, the segmented spline functions are statistically fit to local data. The statistically corrected spline functions are connected at nodes called "knots." In linear regression, the "resolution" of the fit can be determined by two main aspects of data: the shape of data and the order of regression. In general, increasing the level of regression to appropriate level by having more basis functions can decrease the error of the fit. This is analoguous to having appropriately inceased number of knots for the fit for spline fitting. In general, the increased number of knots can decrease the

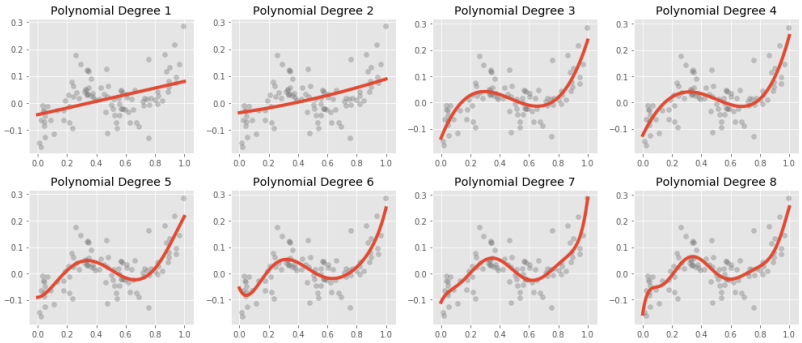

Figure 2.2: Different polynomial regressive fit for a given data[3]

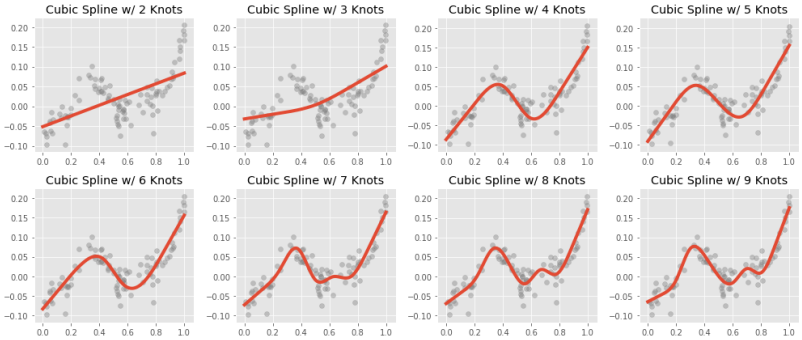

Figure 2.3: Different cubic spline fits for a given data[3]

error. A toy example is shown below in figures 2.2 and 2.3.

Figure 2.2 illustrates the fitting of data as the terms in polynomial regression increases. As the level of regression increases, we see that the fit could dramatically change shapes, especially at the edges. Specifically, inspecting the right edges of degrees 7 to 9 in figure 2.2, edges fluctuate due to lack of data points beyond. On the other hand, right edges are fixed downward all figures for 2.3. This is perhaps better illustrated with edge cases, such as outlier points shown in figures 2.4 and 2.5. Figure 2.4 illustrates that the curvature of the entire fit has been affected as soon as an outlier is added. This effect is much less prominent in 2.5, and the natural cubic

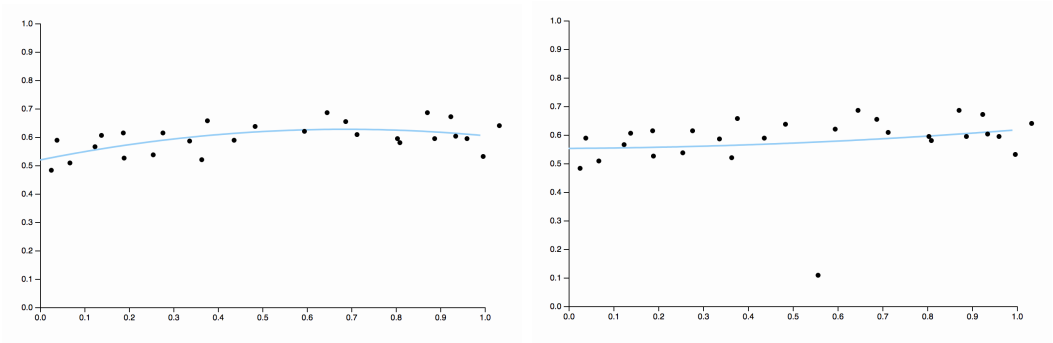

(a) Regressive Fit Before Adding an Outlier (b) Regressive Fit After Adding an Outlier

Figure 2.4: Polynomial Regressive Fit

spline mitigates local variations taking global effects.

With established benefits over linear regression, the modeling using spline fitting are discussed. In general spline fitting, the two primary choices to tune the model are the choice of spline function and number of knots. Determining what choices are best for modeling are statistically justified, using error analysis and cross validation. In the next section, the model for fitting is more precisely defined in Matlab context.

2.3.2 Thin Plate Spline Fitting using Matlab's tpaps package

The above section describes the discrete splines. However, placement of the knots and the number of knots are a significant challenge with discrete spline models. Then, it is a natural choice to use a continuous spline with "bending energy" as a hyperparameter, or a global tuning parameter for a given model. Thin plate spline fitting is a continuous analogue to the discrete splines.

As discussed in the previous section, the discrete splines find fits section by section. Considering a discrete splines for knots placed at $x_1, x_2, ...x_n$, the approximate fit is

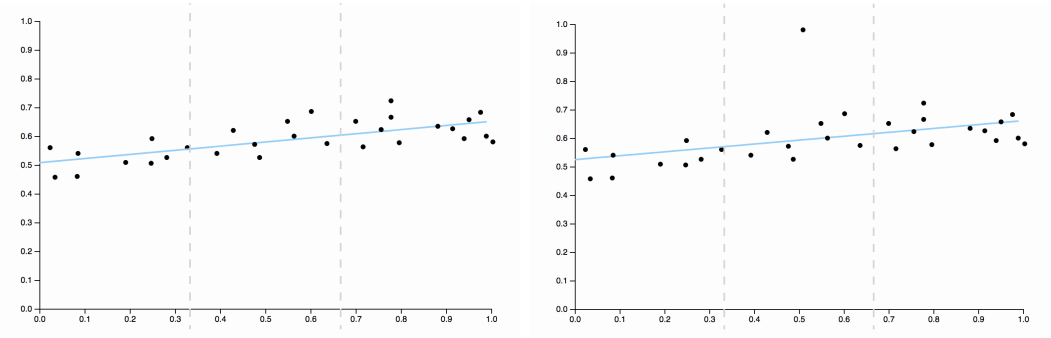

(a) Spline Fit Before Adding an Outlier (b) Spline Fit After Adding an Outlier

Figure 2.5: Natural Cubic Spline Fit

a linear combination of smoothing functions

$$y_i = f_1(x_{1i}) + f_2(x_{2i}, x_{3i}) + f_2(x_{4i}, x_{5i}) + ... + \epsilon_i, \tag{2.28}$$

where each segment is fit by minimizing the mean squared error

$$||y - f||^2. \tag{2.29}$$

In order to remove the dependency of knots, the above can be approximated using the Hilbert space kernels. Assuming that the fitting function is a linear combination of Hilbert space kernel functions, the minimization problem then becomes

$$||y - f||^2 + \lambda \int f''(x)^2 df. \tag{2.30}$$

The second term from the above minimization quantity is the Hilbert space energy criterion. To incorporate the thin plate smoothing criterion, the energy is modified to include the bending energy term

$$\int \left(\left| \frac{\partial^2 f}{\partial x_1^2} \right|^2 + 2 \left| \frac{\partial^2 f}{\partial x_1 \partial x_2} \right|^2 + \left| \frac{\partial^2 f}{\partial x_2^2} \right|^2 \right) dx_1 dx_2. \tag{2.31}$$

Matlab's thin plate spline package "tpaps" then organizes the minimization energy as

$$E_{tpaps} = pE(f) + (1-p)R(f), \tag{2.32}$$

where

$$E(f) = \sum_j |y(:,j) - f(x(:,j))|^2 \tag{2.33}$$

and

$$R(f) = \int \left(\left| \frac{\partial^2 f}{\partial x_1^2} \right|^2 + 2 \left| \frac{\partial^2 f}{\partial x_1 \partial x_2} \right|^2 + \left| \frac{\partial^2 f}{\partial x_2^2} \right|^2 \right) dx_1 dx_2. \tag{2.34}$$

Chapter 3

RESULTS

3.1 Curve Fitting Results

3.1.1 Raw Data

In this section, the raw data of the Oseen vortex are exhibited before curve fitting. First two sets of figures, 3.1 and 3.2, are the noiseless data for 600 data points, and dataset numbers 4 and 7. Subfigures a, b, and c are the computationally generated for three different rotation methods. Subfigure d is the analytical vorticity solution that the computational data are compared. The last two sets of figures, 3.3 and 3.4, are the noisy versions of the first two. The noiselevel used is 0.1.

Expectantly, the two noisier figure sets look a bit more "messier." The sets of higher dataset numbers have higher resolution. Fitting of the noisy plots were discussed in the following sections, using Kriging package "DACE" and spline smoothing package "tpaps."

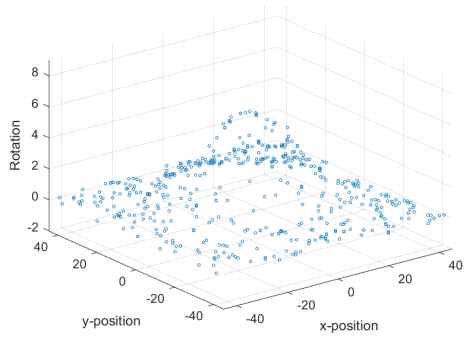

(a) Rotation Method 1

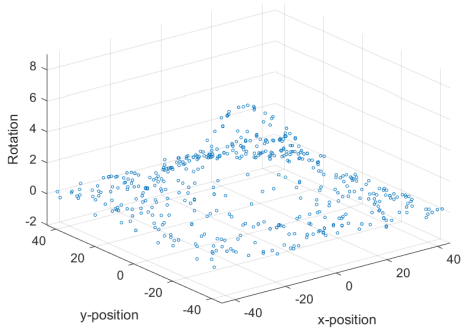

(b) Rotation Method 2

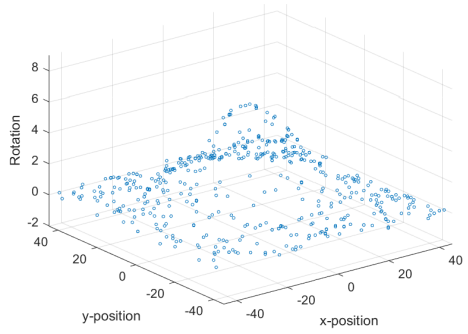

(c) Rotation Method 3

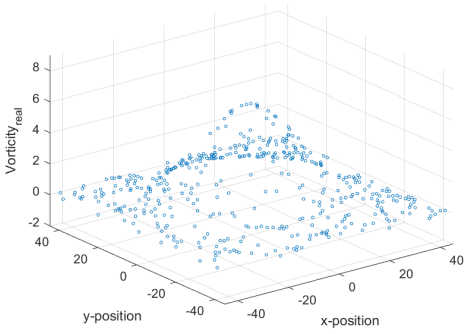

(d) Analytical Vorticity

Figure 3.1: Raw Data for 600 data points, Dataset Number 4, and Noiseless

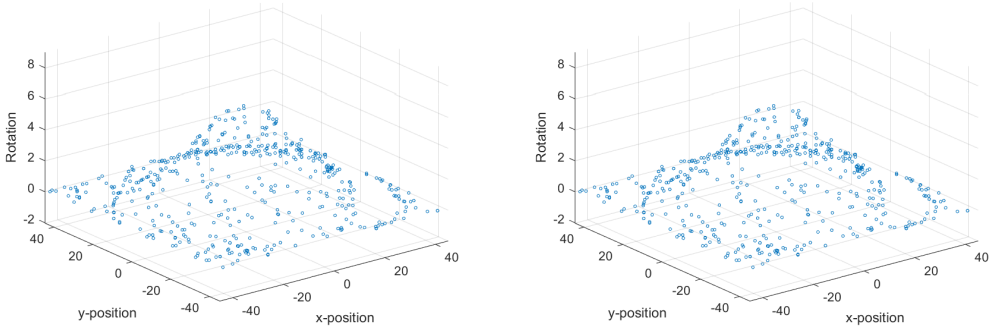

(a) Rotation Method 1

(b) Rotation Method 2

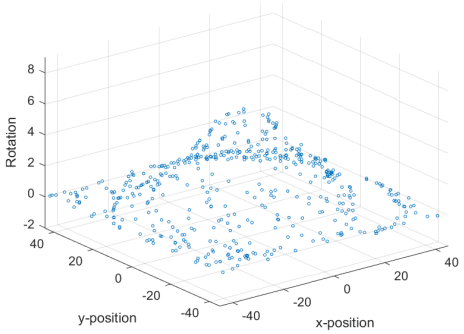

(c) Rotation Method 3

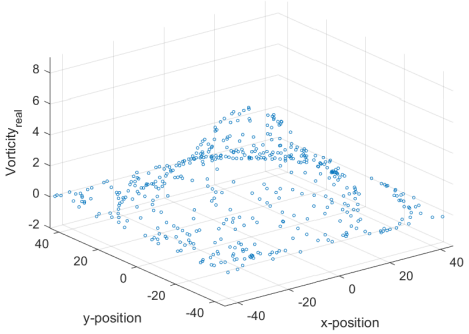

(d) Analytical Vorticity

Figure 3.2: Raw Data for 600 data points, Dataset Number 7, and Noiseless

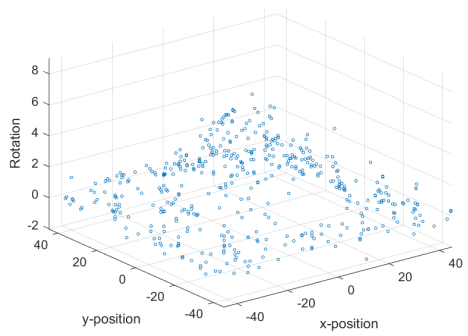

(a) Rotation Method 1

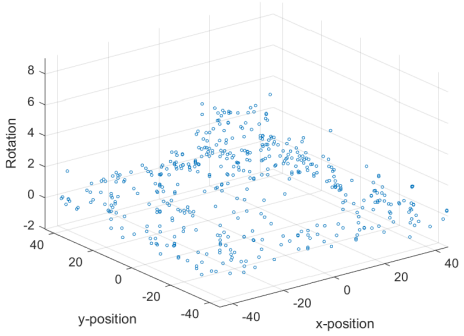

(b) Rotation Method 2

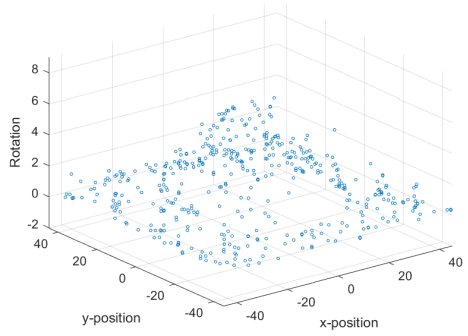

(c) Rotation Method 3

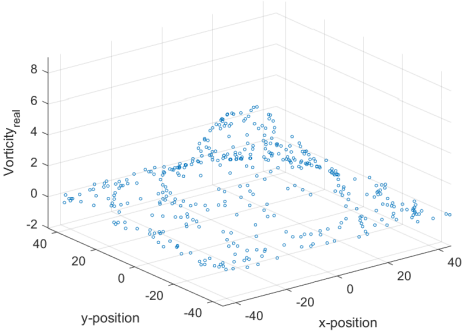

(d) Analytical Vorticity

Figure 3.3: Raw Data for 600 data points, Dataset Number 4, and Noise level 0.1

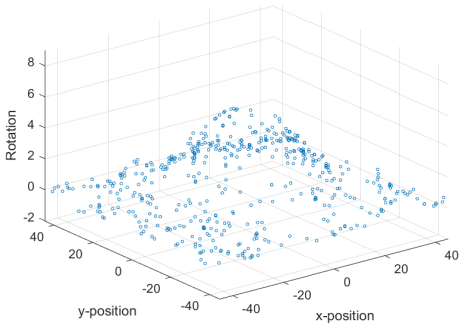

(a) Rotation Method 1

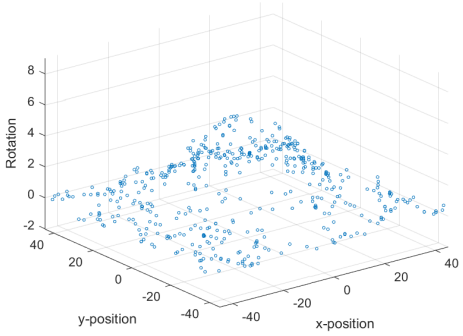

(b) Rotation Method 2

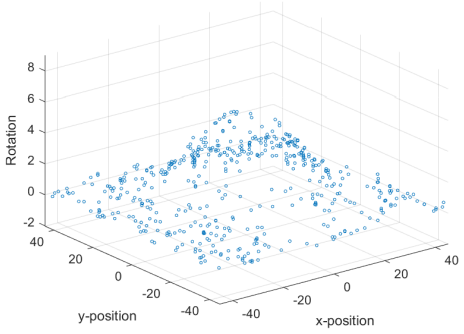

(c) Rotation Method 3

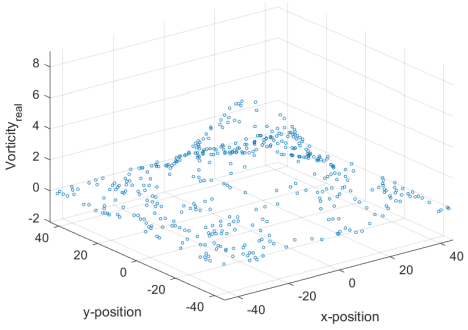

(d) Analytical Vorticity

Figure 3.4: Raw Data for 600 data points, Dataset Number 7, and Noise level 0.1

3.1.2 Regressive Fit Results

For Kriging, plots for each levels of regression are shown in Appendix A. Best parameters of interest such as the θ correlation parameter and level of regression can be determined through statistical analysis discussed in Chapter 4. This chapter discusses the methodology and code, and displays the results.

Code for the Krigging

Using DACE Krigging package developed at Technical University of Denmark, the raw data points are fitted with a surface. First, the variables and domain grids are defined. In this step, the sampling sites are determined as well. Then, the model is fit using the "dacefit" function. Then, the fit is overlayed on top of the raw data points. The table 3.1 shows the general layout of the code.

Table 3.1: Organization of DACE plot generating

Define variables
Define rotational methods and design sites
Choose parameters for the Kriging model
Choose level of regression, noise function, and Θ parameter
Fitting the model
'dacefit' function of DACE package
Evaluating the DACE package
'predictor' function
Plot the model
Overlay the fitted surface to the original data in scatter plot form

Plots from Krigging

A few comparisons are made with the results of Kriging. The fit could have been affected by the rotation methods, levels of regression, number of design sites, or the dataset number. The next few set of figures in this section illustrate comparisons. The next chapter delves into statistical analysis of errors. The complete list of plots for Kriging are listed in Appendix A.

First, the rotation methods are compared. For most groups of datasets, the mean square error was minimized for rotation method 3. The peaks were captured best with rotation method 3 as well.

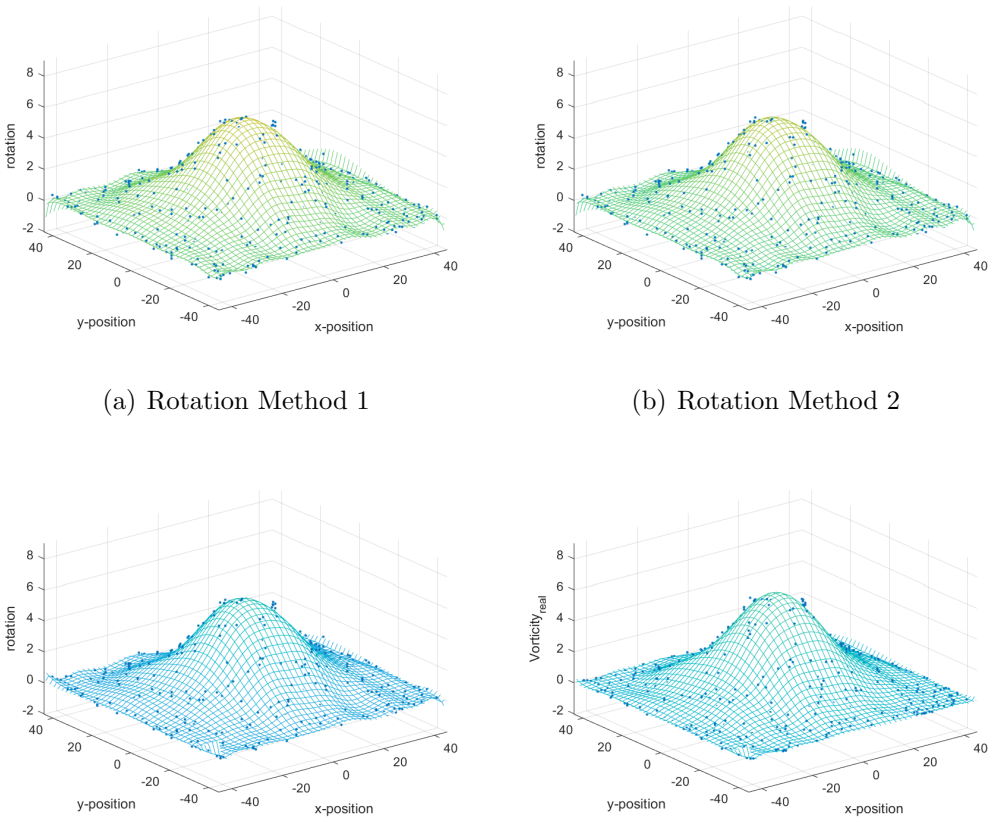

(a) Rotation Method 1

(b) Rotation Method 2

(c) Rotation Method 3

(d) Analytical Vorticity

Figure 3.5: 2nd level regressive fit for 600 data points, Dataset Number 10, and Noise level 0.1

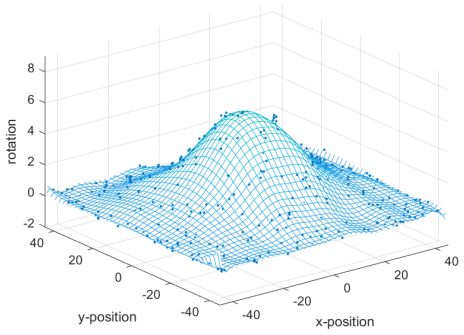

(a) Regression Level 0

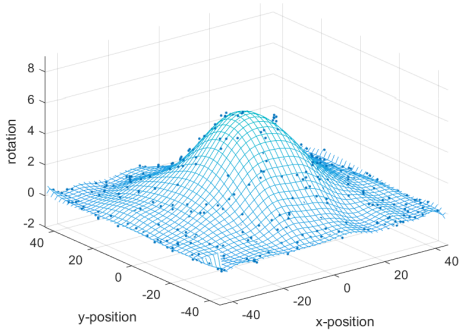

(b) Regression Level 1

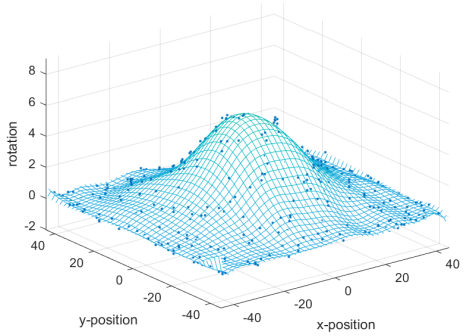

(c) Regression Level 2

Figure 3.6: Comparison of levels of regression

As levels of regression increases, the error decreased. The 2nd level regression gave the best results for most sets of data. Since the shape of the datasets are Gaussian, the parabolic shape was perhaps captured the Gaussian shape the best.

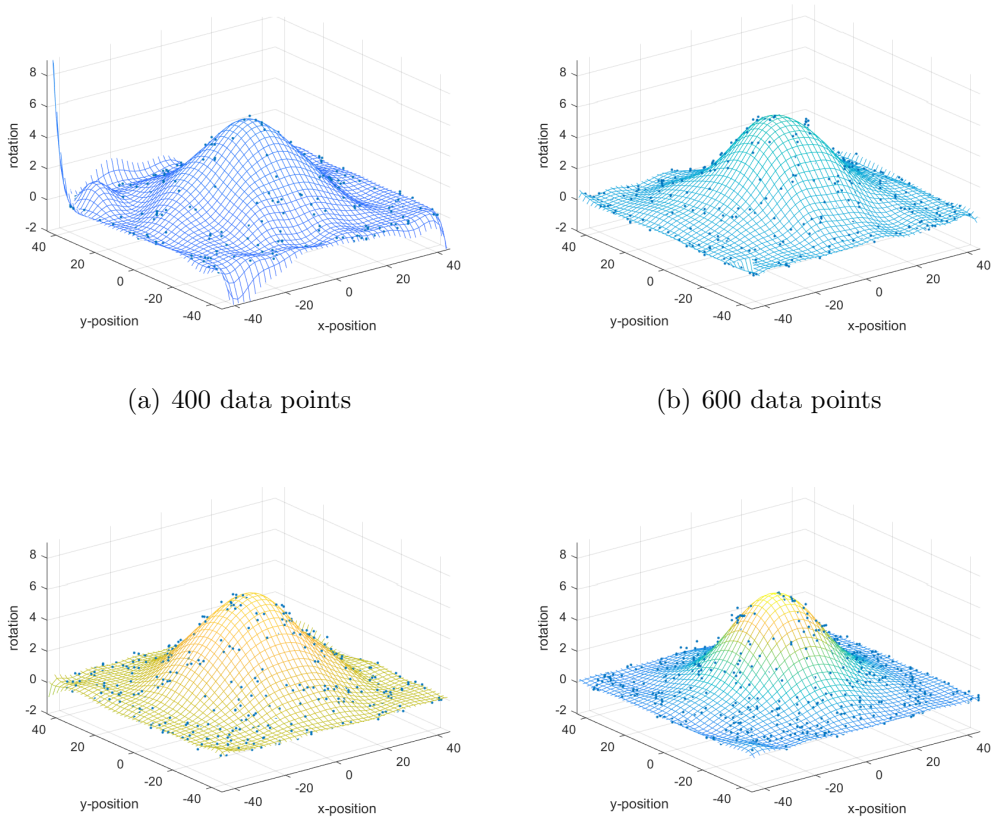

(a) 400 data points

(b) 600 data points

(c) 800 data points

(d) 1000 data points

Figure 3.7: Comparison of number of data points

Another comparison was the number of data points, which in turn would the number of sites where the fit was designed. Naturally, the increasing number of data points gave the best fit. However, large number of data points are limited by experimental limitations.

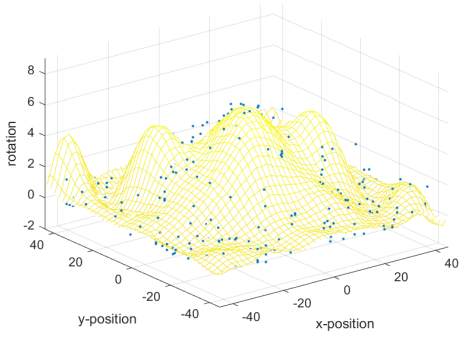

(a) Dataset Number 4

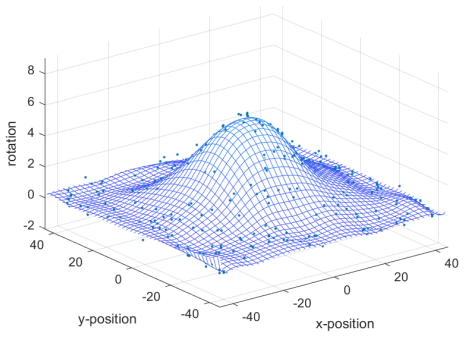

(b) Dataset Number 7

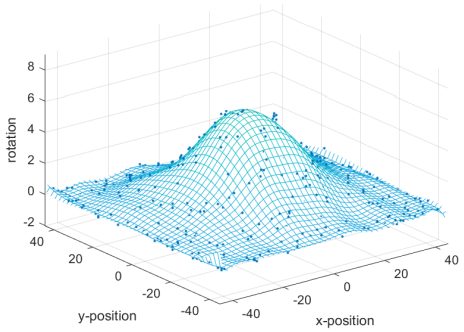

(c) Dataset Number 10

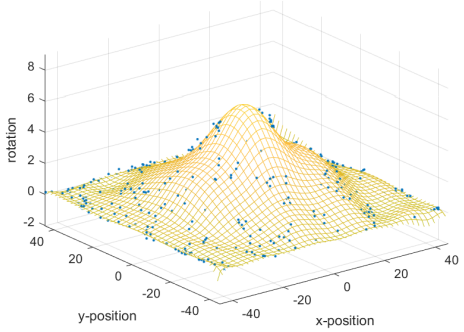

(d) Dataset Number 13

Figure 3.8: Comparison of Dataset Numbers

Then, the dataset numbers are also considered for the plots. The increasing dataset numbers gave better fits.

3.1.3 Spline Fitting Results

Similarly, the spline fitting results are compared as well. The number of data points, rotational methods, and dataset numbers are discussed for comparison. The statistical comparisons are shown in the next chapter.

First, the spline fits were found for each rotation method and compared visually. Similar to the Kriging plot results, the errors are minimized for rotation method 3. Visibly, rotation method 3 captures the peak of the Oseen vortex the best and yields the smoothest results.

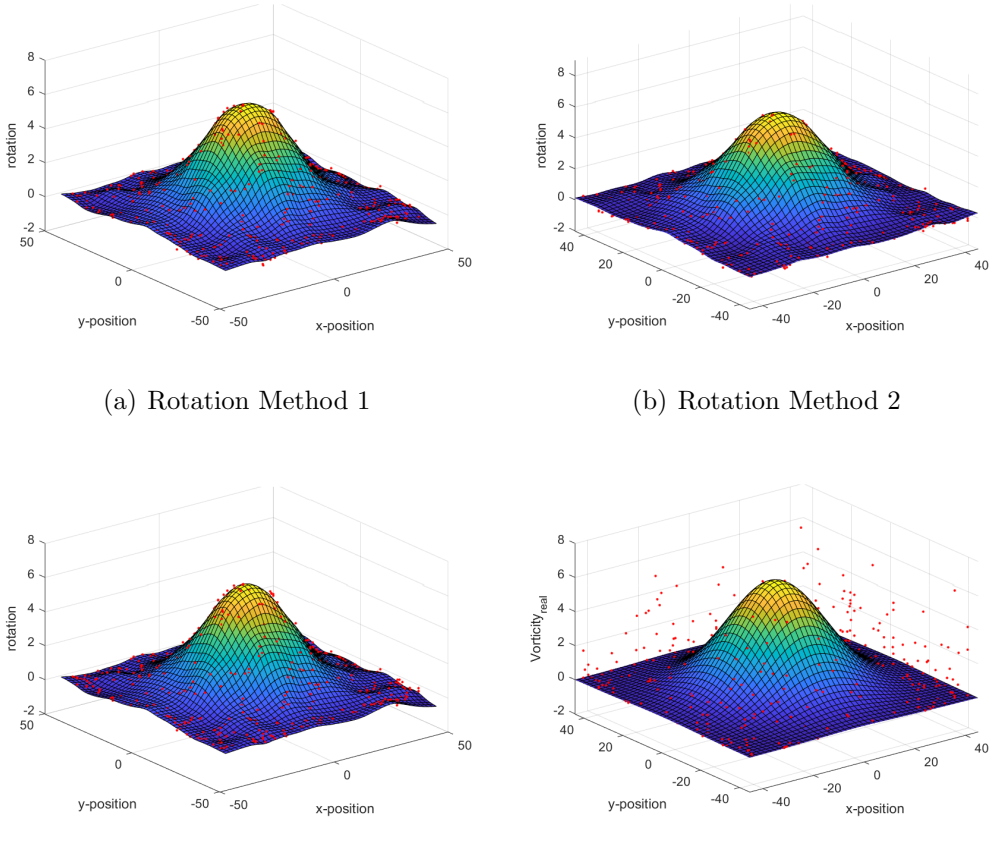

(a) Rotation Method 1

(b) Rotation Method 2

(c) Rotation Method 3

(d) Analytical Vorticity

Figure 3.9: Spline fitting for 600 data points, Dataset Number 10, and Noise level 0.1

Then, the number of data points were varied and the plots were visually compared. The mean squared error is minimized with respect to the data points, and thus, the increasing number of data points yields decreasing mean squared error. The peak was also captured the best with more data points. On the other hand, the increasing number of data points increases the amount of sites for spline fits to match data. This generally restricts smoothness of fit; the model becomes overfit. This can be counter-balanced with a careful choice of parameters, which is further discussed in the next chapter.

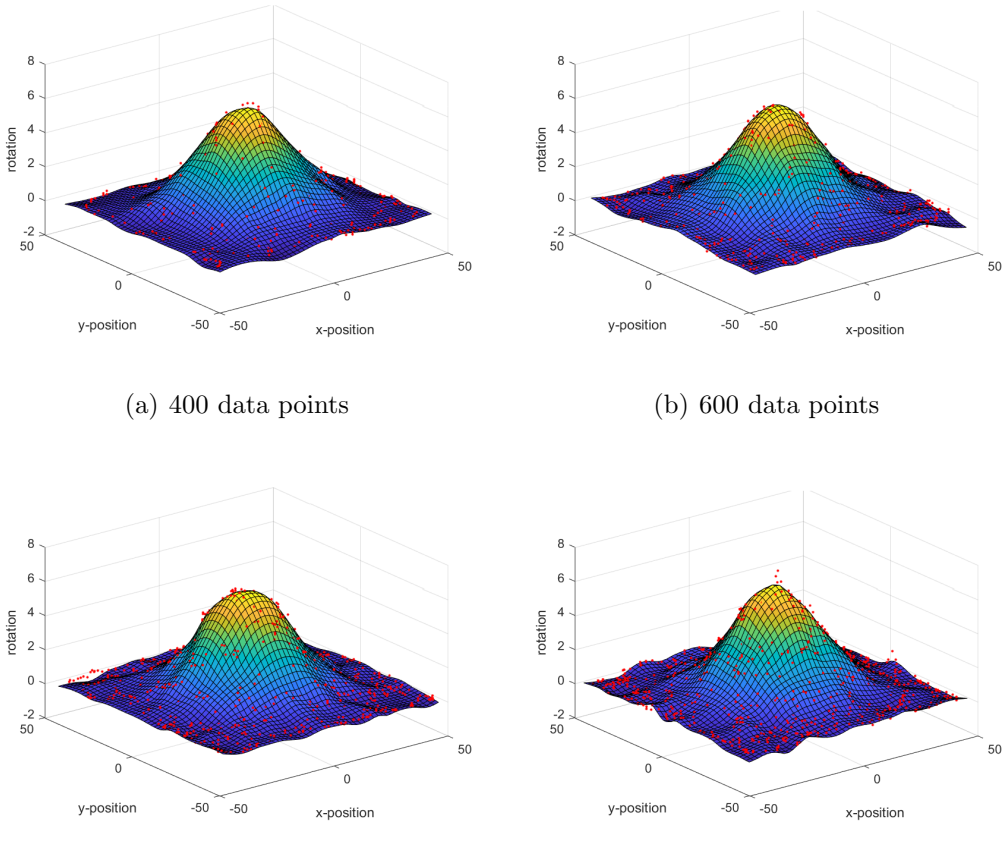

(a) 400 data points

(b) 600 data points

(c) 800 data points

(d) 1000 data points

Figure 3.10: Comparison of data point numbers

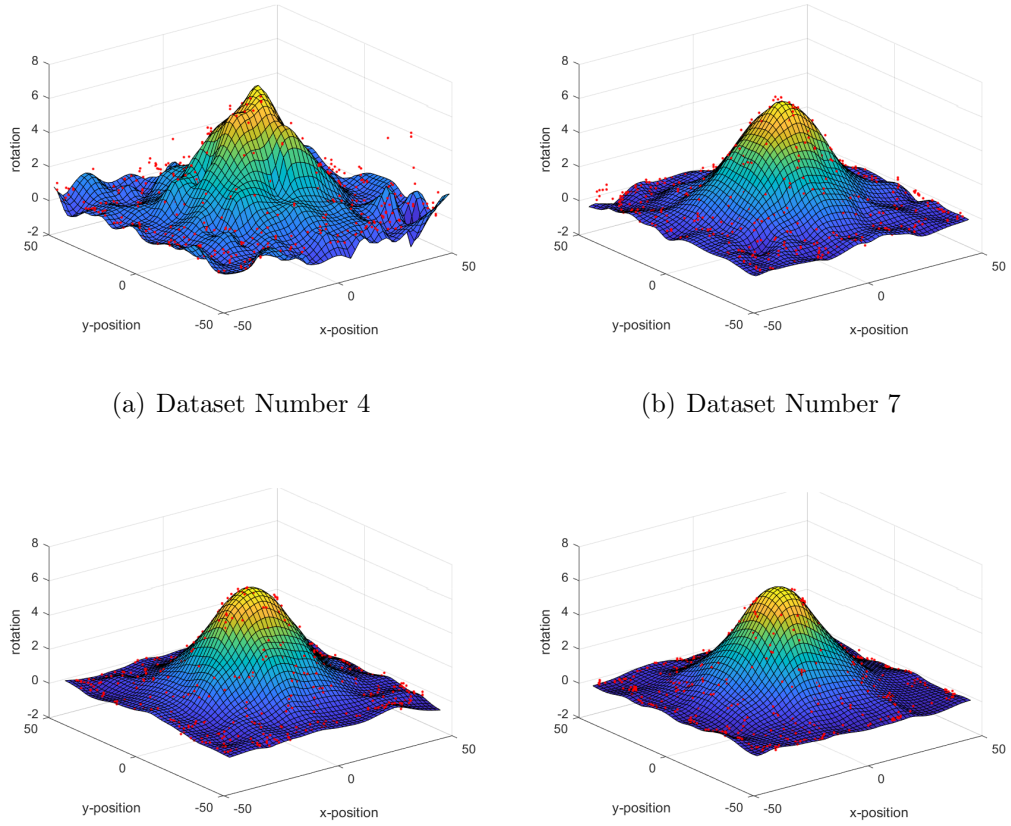

(a) Dataset Number 4

(b) Dataset Number 7

(c) Dataset Number 10

(d) Dataset Number 13

Figure 3.11: Comparison of Dataset Numbers

The increasing dataset number indicates that the fit becomes smoother over time, with decreasing mean squared error.

Chapter 4

DATA ANALYSIS AND STATISTICAL ANALYSIS OF ERRORS

4.1 Statistical Analysis

The computationally generated Oseen vortex data was fit using two different models: kriging and thin plate spline fitting. The dataset is analyzed using both methods in this section. Kriging fits on the dataset is used to interpret a few individual datasets. The smoothing spline has one hyperparameter, which is the smoothing parameter. This makes for an ideal model to work with to do overarching meta-analysis on the overall datasets.

Two methods have differing advantages and disadvantages. The kriging method, linear regressive method, predictively gives lower mean squared error, but the fit is not as smooth as the spline method. The spline fitting takes into account the smoothness in its bending energy. These differences are commented as statistical analysis continues.

4.1.1 DACE

The kriging datasets shown in Chapter 3 and the appendix shows that the fit diverges at the edges. This could be best illustrated by examining the mean squared error. Choosing 600 data points and dataset number 13 for further analysis, the mean squared error for all data points are plotted in 4.1.

The plots in 4.1 are representative of all other dataset behavior, in which the mean squared error is contained within 0.05 around the center, and expands at the

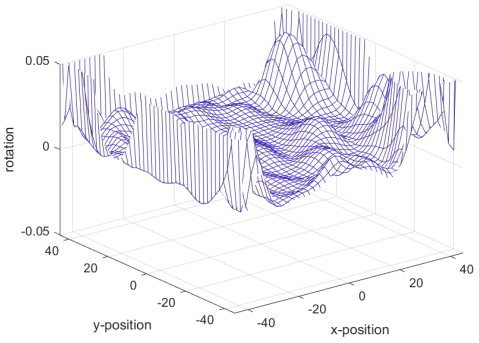

(a) Rotation Method 1

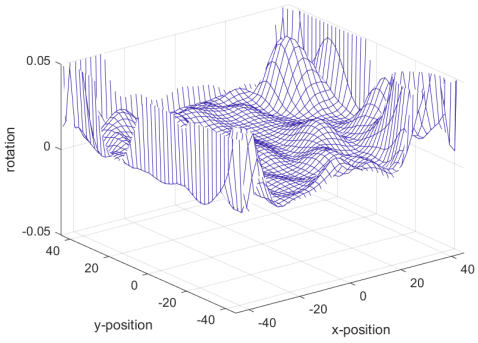

(b) Rotation Method 2

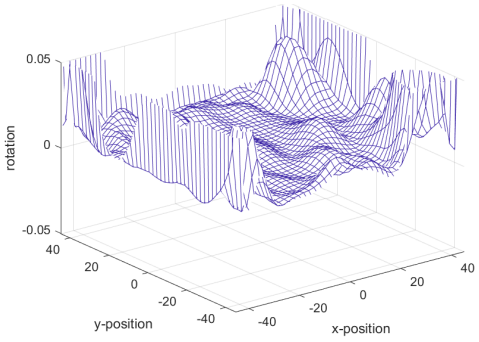

(c) Rotation Method 3

Figure 4.1: Mean Squared Error of Rotation for 600 data points, Dataset Number 13, and Noise level 0.1

edges. This could be explained by lack of data points around the edges. One way to remedy this increased error around the boundary is to impose boundary conditions or to introduce data points around edges to match the mean. The error was relatively small for the fit (averages around 0.03-0.05 overall for most datasets), but there are no smoothness criterion that contains the fit. This could be remedied by further engineering a penalty term for Lagrangian minimization of mean squared error.

4.1.2 tpaps

The advantage of using tpaps is that the model takes into account the smoothness of fit on datasets. The overall comparison of data is also drawn here. Mean squared errors were compared for noiseless and noisy data, varying number of data points, and varying dataset number. Figure 4.2 summarizes the results.

The mean squared error increases with noisy data and the variance of data increased as well. The mean squared error decreased as the number of data points increase, and the variance decreased as well. The mean squared error also decreased as the dataset number decreased. The mean squared error also varied depending on the smoothing parameter, and the optimal smoothing parameter was found by minimizing the mean squared error. Figure 4.3 summarizes the results.

The optimal mean squared error fit is found by process shown in Table 4.1. The best fits were given by smoothing parameter ranging from 0.015 to 0.02. Most optimal choice is around 0.015, but for "messier" data, 0.02 is a better choice of parameter. The messier dataset implies lower dataset number, less number of data points, and noisy.

Table 4.1: Optimal smoothing parameter choice

Optimal parameter choice
Calculate tpaps fit
Calculate Mean Squared Error
Increase tpaps parameter by 0.01 and re-fit the model
Recalculate Mean Squared Error
Repeat until optimal Mean Squared Error reached

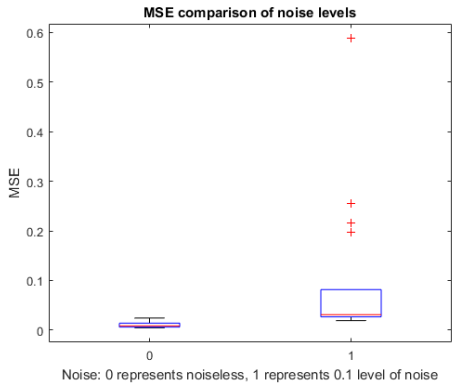

(a) Mean Squared Error comparison for varying noise

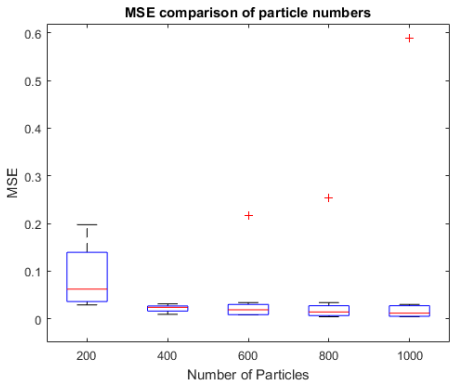

(b) Mean Squared Error comparison for varying number of data points

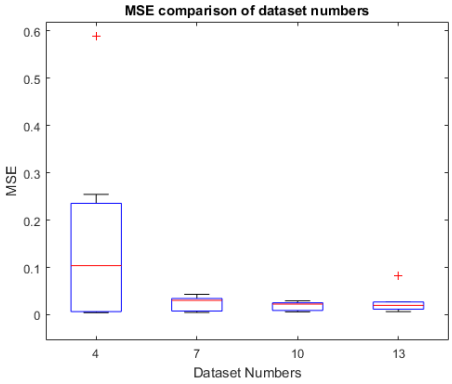

(c) Mean Squared Error comparison for varying dataset number

Figure 4.2: Mean Squared Error (MSE) Comparison. The red line of the box plots represent the median of MSE and + points represent the outliers (beyond 3 standard deviations away from the median). The medians for differing noise levels are 0.0085 and 0.0309. The medians for varying number of data points are 0.0624, 0.0241, 0.0192, and 0.0144. The medians for varying dataset numbers are 0.104, 0.0302, 0.0225, and 0.0197.

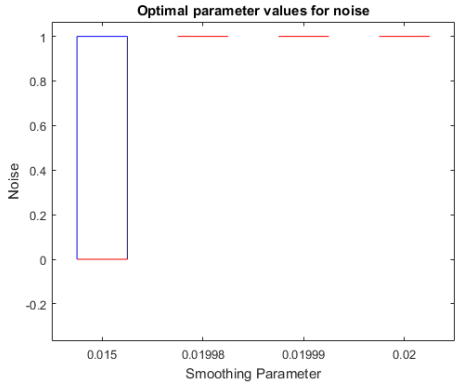

(a) Optimal smoothing parameter range based on noise levels

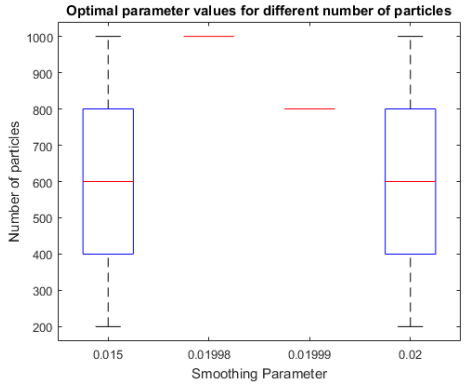

(b) Optimal smoothing parameter range based on numbers of data points

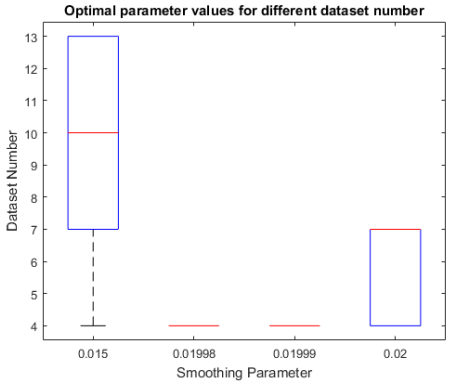

(c) Optimal smoothing parameter range based on dataset numbers

Figure 4.3: Optimal Smoothing Parameters

Chapter 5

CONCLUSION AND FUTURE WORK

5.1 Summary and Conclusion

The computationally generated Oseen vortex data were fit using regression based model and a spline fitting model. The methodologies and theories of regression and Kriging, and spline and thin plate spline models were discussed. Then, the Kriging and thin plate spline models were used to fit datasets of different parameters: data point numbers, dataset numbers, and rotational methods. The mean squared error was plotted for regression analysis on individual sets, and the spline fitting errors were analyzed to discuss the overarching analysis on the entire group of datasets.

5.2 Recommendations for Future Work

These methods for fitting have different benefits and costs. The regression based models tend to give smaller mean squared error, but the smoothness of fit is not taken into account. The smoothness of fit is significant, since the structure of flow could be obscured by a high variance fit. This may be improved by considering boundary conditions or fixing edges by introducing carefully considered fixed edge data points. The spline based models take smoothness of fit into account, but the overall mean squared error could be higher.

A further step is to consider these attributes for models, and engineer an improved model. The two methods could be ensembled. One rudimentary step to ensemble the two models would be to take the average of two fits, and draw error analysis upon data.

BIBLIOGRAPHY

[1] Nielsen Hans Bruun Lophaven, Soren N. and Jacob Sondergaard. *DACE: A Matlab Kriging Toolbox*. Informatics and Mathematical Modelling, Technical University of Denmark, DK-2800 Kgs. Lyngby, Denmark, version 2.0 edition, August 2002.

[2] Simon N. Wood. Thin plate regression splines. *Journal of the Royal Statistical Society. Series B (Statistical Methodology)*, 65(1):95–114, 2003.

[3] Matt Drury. A comparison of basis expansions in regression.

[4] Octave-Forge. tpaps.

[5] Carl de Boor. *Spline Toolbox For Use with Matlab*. Mathworks, The MathWorks, Inc. 3 Apple Hill Drive Natick, MA, 01760-2098, version 3 edition, 1990-2004.

[6] Sandip K. Pawar, Ruud H. M. Abrahams, Niels Deen, Johan Padding, Gert-Jan van der Gulik, Alfred Jongsma, Fredrik Innings, and J A. M. Hans Kuipers. Cjce-article on-expt study. 12 2015.

[7] Richard W. Johnson, Richard Schultz, Patrick J. Roache, Ismail Celik, W Pointer, and Y Hassan. Processes and procedures for application of cfd to nuclear reactor safety analysis. 10 2017.

[8] Part i - viscous evolution of point vortex equilibriua. Master's thesis, University of Southern California, August 2011.

[9] Fanny M. Limon Duparcmeur Don Jacob Nash'at N. Ahmad, Fred H. Proctor. Review of idealized aircraft wake vortex models. https://ntrs.nasa.gov/archive/nasa/casi.ntrs.nasa.gov/20140003974.pdf.

[10] Toby J. Mitchell Jerome Sacks, William J. Welch and Henry P. Wynn. Design and analysis of computer experiments. *Statistical Science*, 4:409–423, November 1989.

[11] Trevor Hastie. *The Elements of Statistical Learning: Data Mining, Inference, and Prediction.* Springer, 12th edition, 2017.

Appendix A

APPENDIX OF FIGURES

This section lists all figures generated and formatted for datasets with data point numbers 200, 400, 600, 800, and 1000, dataset numbers 4, 7, 10, and 13, and noise level of 0 and 0.1. The first section lists all figures with Regressive fitting on the datasets using DACE kriging package, which is essentially linear regression with noisy correlation. Figure sets are then organized with levels of varying regression. The second section lists all figures with spline fitting on the datasets using tpaps function of Matlab. The theory behind the fitting methods are explained in detail in Chapter 2.

A.1 Kriging Fit Using DACE for Datasets

A.1.1 0th Level Regressive Fit

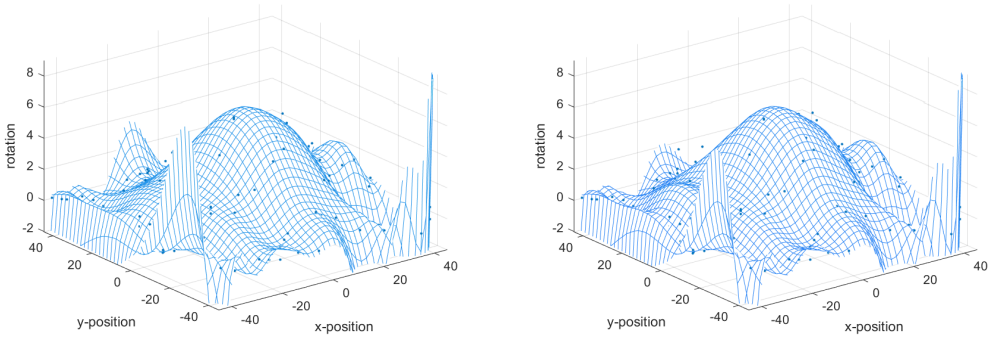

(a) Rotation Method 1

(b) Rotation Method 2

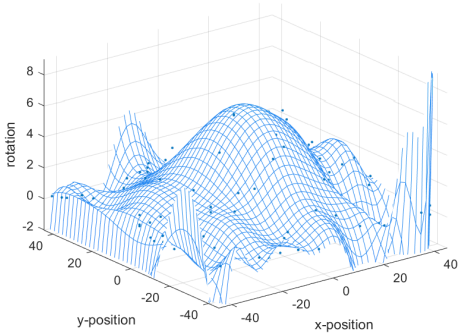

(c) Rotation Method 3

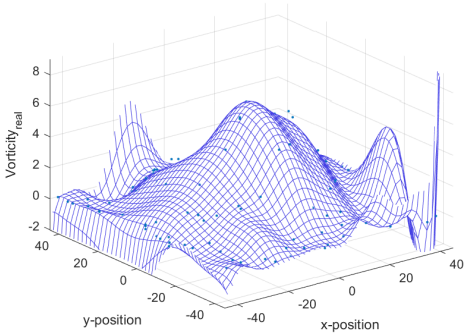

(d) Analytical Vorticity

Figure A.1: 0th level regressive fit for 200 data points, Dataset Number 4, and Noise level 0.1

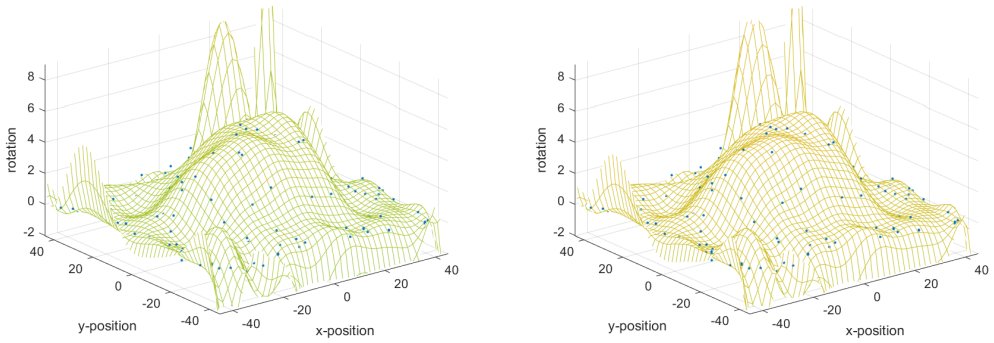

(a) Rotation Method 1

(b) Rotation Method 2

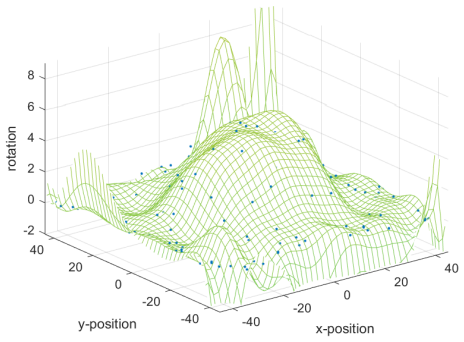

(c) Rotation Method 3

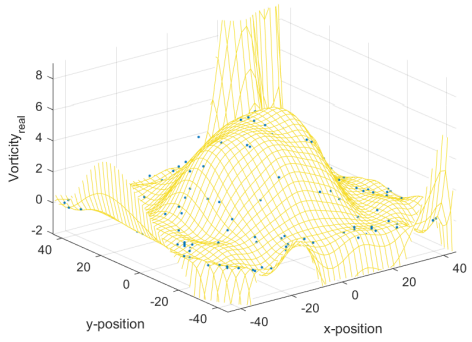

(d) Analytical Vorticity

Figure A.2: 0th level regressive fit for 200 data points, Dataset Number 7, and Noise level 0.1

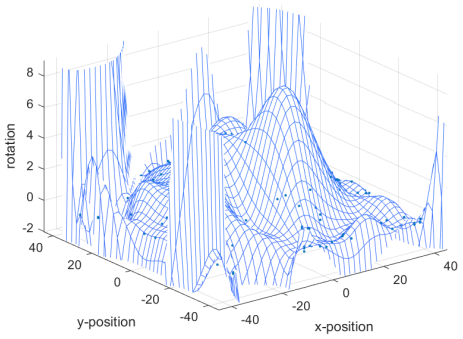

(a) Rotation Method 1

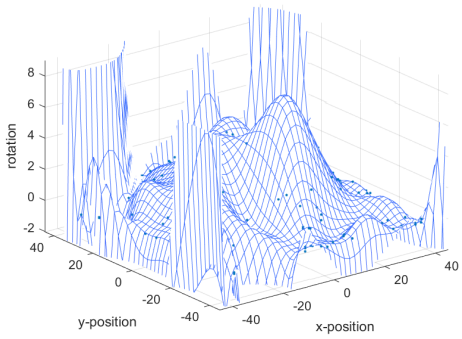

(b) Rotation Method 2

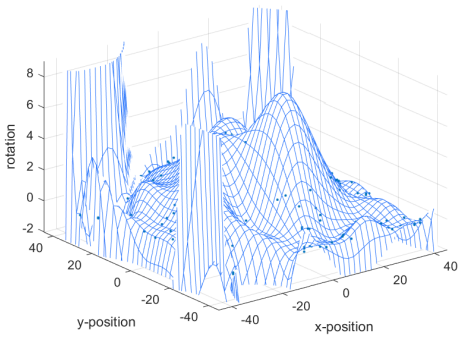

(c) Rotation Method 3

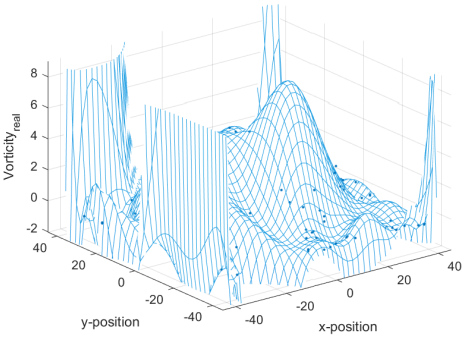

(d) Analytical Vorticity

Figure A.3: 0th level regressive fit for 200 data points, Dataset Number 10, and Noise level 0.1

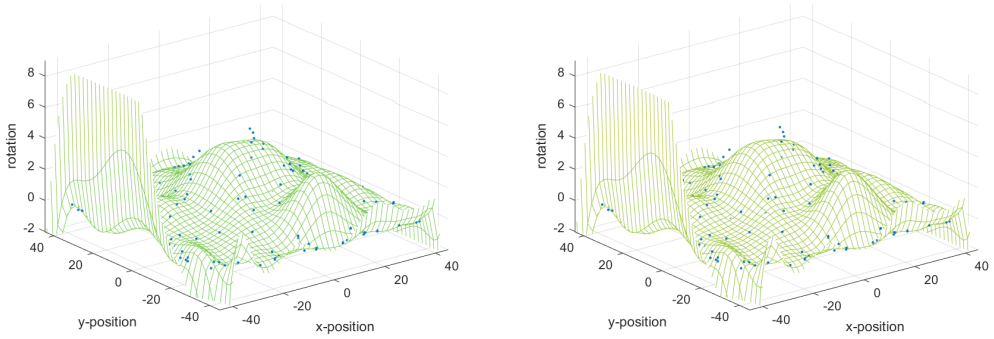

(a) Rotation Method 1

(b) Rotation Method 2

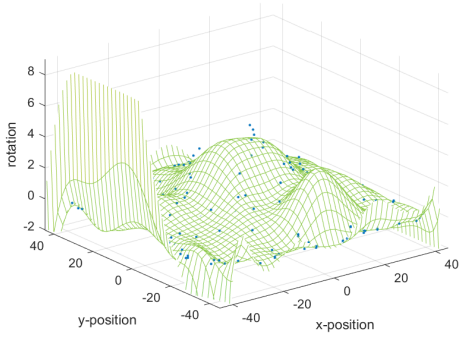

(c) Rotation Method 3

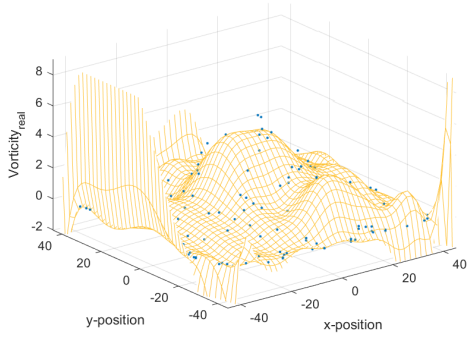

(d) Analytical Vorticity

Figure A.4: 0th level regressive fit for 200 data points, Dataset Number 13, and Noise level 0.1

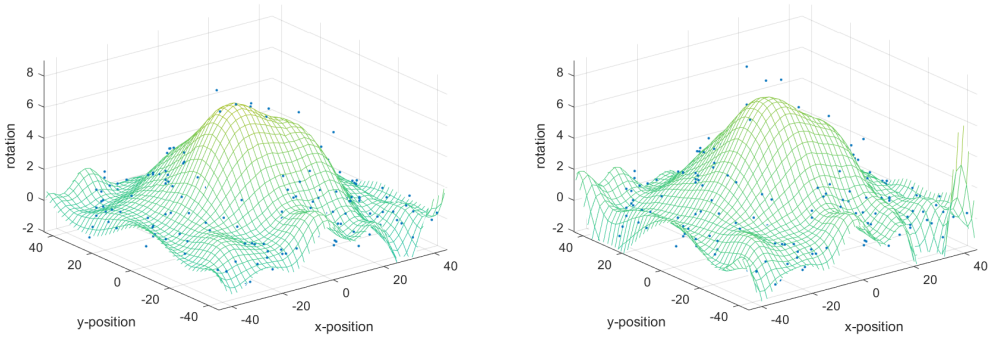

(a) Rotation Method 1

(b) Rotation Method 2

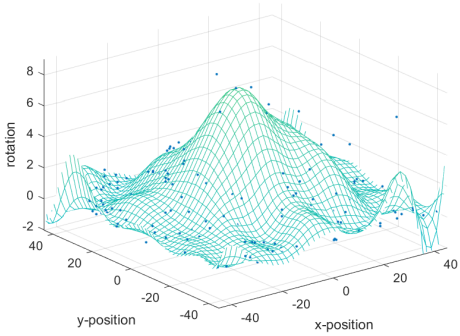

(c) Rotation Method 3

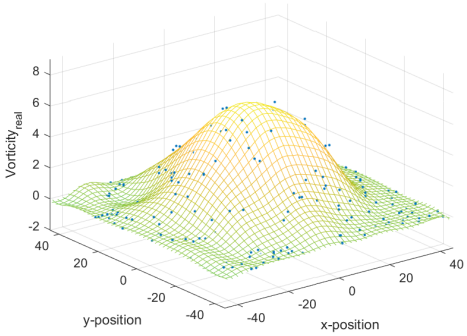

(d) Analytical Vorticity

Figure A.5: 0th level regressive fit for 400 data points, Dataset Number 4, and Noise level 0.1

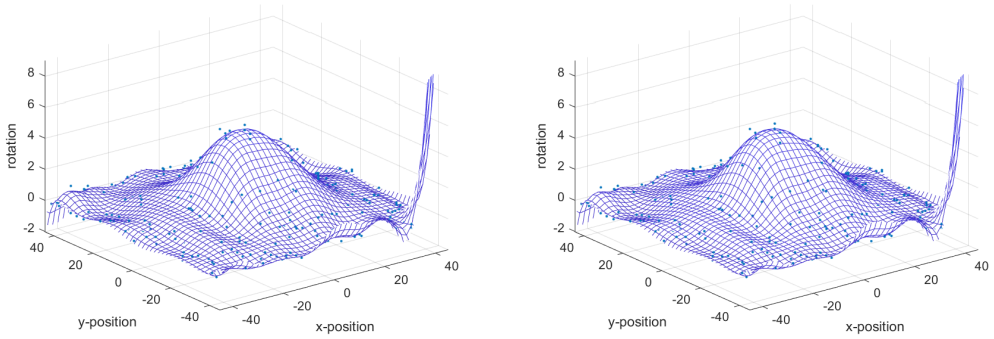

(a) Rotation Method 1

(b) Rotation Method 2

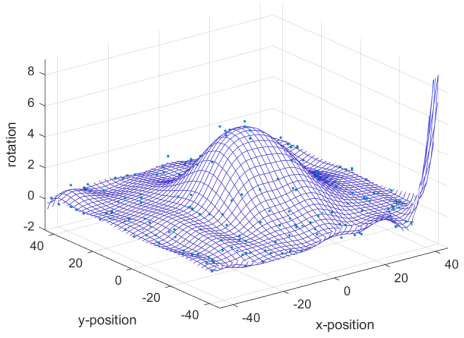

(c) Rotation Method 3

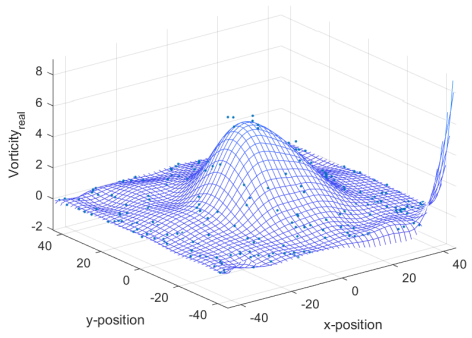

(d) Analytical Vorticity

Figure A.6: 0th level regressive fit for 400 data points, Dataset Number 7, and Noise level 0.1

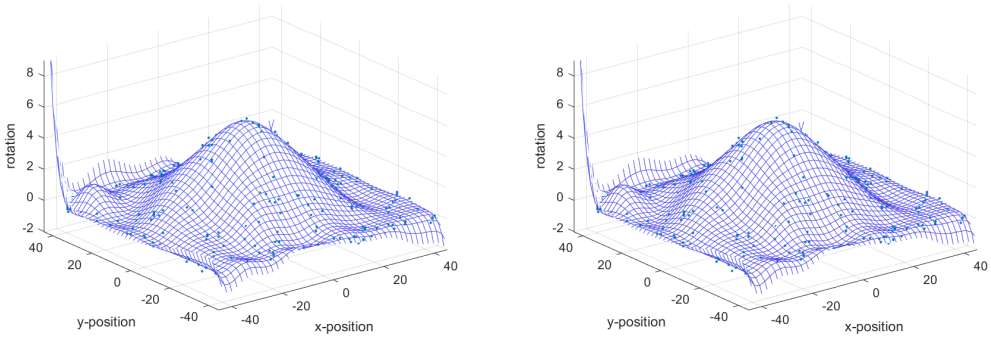

(a) Rotation Method 1

(b) Rotation Method 2

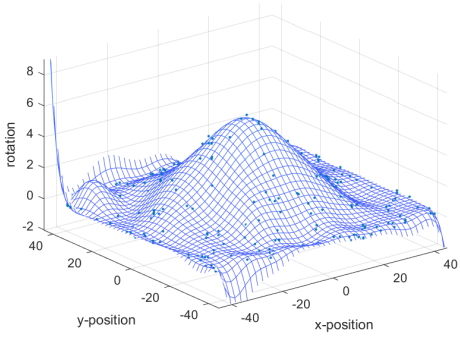

(c) Rotation Method 3

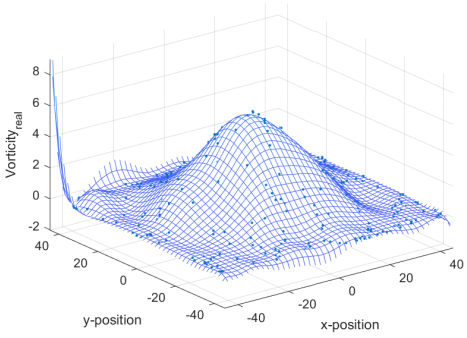

(d) Analytical Vorticity

Figure A.7: 0th level regressive fit for 400 data points, Dataset Number 10, and Noise level 0.1

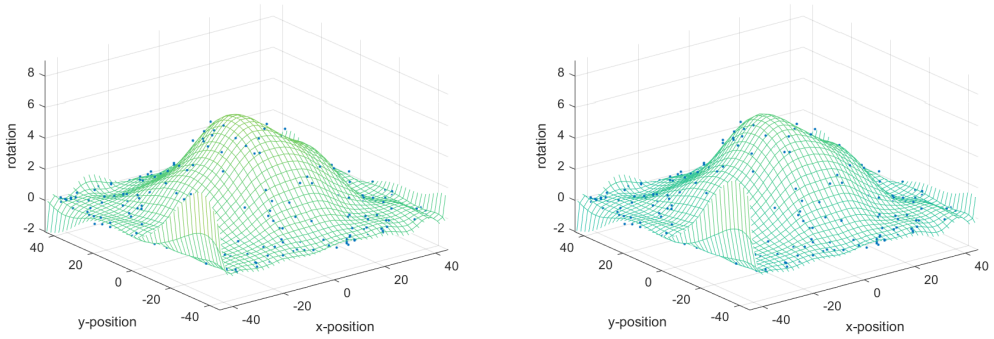

(a) Rotation Method 1

(b) Rotation Method 2

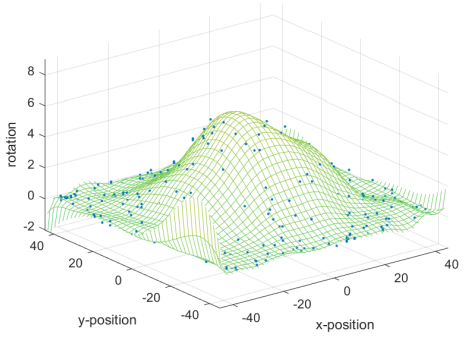

(c) Rotation Method 3

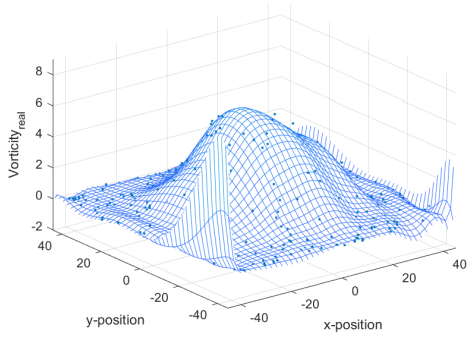

(d) Analytical Vorticity

Figure A.8: 0th level regressive fit for 400 data points, Dataset Number 13, and Noise level 0.1

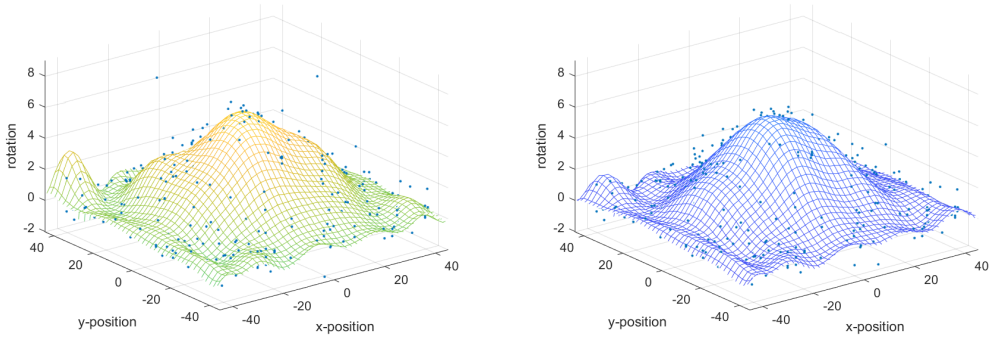

(a) Rotation Method 1

(b) Rotation Method 2

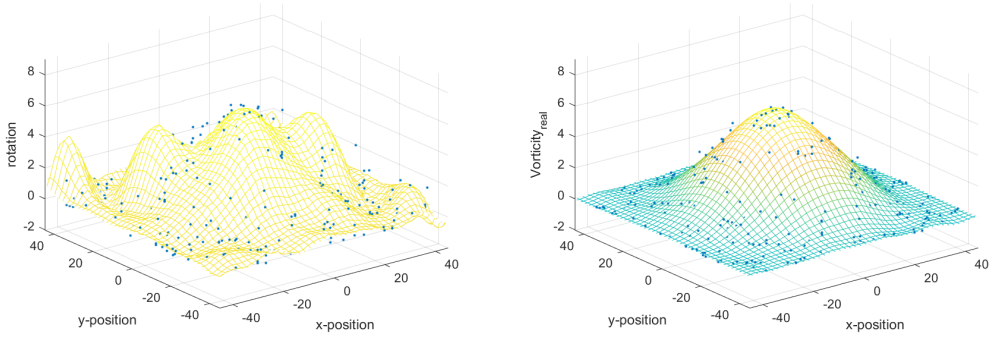

(c) Rotation Method 3

(d) Analytical Vorticity

Figure A.9: 0th level regressive fit for 600 data points, Dataset Number 4, and Noise level 0.1

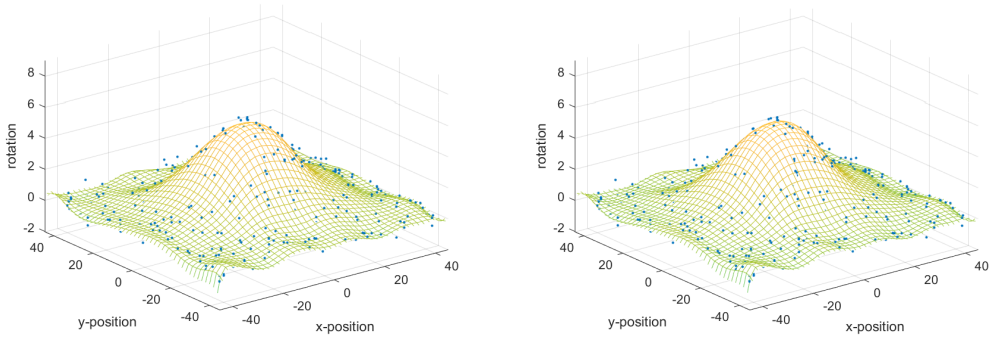

(a) Rotation Method 1

(b) Rotation Method 2

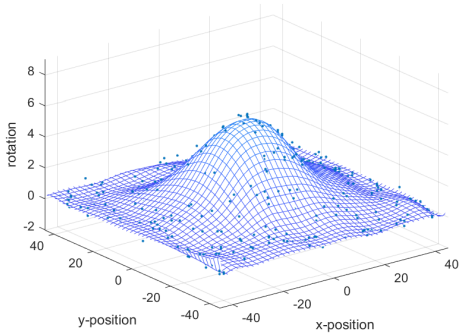

(c) Rotation Method 3

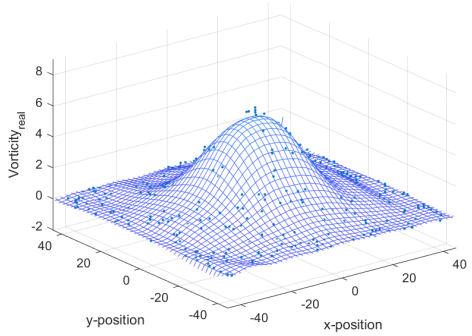

(d) Analytical Vorticity

Figure A.10: 0th level regressive fit for 600 data points, Dataset Number 7, and Noise level 0.1

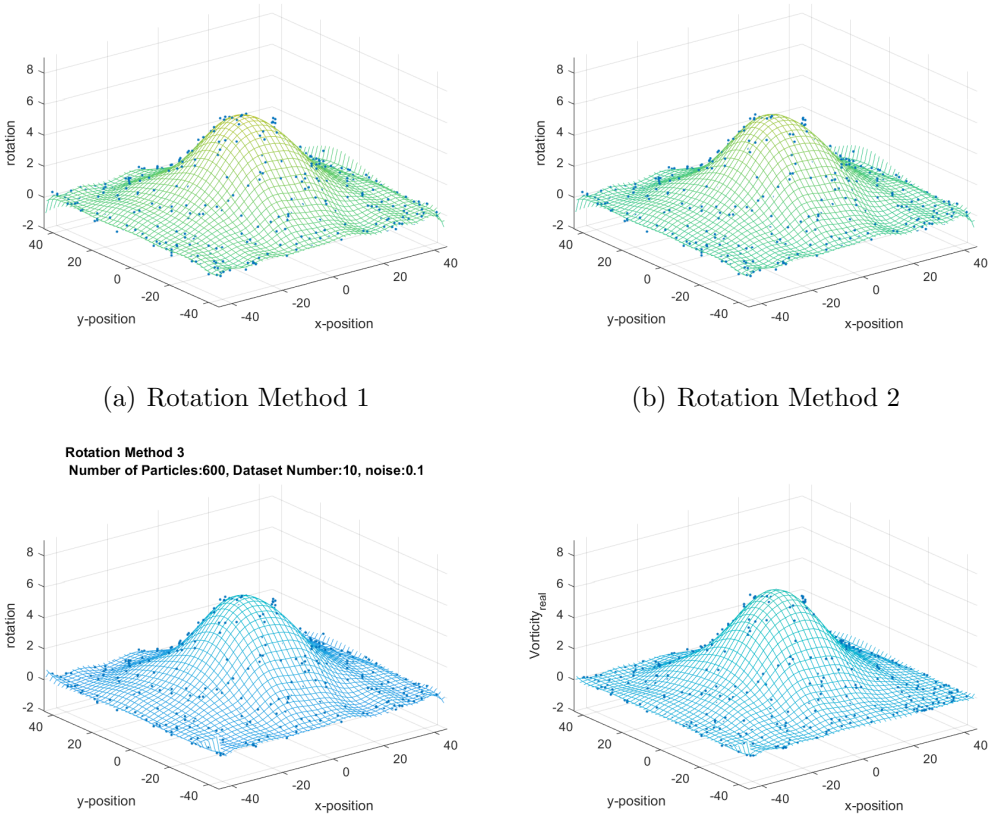

(a) Rotation Method 1

(b) Rotation Method 2

(c) Rotation Method 3

(d) Analytical Vorticity

Figure A.11: 0th level regressive fit for 600 data points, Dataset Number 10, and Noise level 0.1

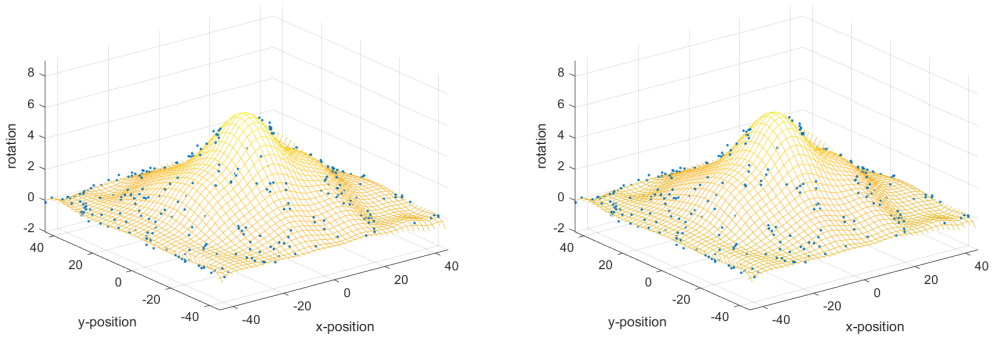

(a) Rotation Method 1

(b) Rotation Method 2

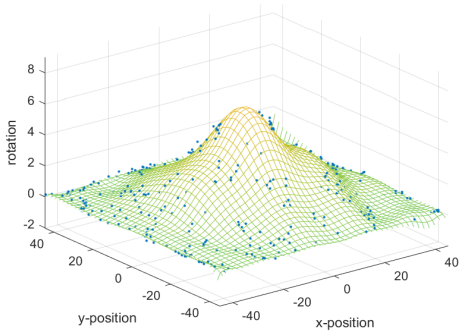

(c) Rotation Method 3

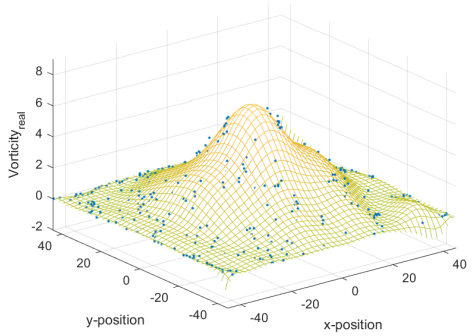

(d) Analytical Vorticity

Figure A.12: 0th level regressive fit for 600 data points, Dataset Number 13, and Noise level 0.1

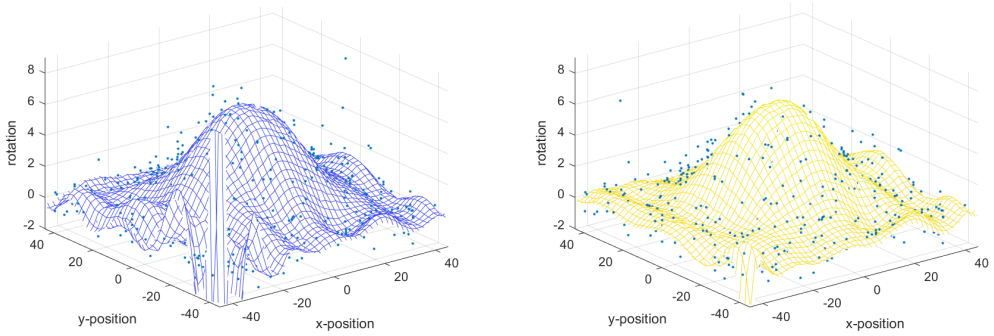

(a) Rotation Method 1

(b) Rotation Method 2

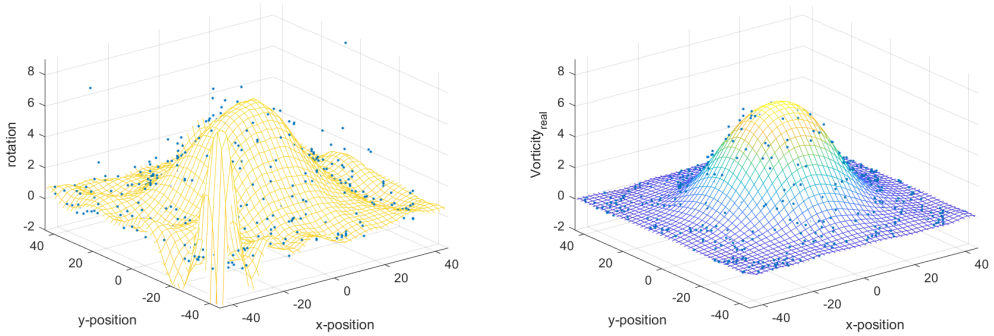

(c) Rotation Method 3

(d) Analytical Vorticity

Figure A.13: 0th level regressive fit for 800 data points, Dataset Number 4, and Noise level 0.1

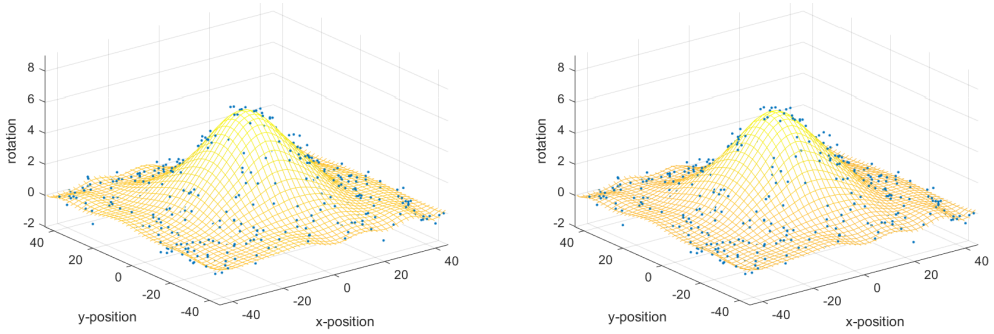

(a) Rotation Method 1

(b) Rotation Method 2

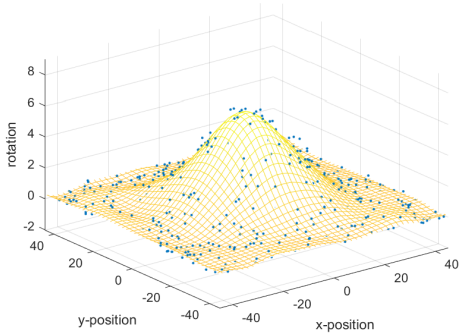

(c) Rotation Method 3

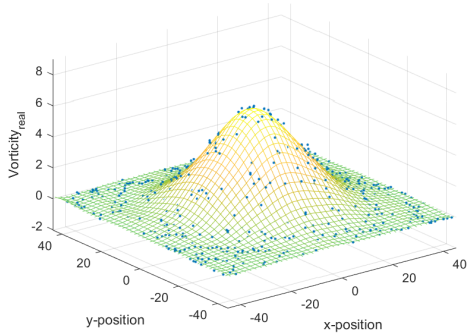

(d) Analytical Vorticity

Figure A.14: 0th level regressive fit for 800 data points, Dataset Number 7, and Noise level 0.1

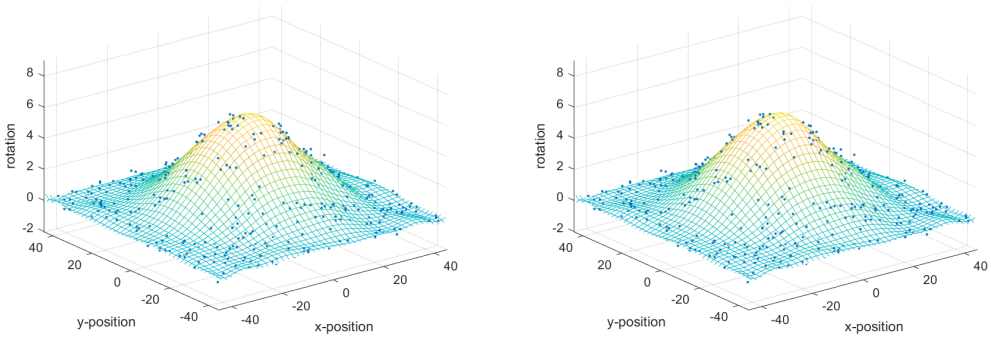

(a) Rotation Method 1

(b) Rotation Method 2

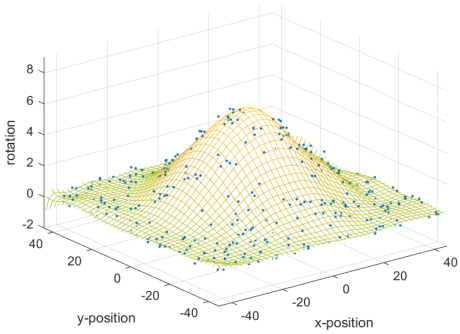

(c) Rotation Method 3

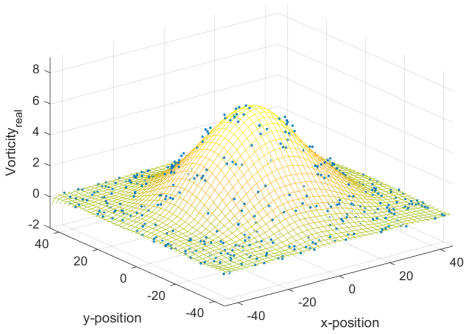

(d) Analytical Vorticity

Figure A.15: 0th level regressive fit for 800 data points, Dataset Number 10, and Noise level 0.1

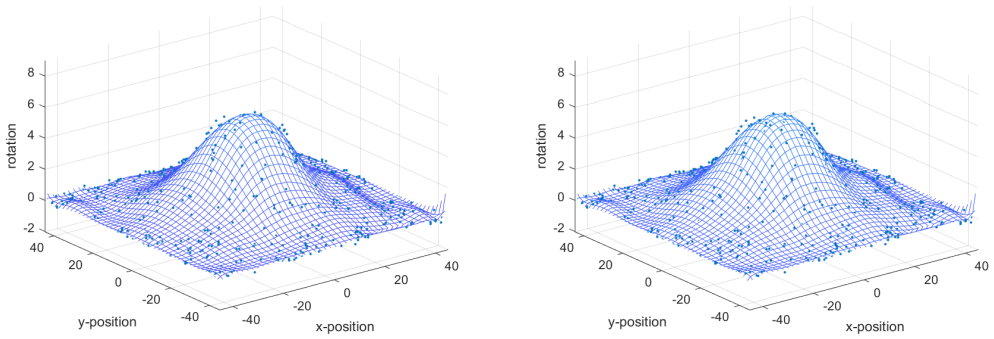

(a) Rotation Method 1

(b) Rotation Method 2

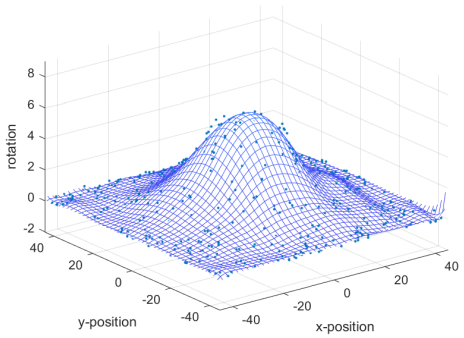

(c) Rotation Method 3

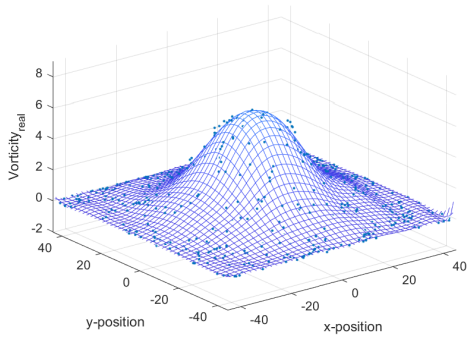

(d) Analytical Vorticity

Figure A.16: 0th level regressive fit for 800 data points, Dataset Number 13, and Noise level 0.1

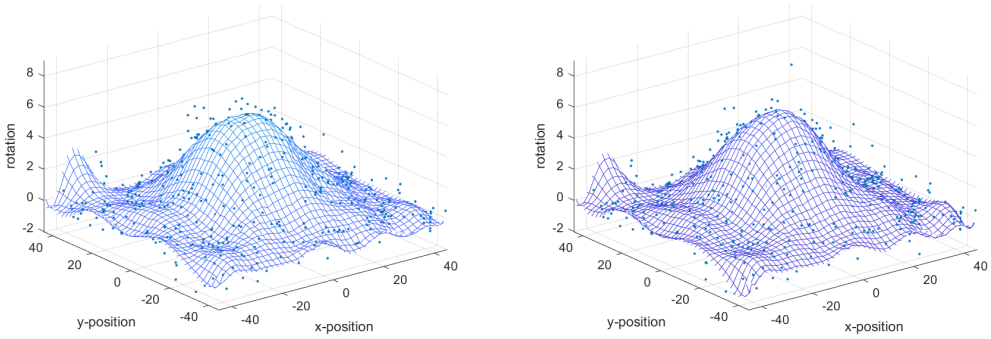

(a) Rotation Method 1

(b) Rotation Method 2

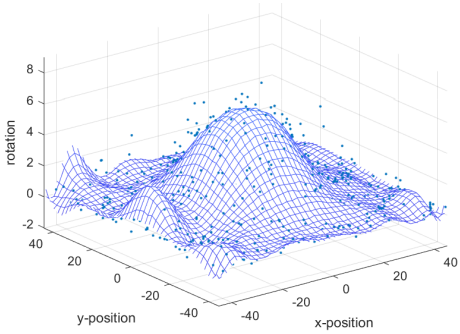

(c) Rotation Method 3

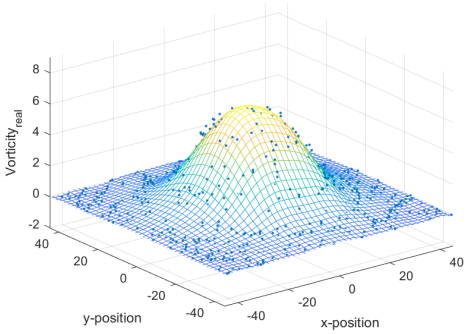

(d) Analytical Vorticity

Figure A.17: 0th level regressive fit for 1000 data points, Dataset Number 4, and Noise level 0.1

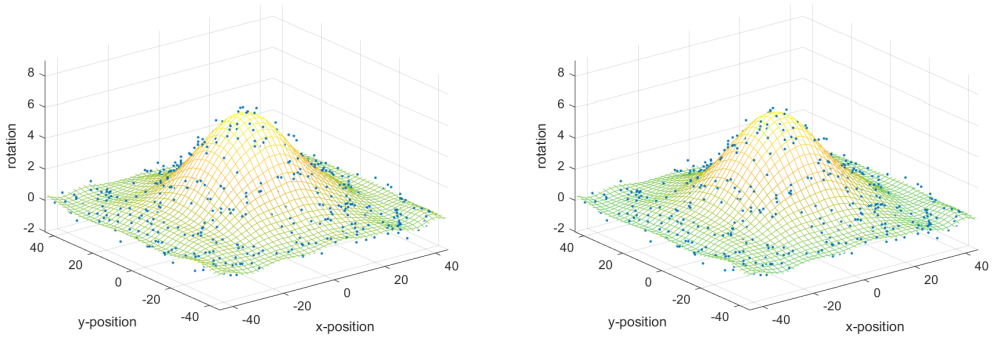

(a) Rotation Method 1

(b) Rotation Method 2

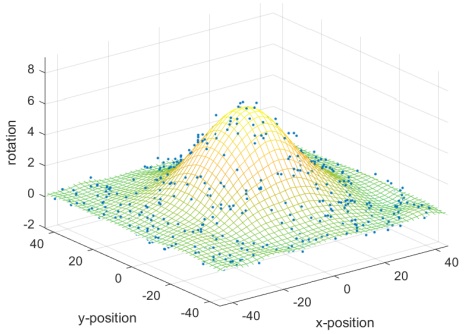

(c) Rotation Method 3

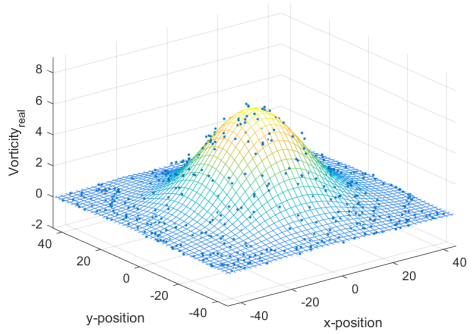

(d) Analytical Vorticity

Figure A.18: 0th level regressive fit for 1000 data points, Dataset Number 7, and Noise level 0.1

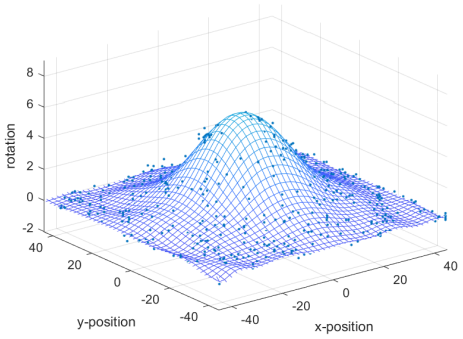

(a) Rotation Method 1

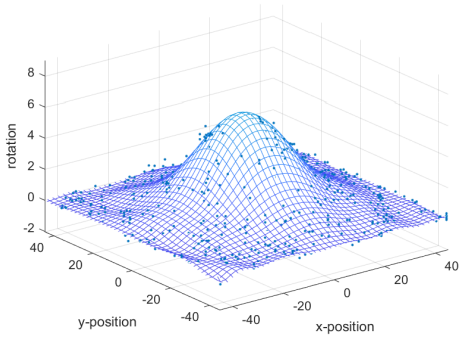

(b) Rotation Method 2

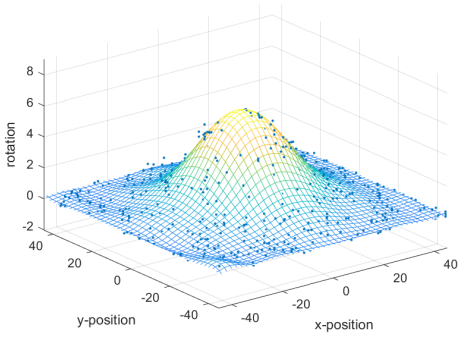

(c) Rotation Method 3

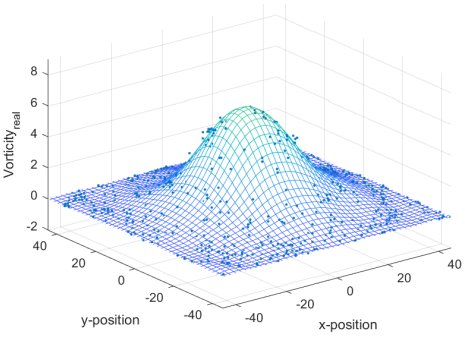

(d) Analytical Vorticity

Figure A.19: 0th level regressive fit for 1000 data points, Dataset Number 10, and Noise level 0.1

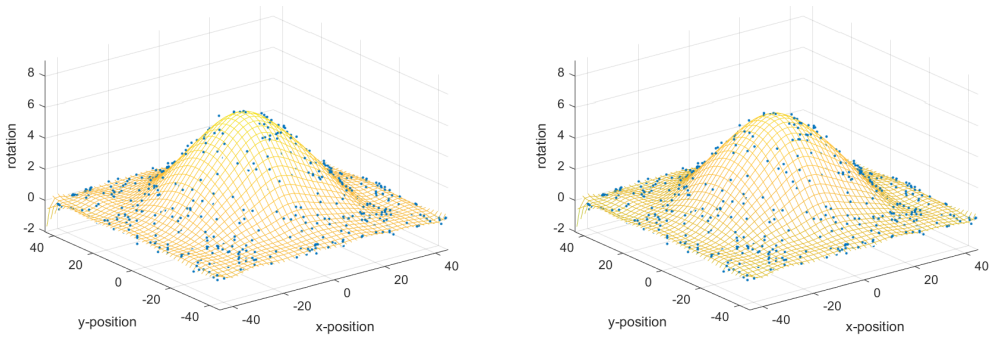

(a) Rotation Method 1

(b) Rotation Method 2

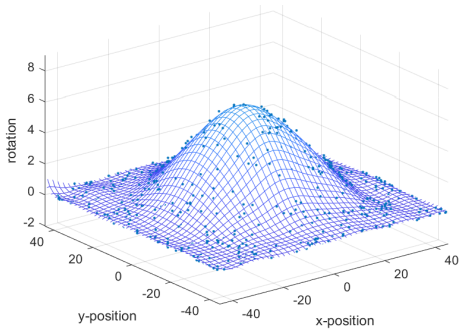

(c) Rotation Method 3

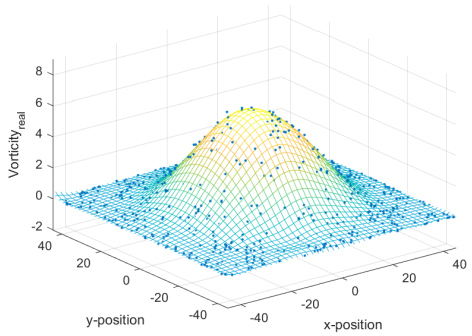

(d) Analytical Vorticity

Figure A.20: 0th level regressive fit for 1000 data points, Dataset Number 13, and Noise level 0.1

A.1.2 1st Level Regressive Fit

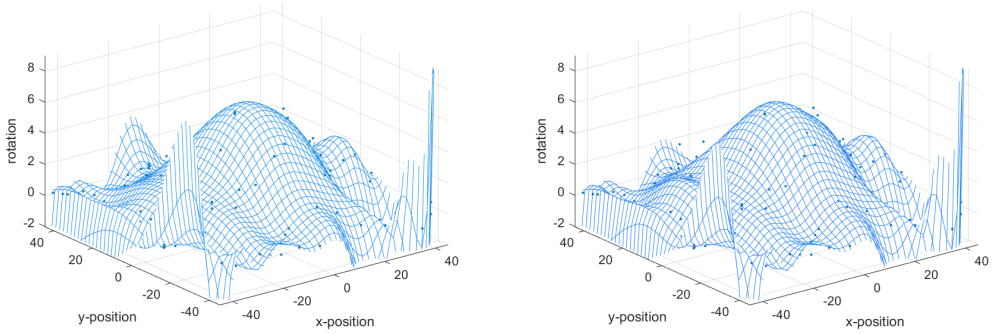

(a) Rotation Method 1

(b) Rotation Method 2

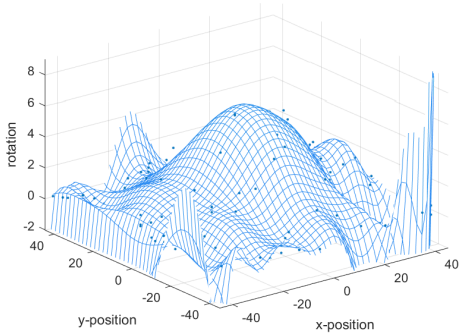

(c) Rotation Method 3

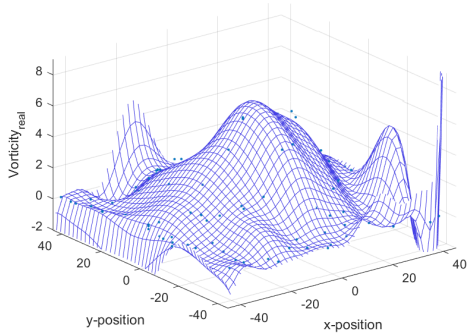

(d) Analytical Vorticity

Figure A.21: 1st level regressive fit for 200 data points, Dataset Number 4, and Noise level 0.1

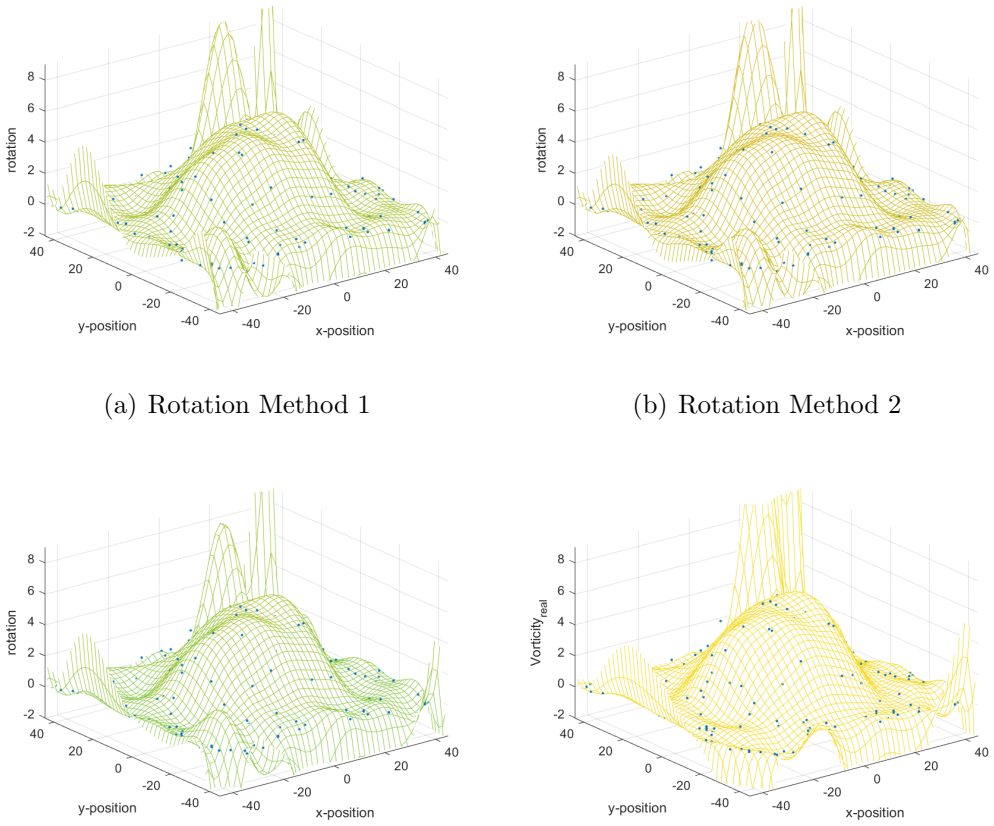

(a) Rotation Method 1

(b) Rotation Method 2

(c) Rotation Method 3

(d) Analytical Vorticity

Figure A.22: 1st level regressive fit for 200 data points, Dataset Number 7, and Noise level 0.1

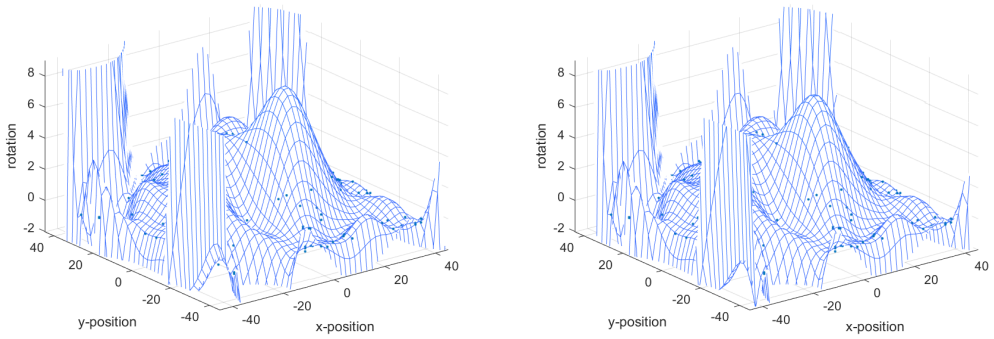

(a) Rotation Method 1

(b) Rotation Method 2

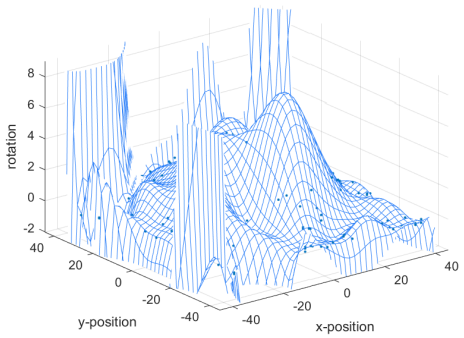

(c) Rotation Method 3

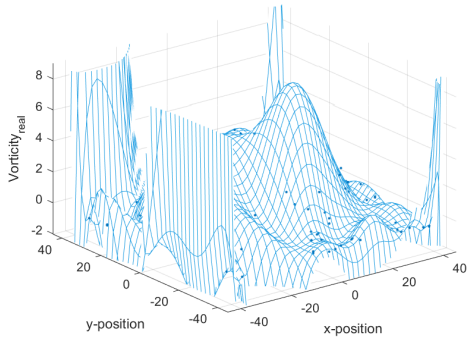

(d) Analytical Vorticity

Figure A.23: 1st level regressive fit for 200 data points, Dataset Number 10, and Noise level 0.1

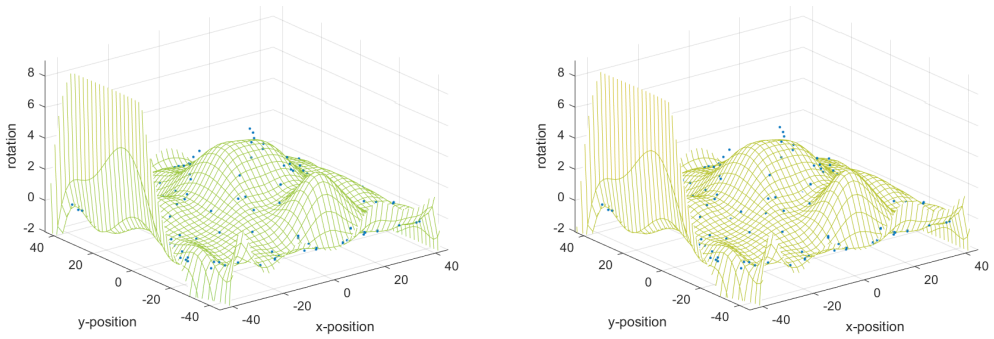

(a) Rotation Method 1

(b) Rotation Method 2

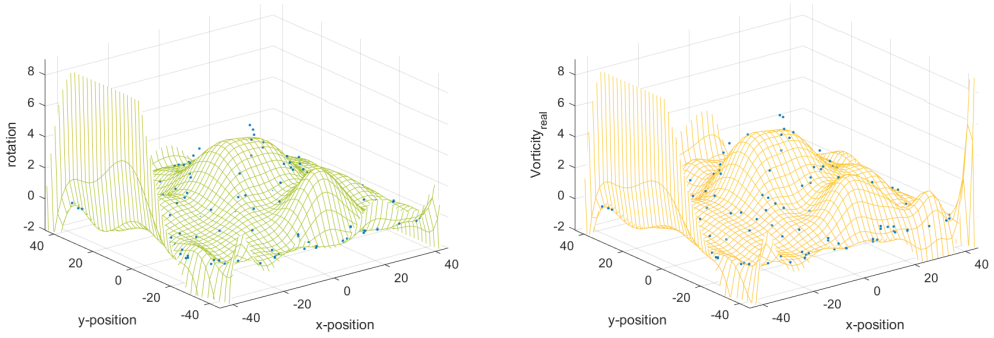

(c) Rotation Method 3

(d) Analytical Vorticity

Figure A.24: 1st level regressive fit for 200 data points, Dataset Number 13, and Noise level 0.1

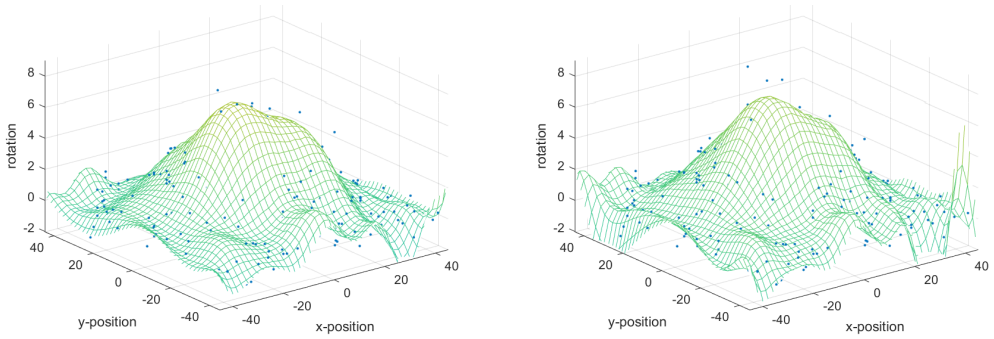

(a) Rotation Method 1

(b) Rotation Method 2

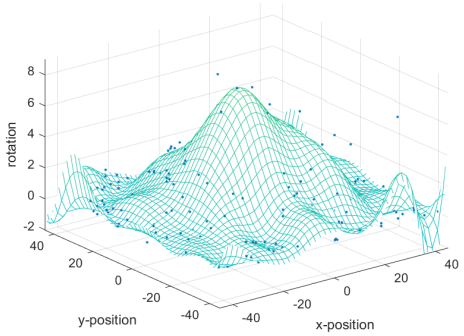

(c) Rotation Method 3

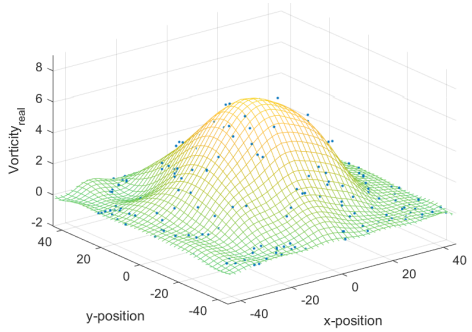

(d) Analytical Vorticity

Figure A.25: 1st level regressive fit for 400 data points, Dataset Number 4, and Noise level 0.1

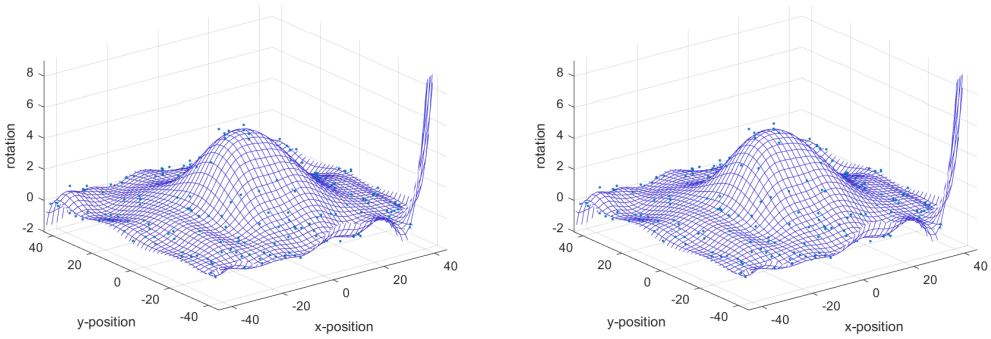

(a) Rotation Method 1

(b) Rotation Method 2

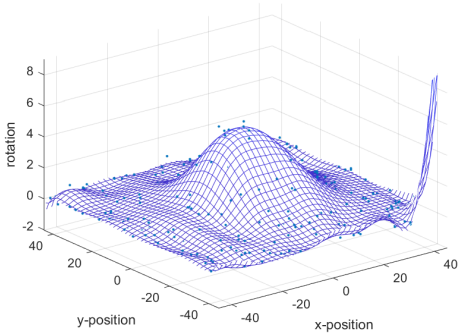

(c) Rotation Method 3

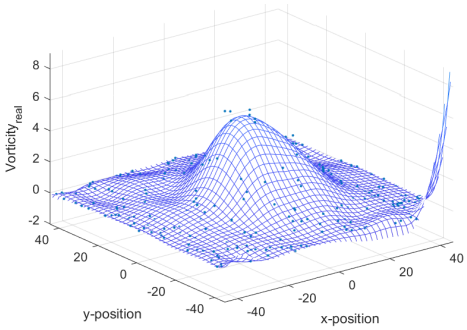

(d) Analytical Vorticity

Figure A.26: 1st level regressive fit for 400 data points, Dataset Number 7, and Noise level 0.1

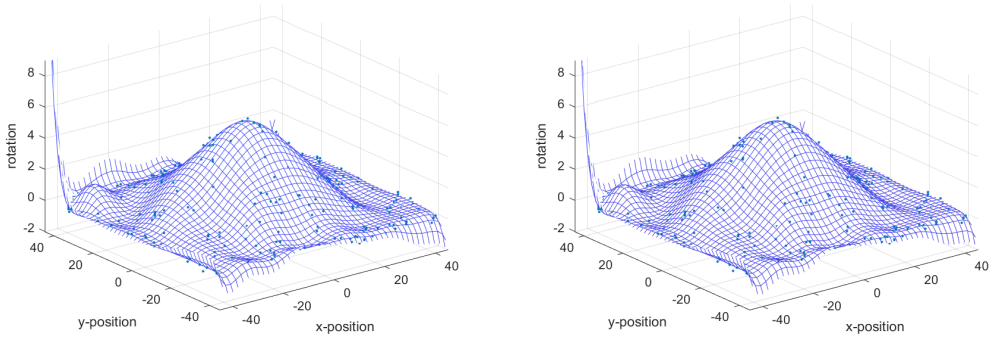

(a) Rotation Method 1

(b) Rotation Method 2

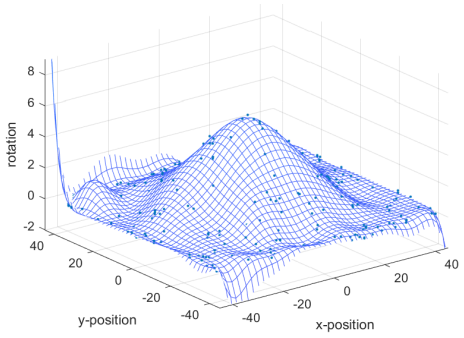

(c) Rotation Method 3

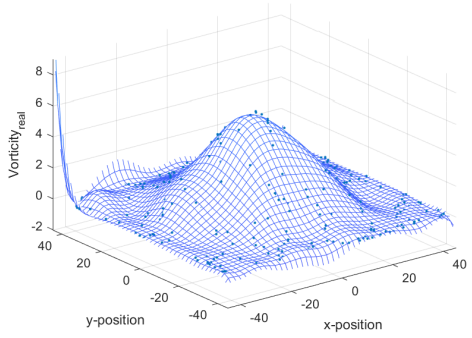

(d) Analytical Vorticity

Figure A.27: 1st level regressive fit for 400 data points, Dataset Number 10, and Noise level 0.1

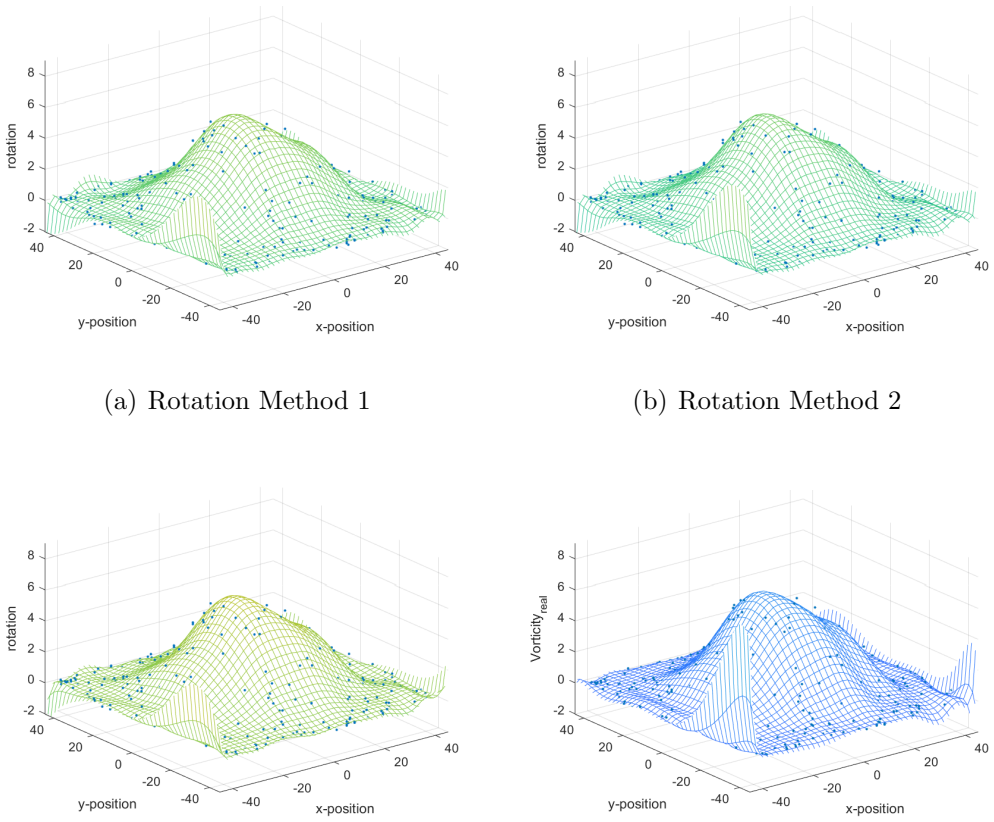

(a) Rotation Method 1

(b) Rotation Method 2

(c) Rotation Method 3

(d) Analytical Vorticity

Figure A.28: 1st level regressive fit for 400 data points, Dataset Number 13, and Noise level 0.1

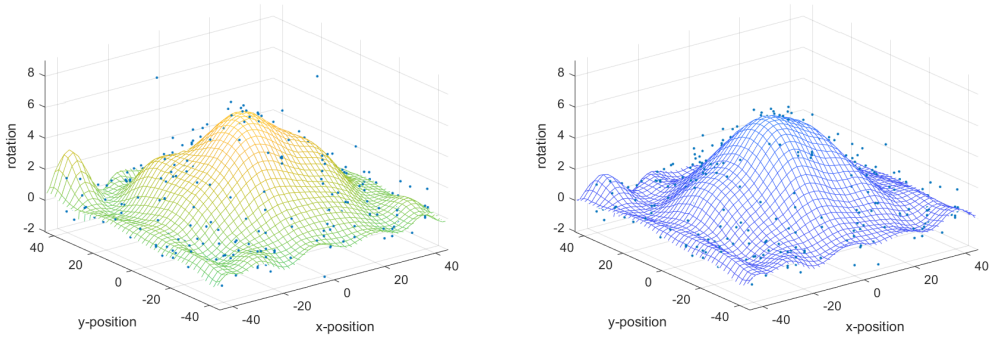

(a) Rotation Method 1

(b) Rotation Method 2

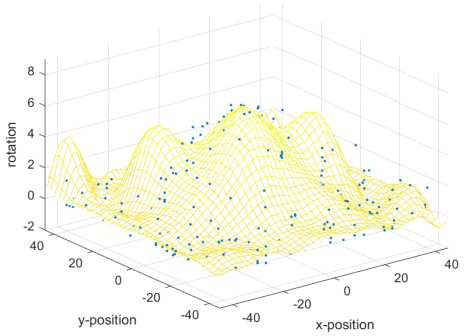

(c) Rotation Method 3

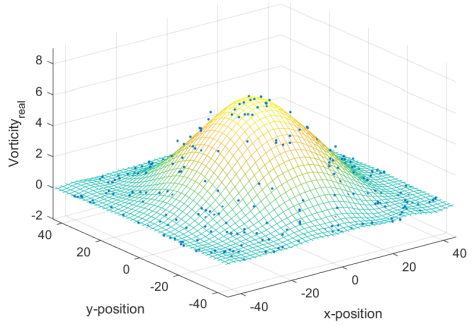

(d) Analytical Vorticity

Figure A.29: 1st level regressive fit for 600 data points, Dataset Number 4, and Noise level 0.1

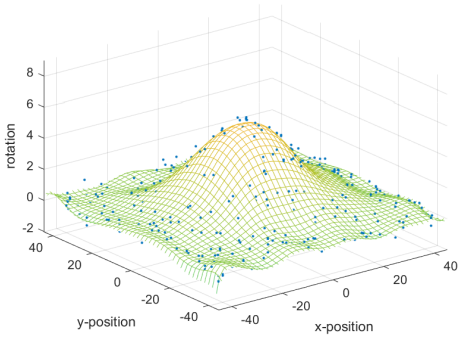

(a) Rotation Method 1

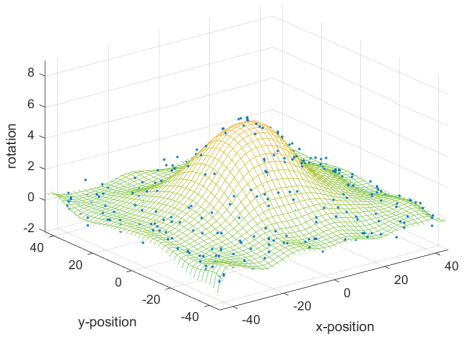

(b) Rotation Method 2

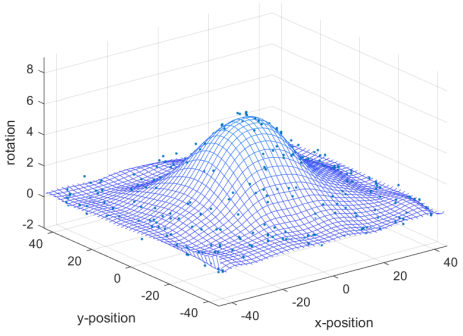

(c) Rotation Method 3

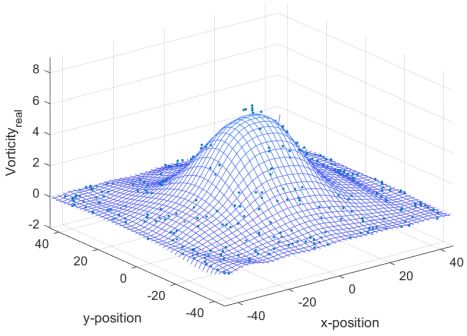

(d) Analytical Vorticity

Figure A.30: 1st level regressive fit for 600 data points, Dataset Number 7, and Noise level 0.1

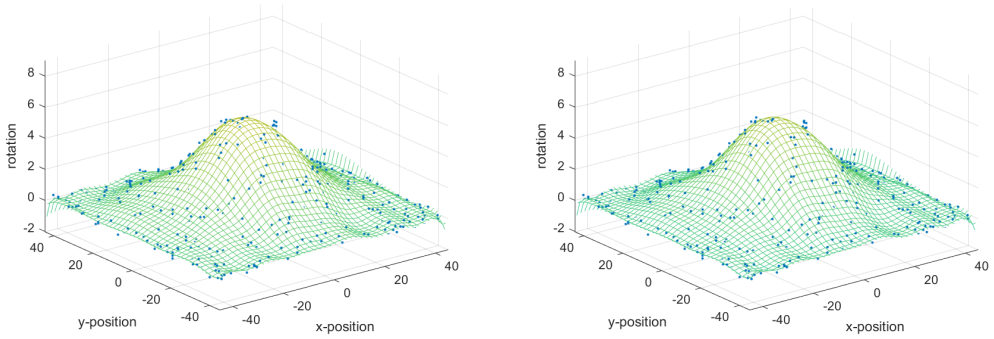

(a) Rotation Method 1

(b) Rotation Method 2

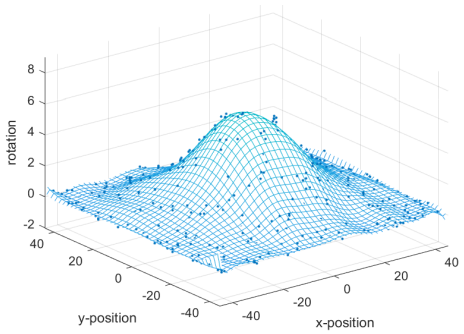

(c) Rotation Method 3

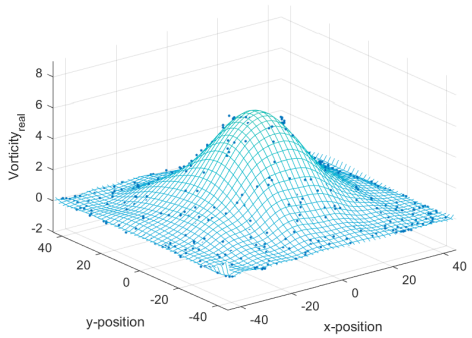

(d) Analytical Vorticity

Figure A.31: 1st level regressive fit for 600 data points, Dataset Number 10, and Noise level 0.1

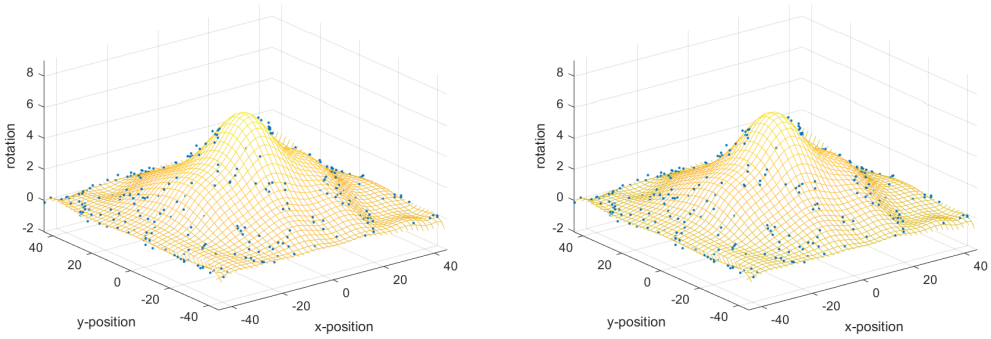

(a) Rotation Method 1

(b) Rotation Method 2

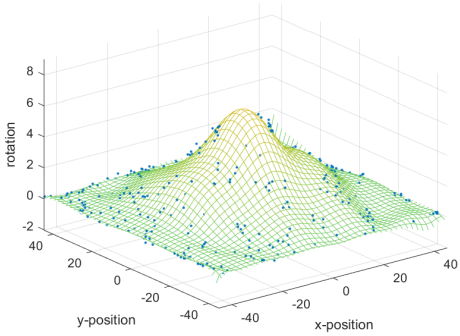

(c) Rotation Method 3

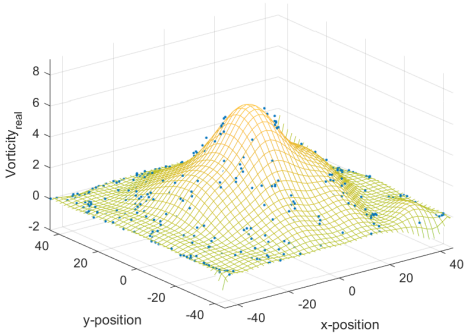

(d) Analytical Vorticity

Figure A.32: 1st level regressive fit for 600 data points, Dataset Number 13, and Noise level 0.1

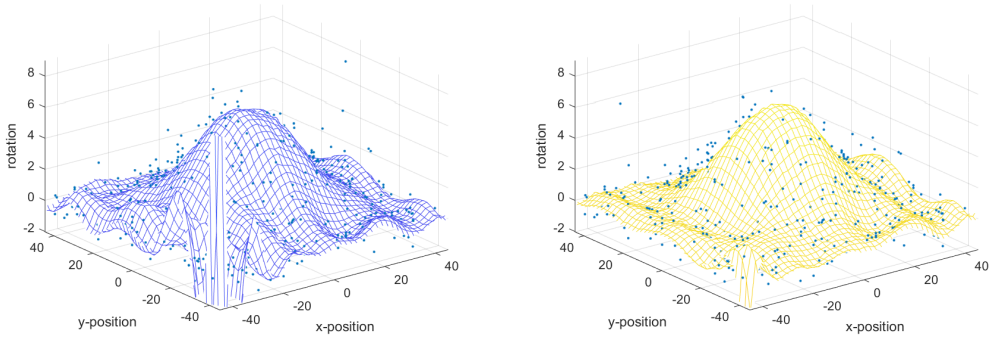

(a) Rotation Method 1

(b) Rotation Method 2

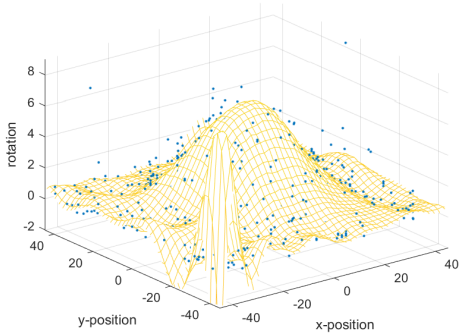

(c) Rotation Method 3

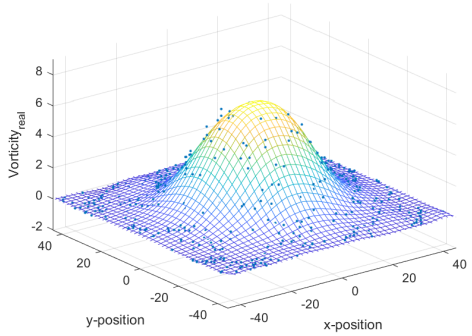

(d) Analytical Vorticity

Figure A.33: 1st level regressive fit for 800 data points, Dataset Number 4, and Noise level 0.1

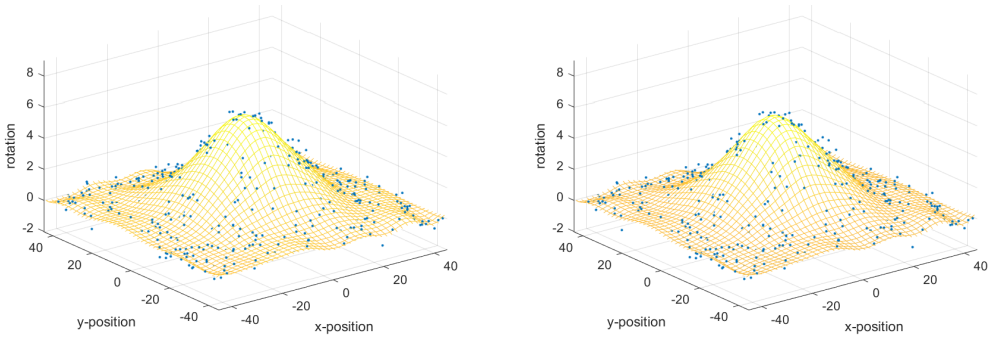

(a) Rotation Method 1

(b) Rotation Method 2

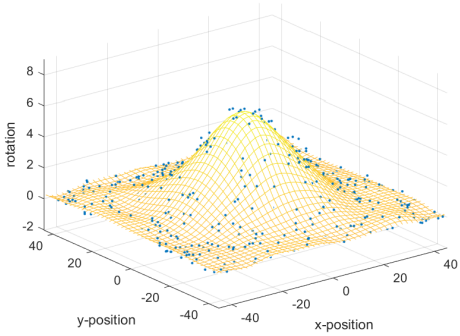

(c) Rotation Method 3

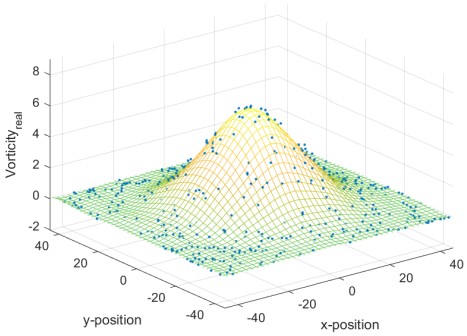

(d) Analytical Vorticity

Figure A.34: 1st level regressive fit for 800 data points, Dataset Number 7, and Noise level 0.1

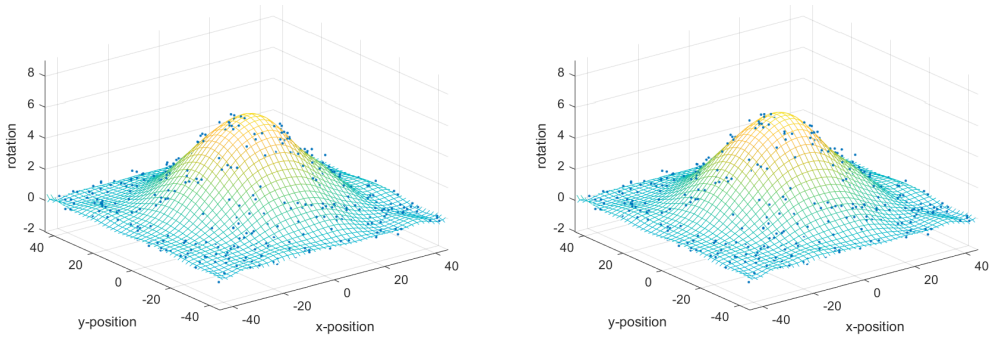

(a) Rotation Method 1

(b) Rotation Method 2

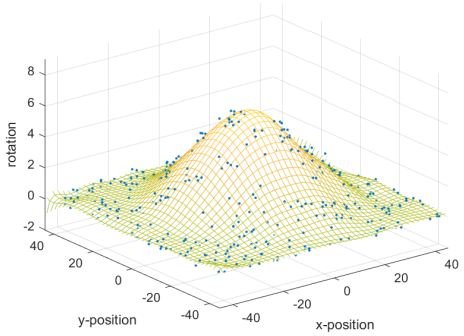

(c) Rotation Method 3

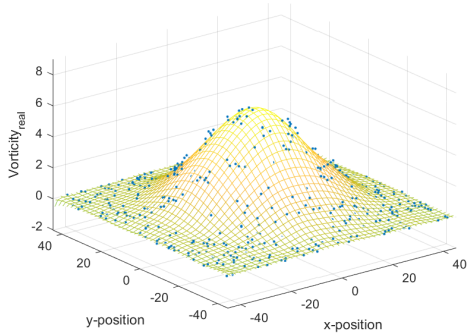

(d) Analytical Vorticity

Figure A.35: 1st level regressive fit for 800 data points, Dataset Number 10, and Noise level 0.1

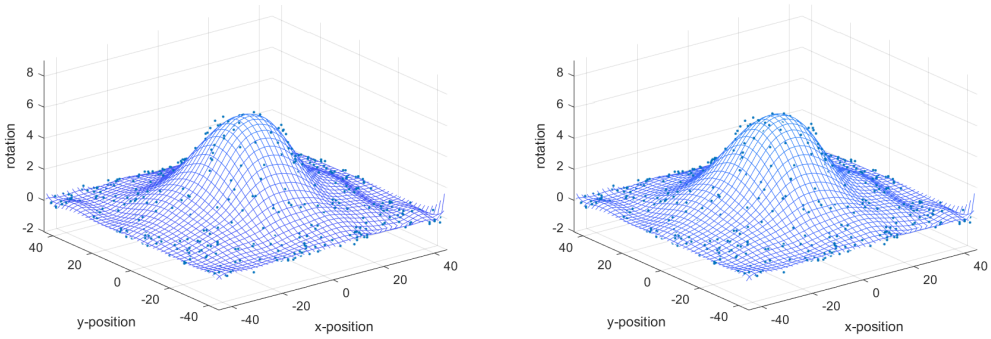

(a) Rotation Method 1

(b) Rotation Method 2

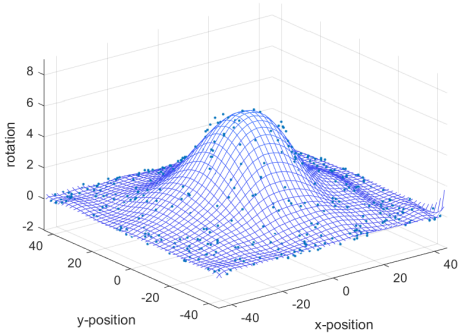

(c) Rotation Method 3

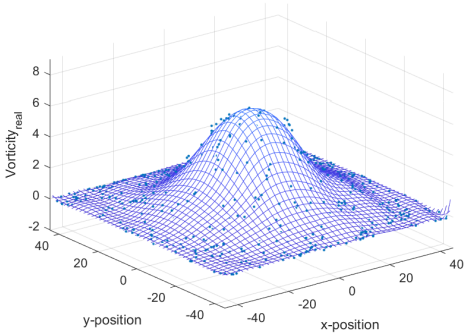

(d) Analytical Vorticity

Figure A.36: 1st level regressive fit for 800 data points, Dataset Number 13, and Noise level 0.1

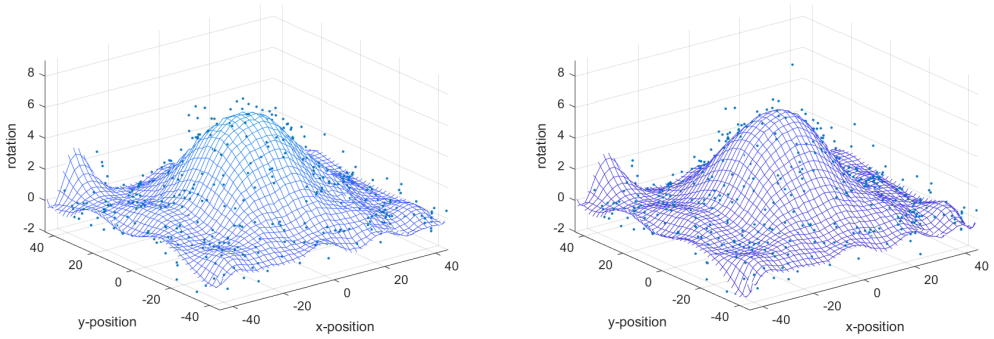

(a) Rotation Method 1

(b) Rotation Method 2

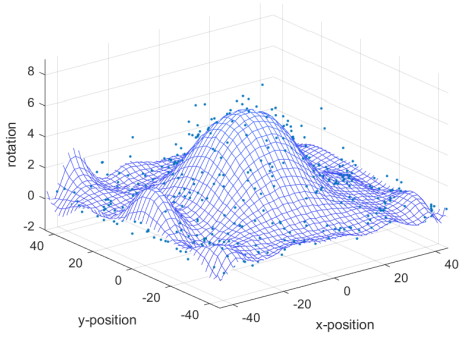

(c) Rotation Method 3

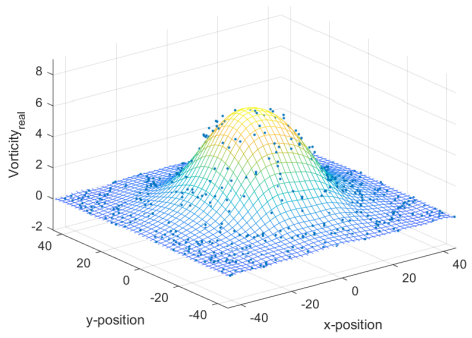

(d) Analytical Vorticity

Figure A.37: 1st level regressive fit for 1000 data points, Dataset Number 4, and Noise level 0.1

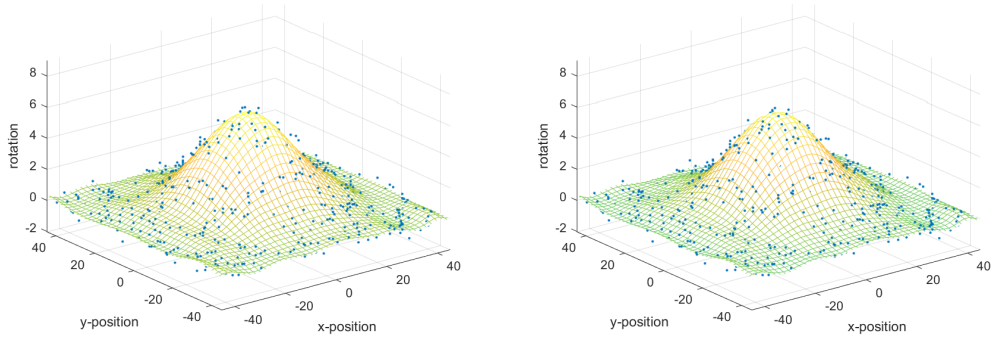

(a) Rotation Method 1

(b) Rotation Method 2

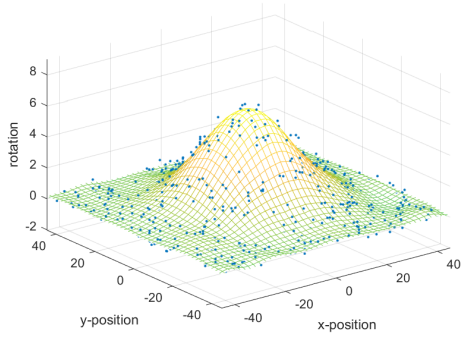

(c) Rotation Method 3

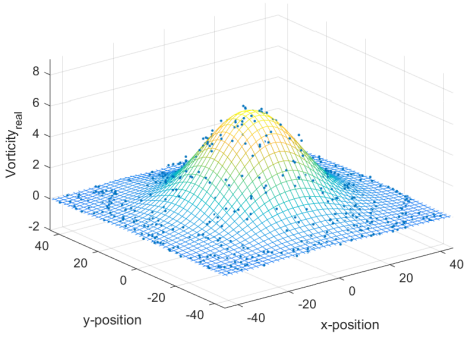

(d) Analytical Vorticity

Figure A.38: 1st level regressive fit for 1000 data points, Dataset Number 7, and Noise level 0.1

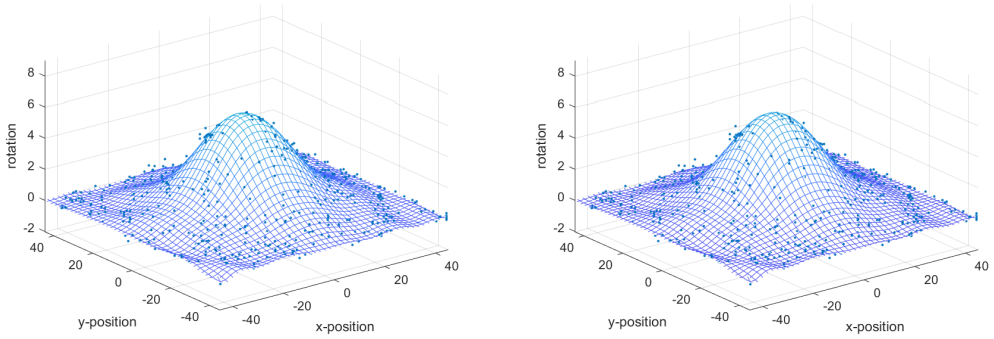

(a) Rotation Method 1

(b) Rotation Method 2

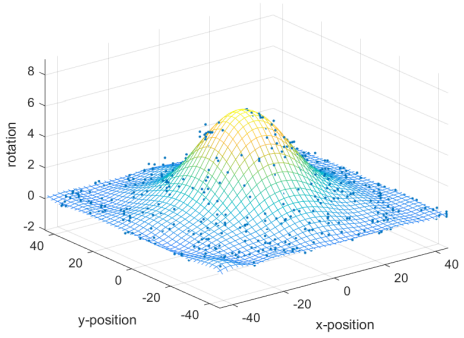

(c) Rotation Method 3

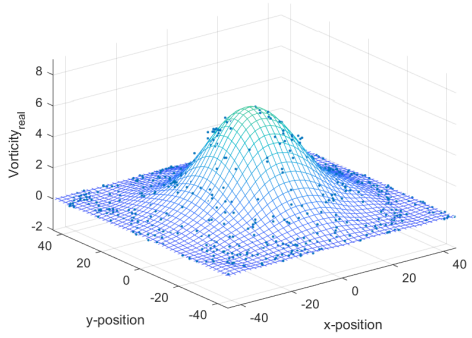

(d) Analytical Vorticity

Figure A.39: 1st level regressive fit for 1000 data points, Dataset Number 10, and Noise level 0.1

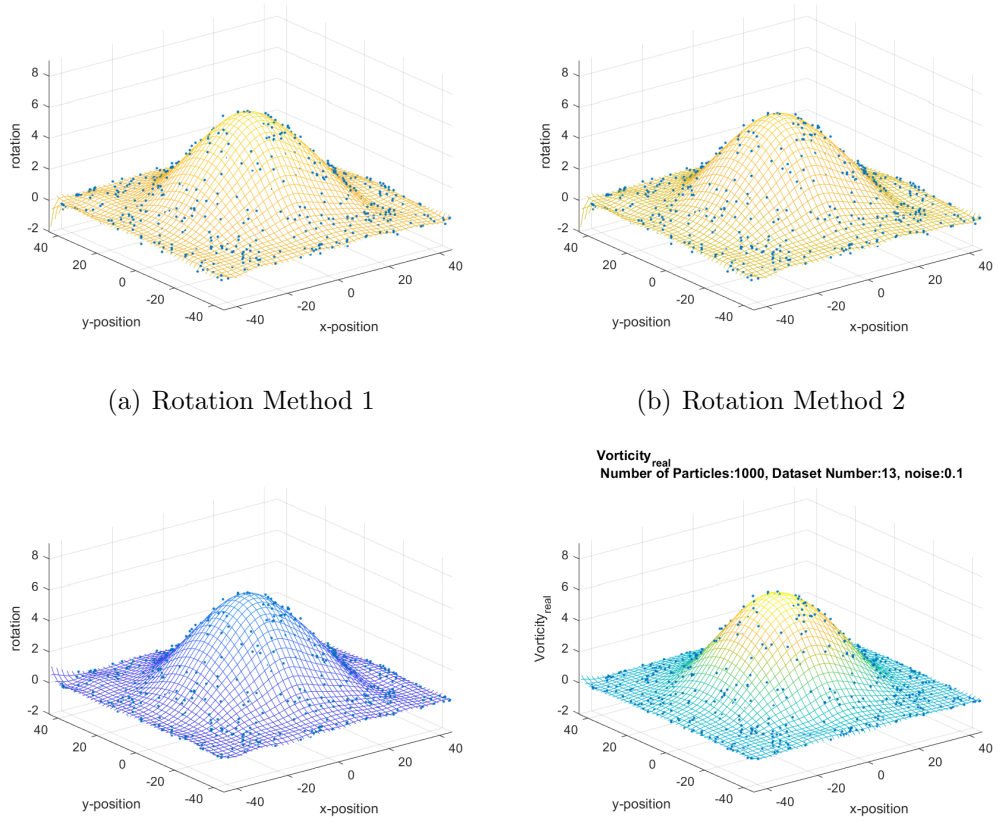

(a) Rotation Method 1

(b) Rotation Method 2

(c) Rotation Method 3

(d) Analytical Vorticity

Figure A.40: 1st level regressive fit for 1000 data points, Dataset Number 13, and Noise level 0.1

A.1.3 2nd Level Regressive Fit

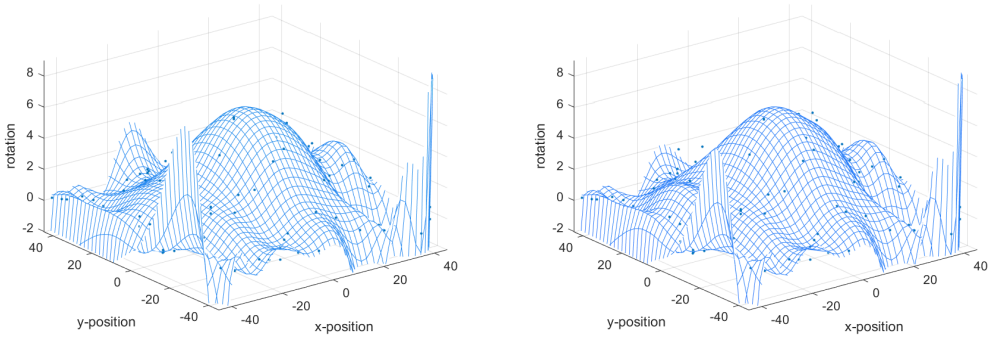

(a) Rotation Method 1

(b) Rotation Method 2

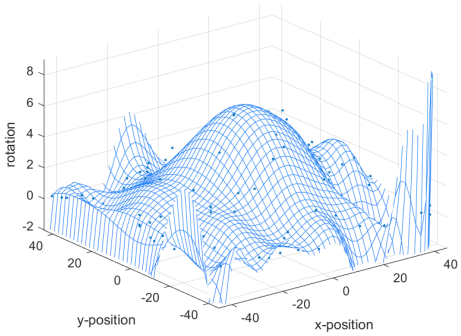

(c) Rotation Method 3

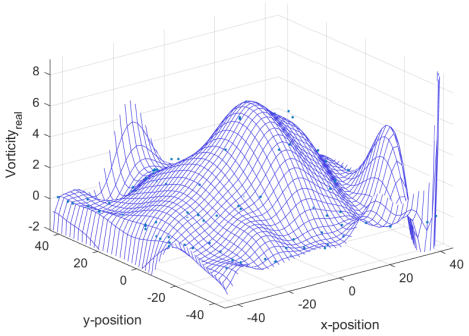

(d) Analytical Vorticity

Figure A.41: 2nd level regressive fit for 200 data points, Dataset Number 4, and Noise level 0.1

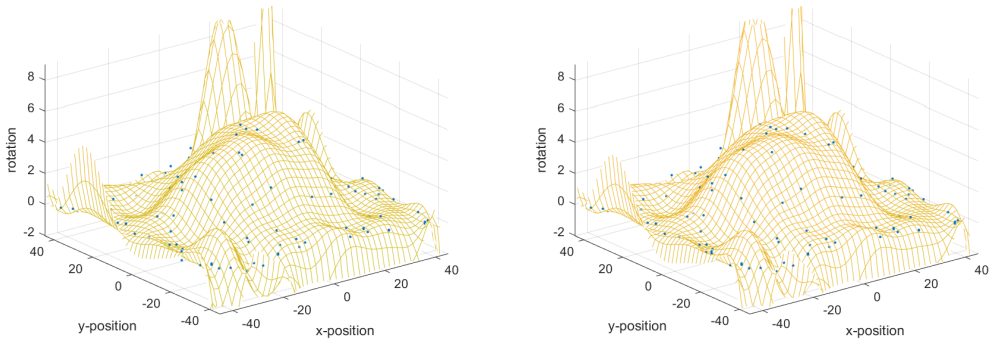

(a) Rotation Method 1

(b) Rotation Method 2

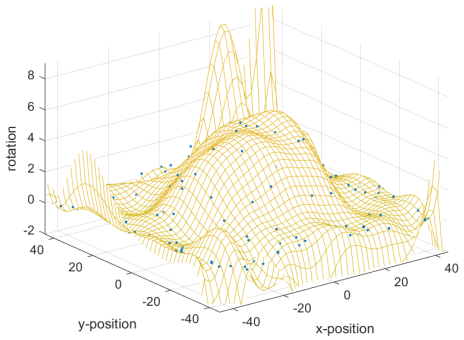

(c) Rotation Method 3

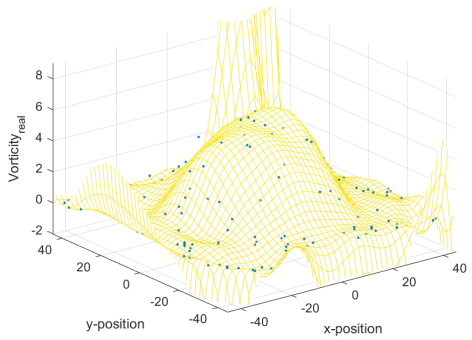

(d) Analytical Vorticity

Figure A.42: 2nd level regressive fit for 200 data points, Dataset Number 7, and Noise level 0.1

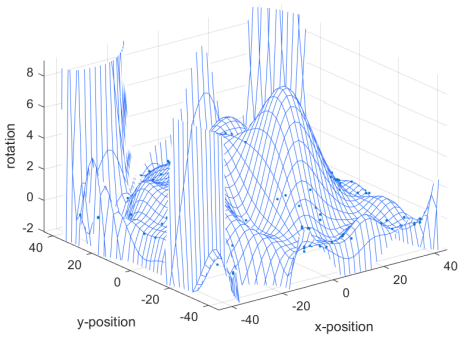

(a) Rotation Method 1

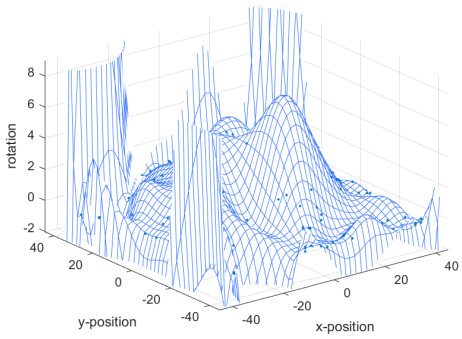

(b) Rotation Method 2

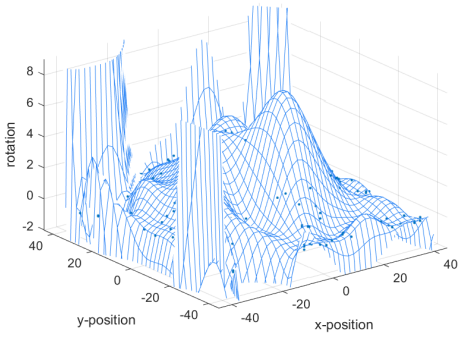

(c) Rotation Method 3

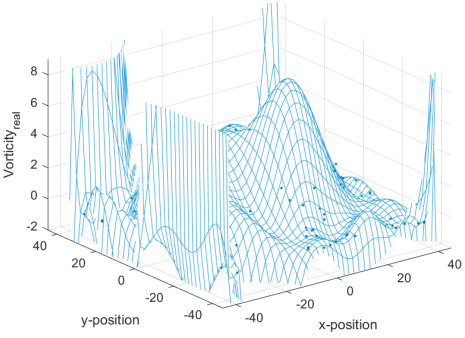

(d) Analytical Vorticity

Figure A.43: 2nd level regressive fit for 200 data points, Dataset Number 10, and Noise level 0.1

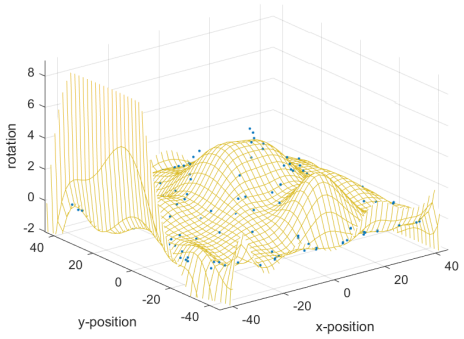

(a) Rotation Method 1

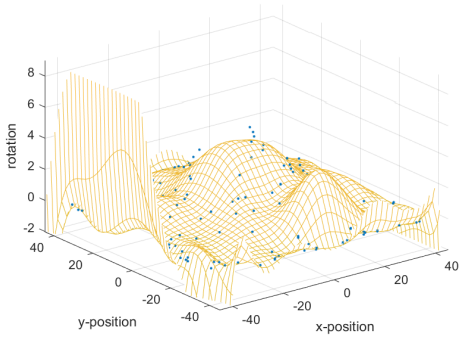

(b) Rotation Method 2

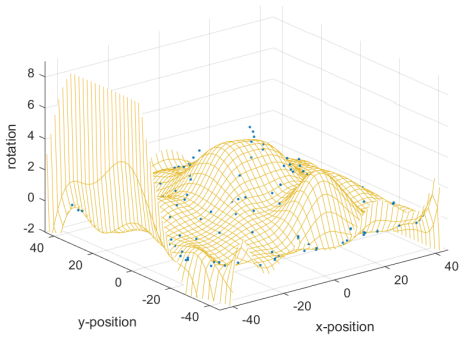

(c) Rotation Method 3

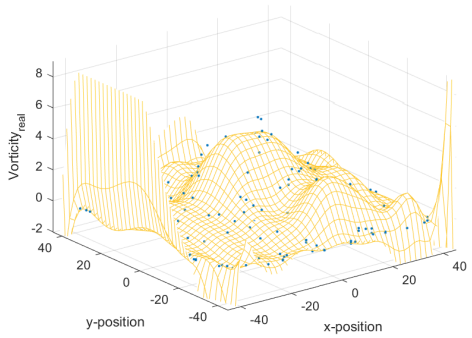

(d) Analytical Vorticity

Figure A.44: 2nd level regressive fit for 200 data points, Dataset Number 13, and Noise level 0.1

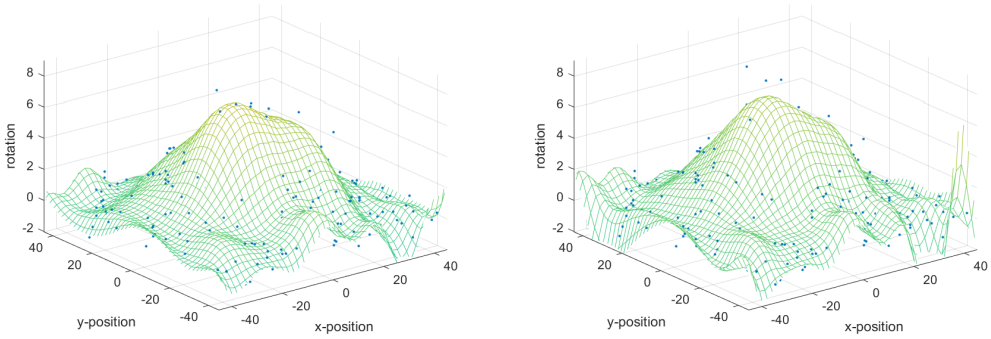

(a) Rotation Method 1

(b) Rotation Method 2

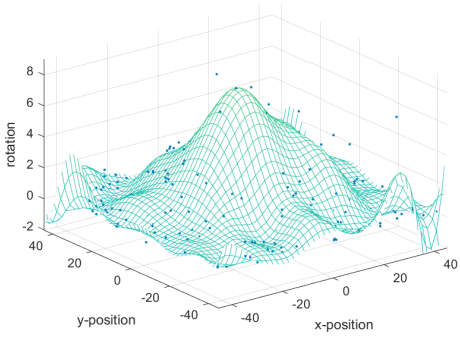

(c) Rotation Method 3

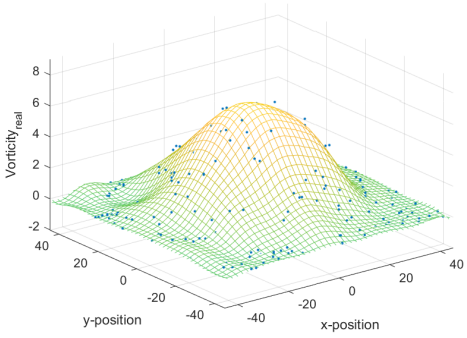

(d) Analytical Vorticity

Figure A.45: 2nd level regressive fit for 400 data points, Dataset Number 4, and Noise level 0.1

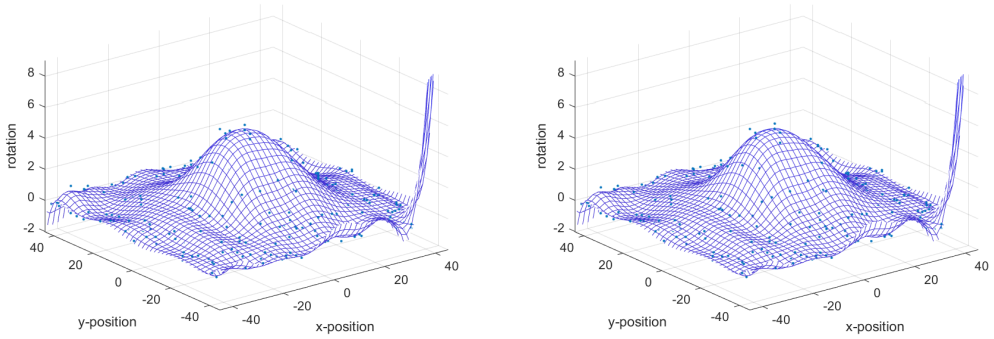

(a) Rotation Method 1

(b) Rotation Method 2

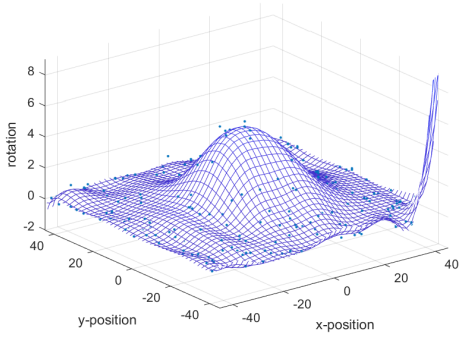

(c) Rotation Method 3

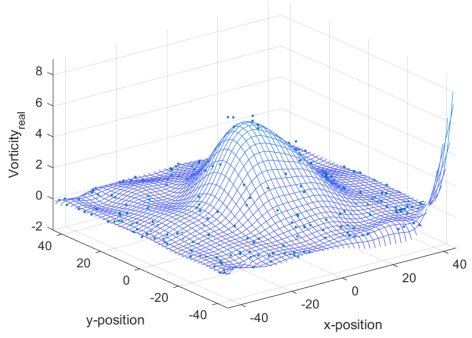

(d) Analytical Vorticity

Figure A.46: 2nd level regressive fit 400 data points, Dataset Number 7, and Noise level 0.1

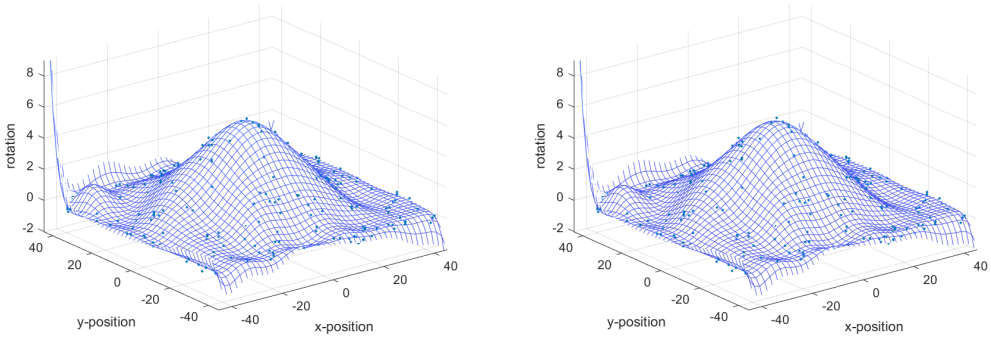

(a) Rotation Method 1

(b) Rotation Method 2

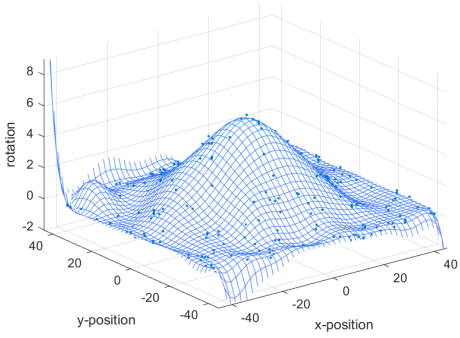

(c) Rotation Method 3

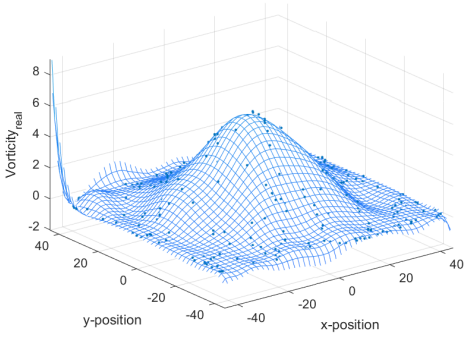

(d) Analytical Vorticity

Figure A.47: 2nd level regressive fit for 400 data points, Dataset Number 10, and Noise level 0.1

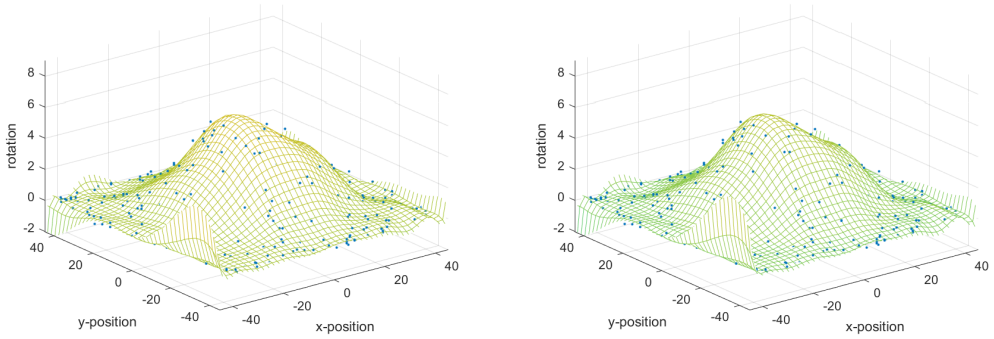

(a) Rotation Method 1

(b) Rotation Method 2

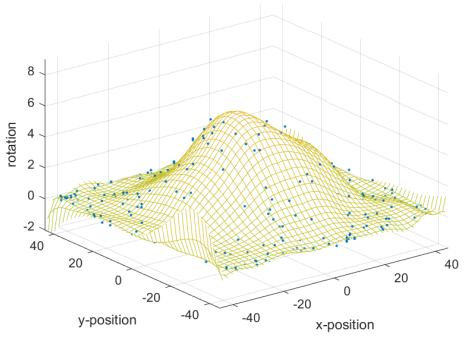

(c) Rotation Method 3

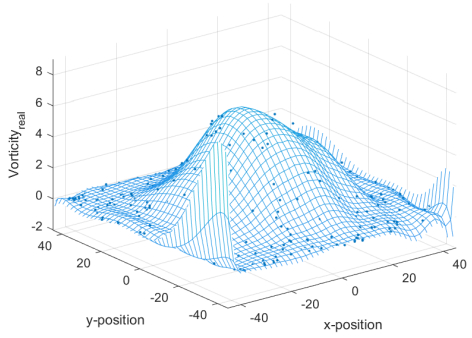

(d) Analytical Vorticity

Figure A.48: 2nd level regressive fit for 400 data points, Dataset Number 13, and Noise level 0.1

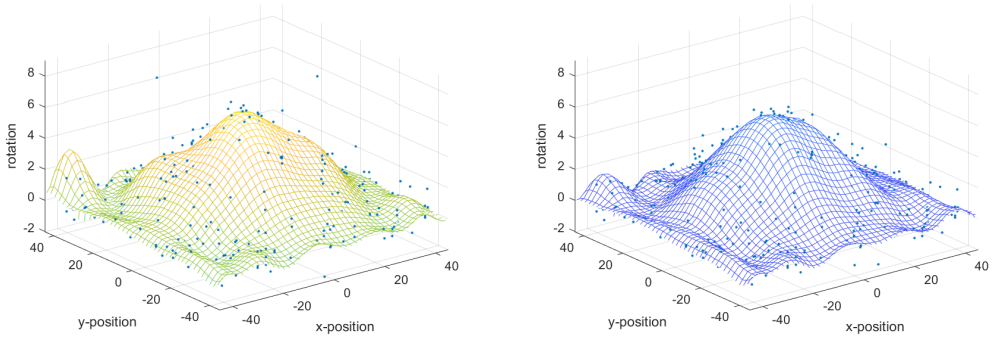

(a) Rotation Method 1

(b) Rotation Method 2

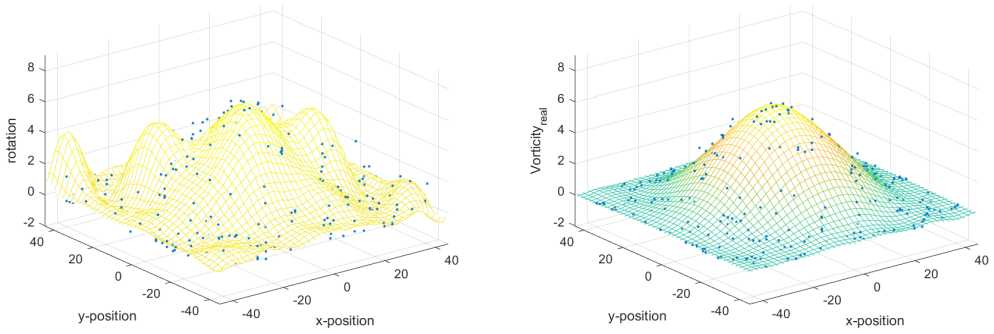

(c) Rotation Method 3

(d) Analytical Vorticity

Figure A.49: 2nd level regressive fit for 600 data points, Dataset Number 4, and Noise level 0.1

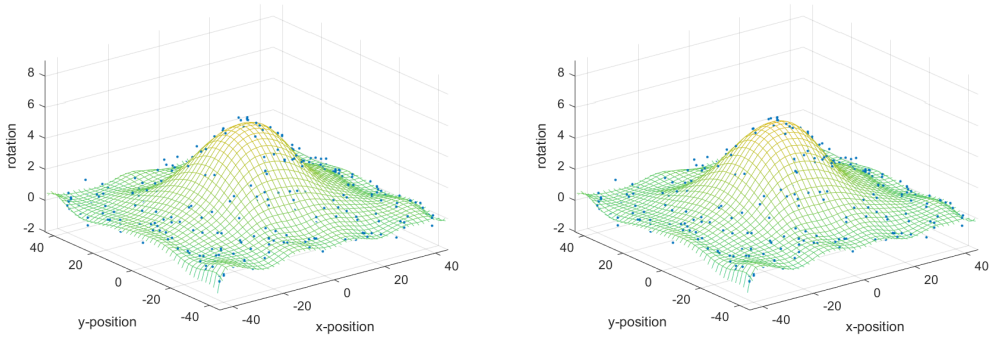

(a) Rotation Method 1

(b) Rotation Method 2

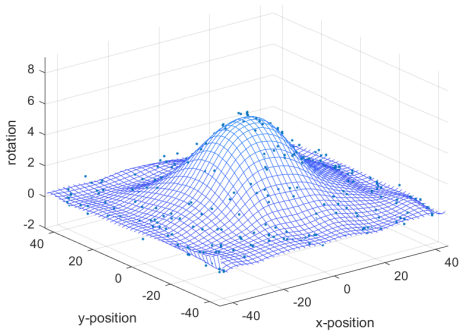

(c) Rotation Method 3

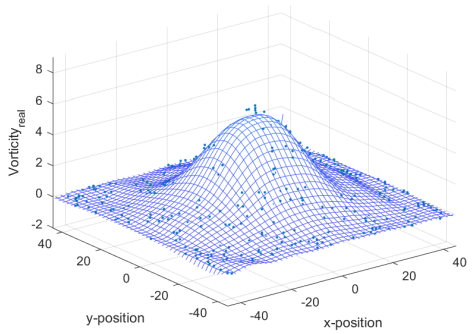

(d) Analytical Vorticity

Figure A.50: 2nd level regressive fit for 600 data points, Dataset Number 7, and Noise level 0.1

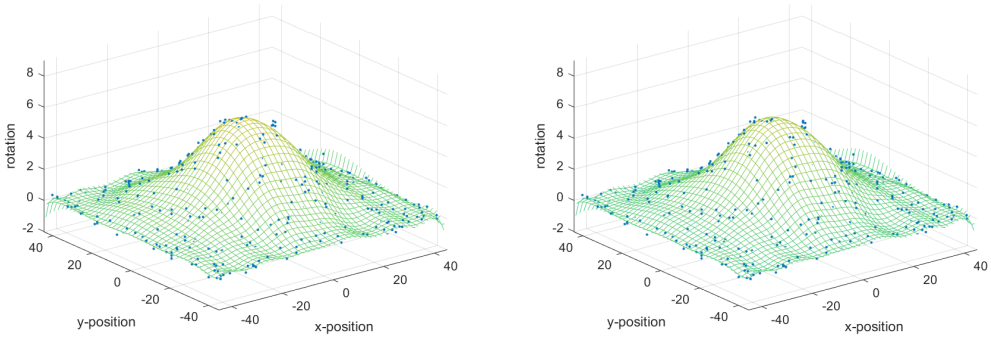

(a) Rotation Method 1

(b) Rotation Method 2

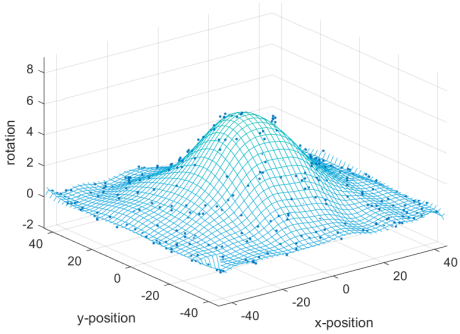

(c) Rotation Method 3

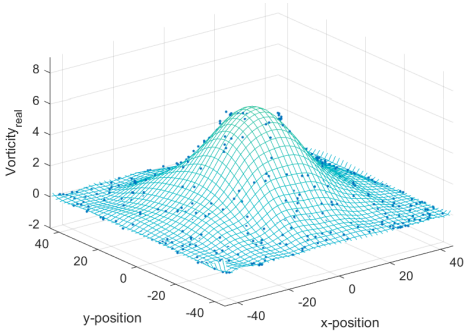

(d) Analytical Vorticity

Figure A.51: 2nd level regressive fit for 600 data points, Dataset Number 10, and Noise level 0.1

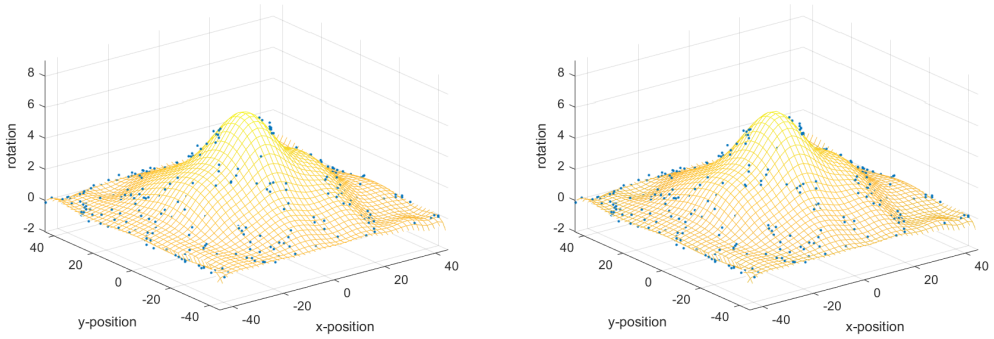

(a) Rotation Method 1

(b) Rotation Method 2

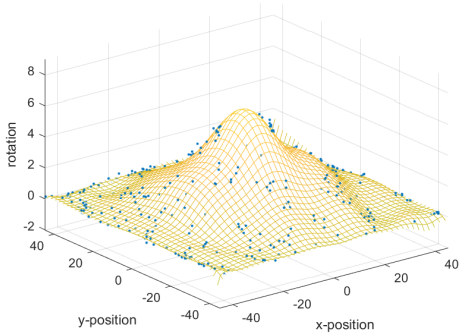

(c) Rotation Method 3

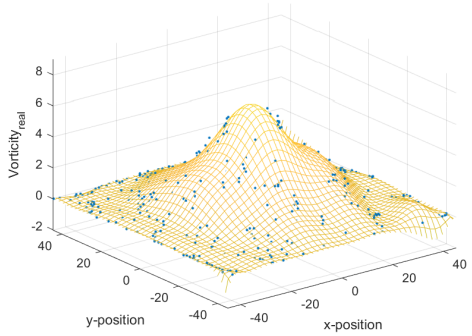

(d) Analytical Vorticity

Figure A.52: 2nd level regressive fit for 600 data points, Dataset Number 13, and Noise level 0.1

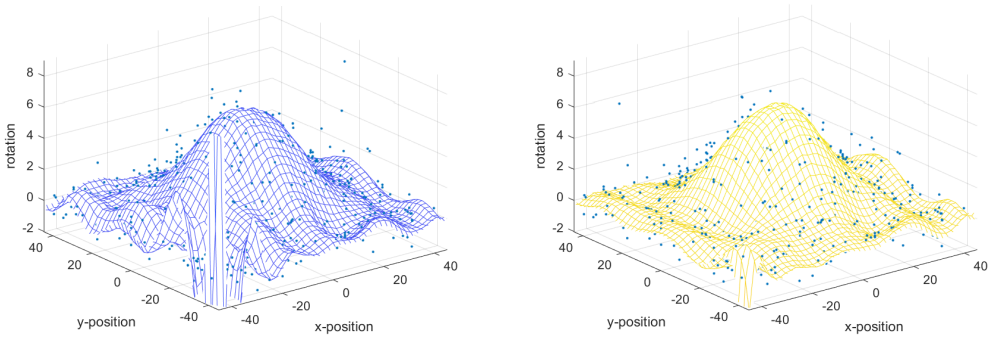

(a) Rotation Method 1

(b) Rotation Method 2

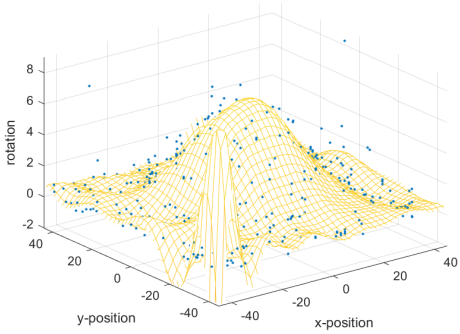

(c) Rotation Method 3

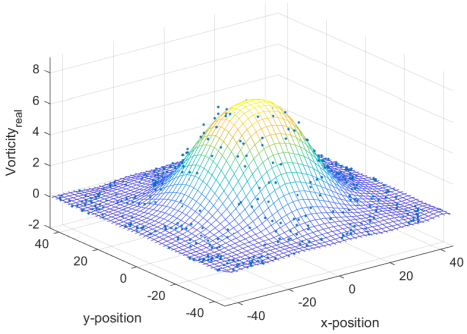

(d) Analytical Vorticity

Figure A.53: 2nd level regressive fit for 800 data points, Dataset Number 4, and Noise level 0.1

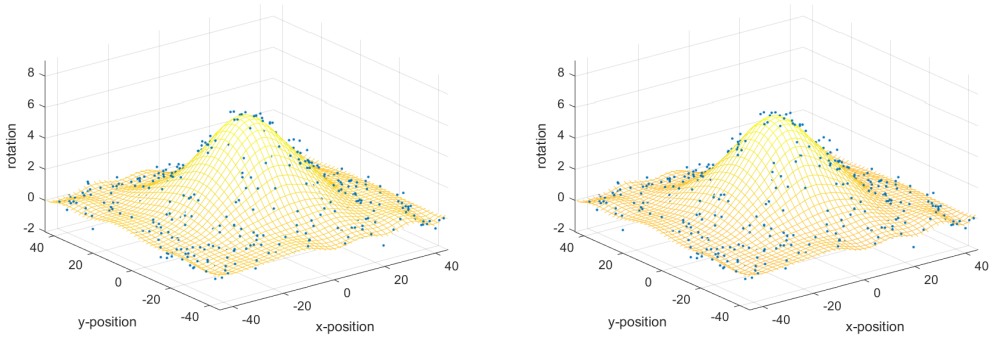

(a) Rotation Method 1

(b) Rotation Method 2

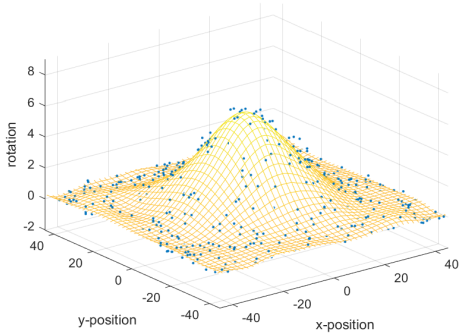

(c) Rotation Method 3

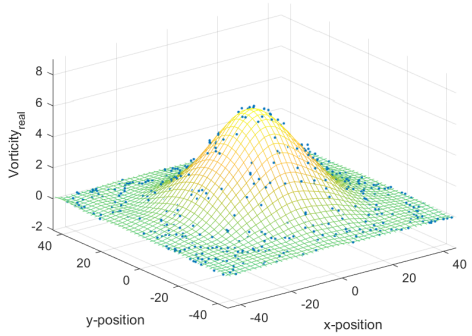

(d) Analytical Vorticity

Figure A.54: 2nd level regressive fit for 800 data points, Dataset Number 7, and Noise level 0.1

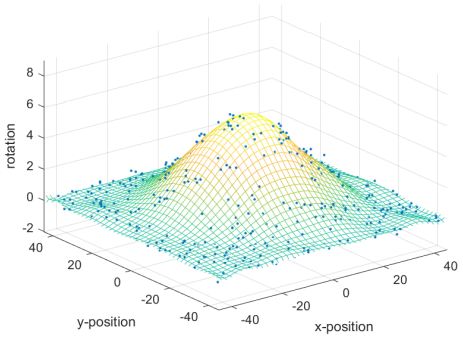

(a) Rotation Method 1

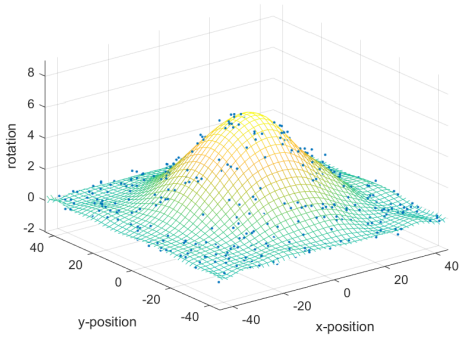

(b) Rotation Method 2

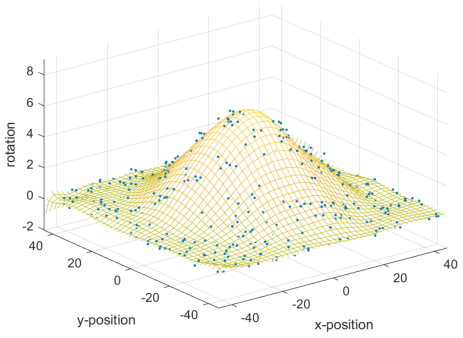

(c) Rotation Method 3

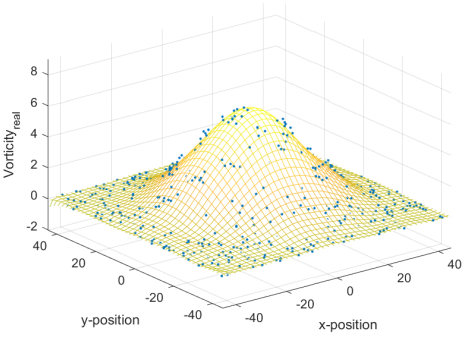

(d) Analytical Vorticity

Figure A.55: 2nd level regressive fit for 800 data points, Dataset Number 10, and Noise level 0.1

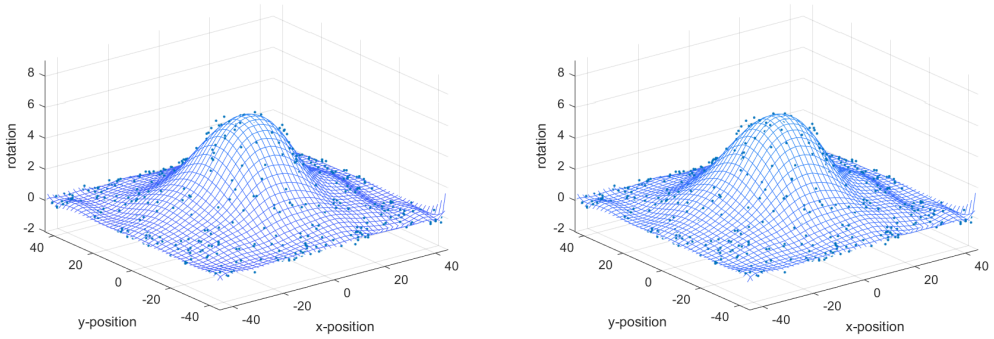

(a) Rotation Method 1

(b) Rotation Method 2

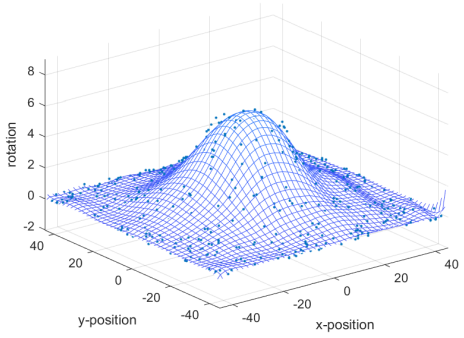

(c) Rotation Method 3

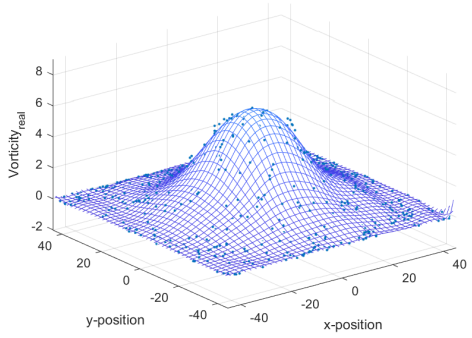

(d) Analytical Vorticity

Figure A.56: 2nd level regressive fit for 800 data points, Dataset Number 13, and Noise level 0.1

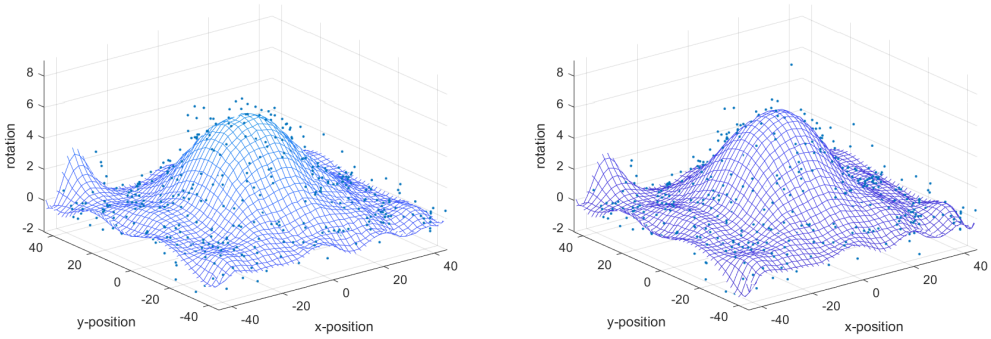

(a) Rotation Method 1

(b) Rotation Method 2

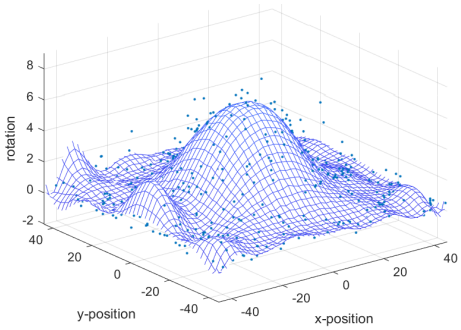

(c) Rotation Method 3

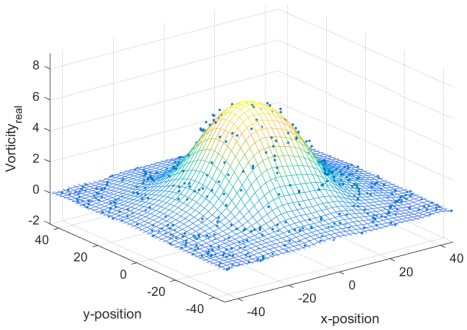

(d) Analytical Vorticity

Figure A.57: 2nd level regressive fit for 1000 data points, Dataset Number 4, and Noise level 0.1

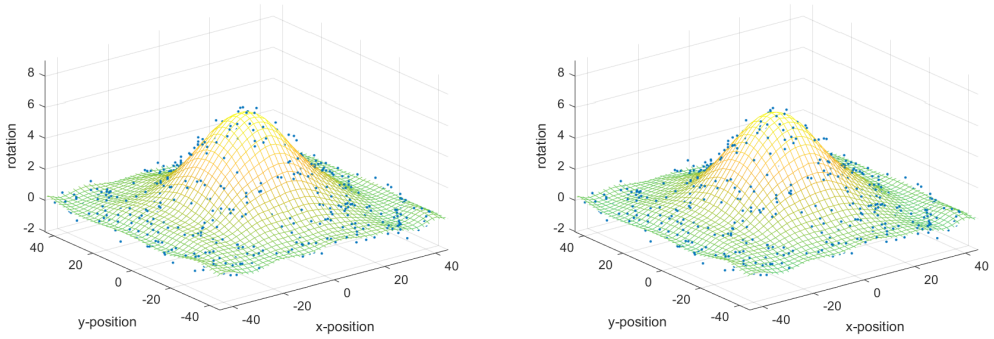

(a) Rotation Method 1

(b) Rotation Method 2

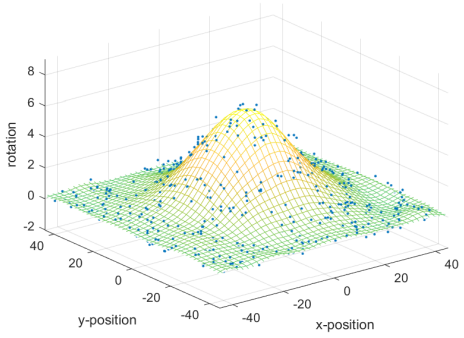

(c) Rotation Method 3

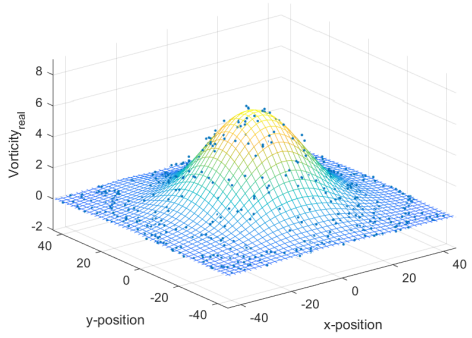

(d) Analytical Vorticity

Figure A.58: 2nd level regressive fit for 1000 data points, Dataset Number 7, and Noise level 0.1

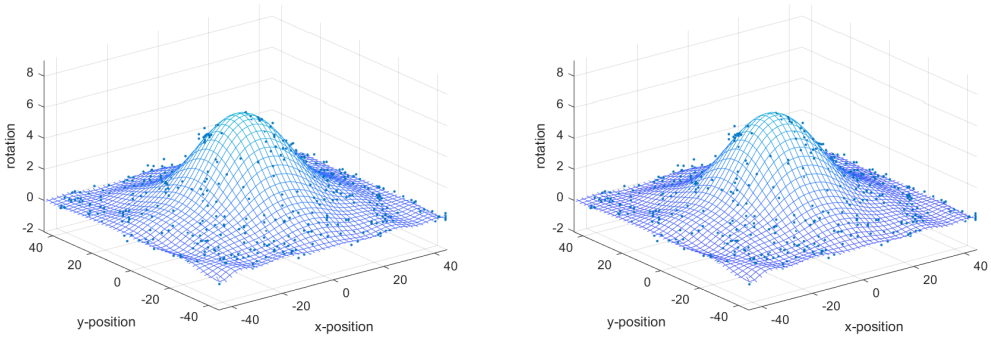

(a) Rotation Method 1

(b) Rotation Method 2

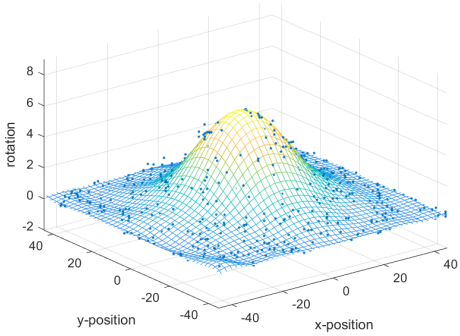

(c) Rotation Method 3

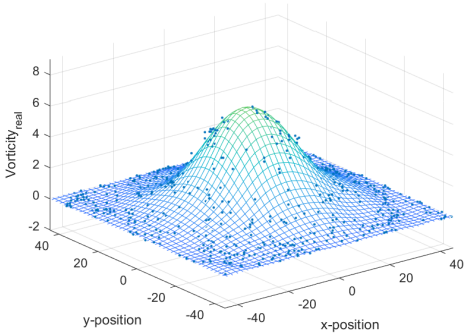

(d) Analytical Vorticity

Figure A.59: 2nd level regressive fit for 1000 data points, Dataset Number 10, and Noise level 0.1

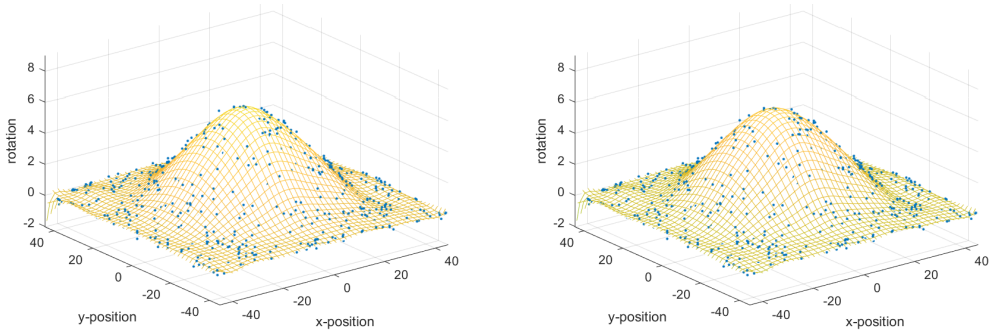

(a) Rotation Method 1

(b) Rotation Method 2

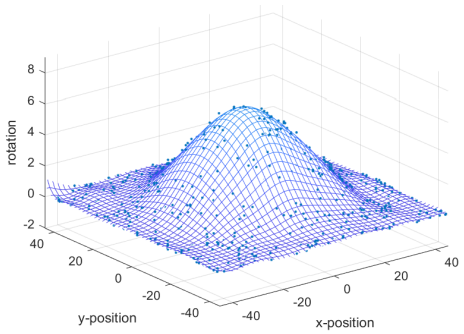

(c) Rotation Method 3

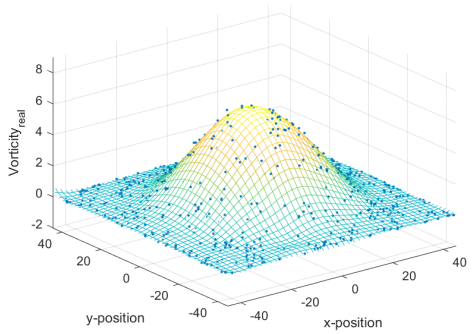

(d) Analytical Vorticity

Figure A.60: 2nd level regressive fit for 1000 data points, Dataset Number 13, and Noise level 0.1

A.2 Spline Fit Using tpaps for Datasets

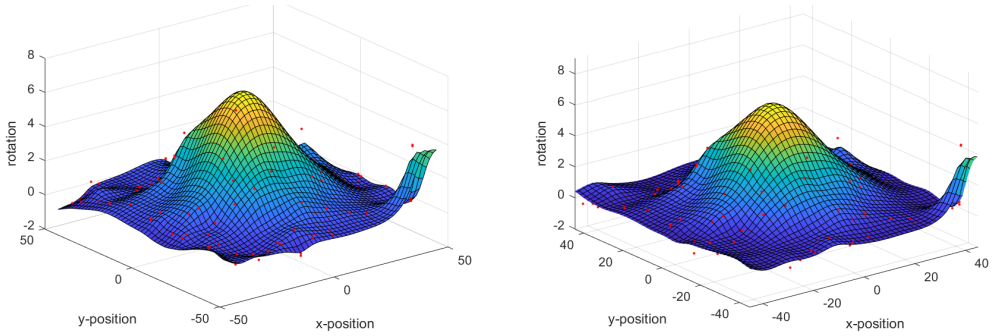

(a) Rotation Method 1

(b) Rotation Method 2

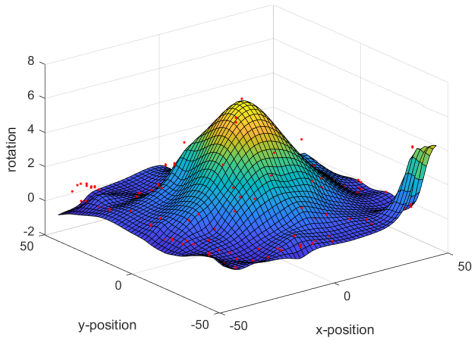

(c) Rotation Method 3

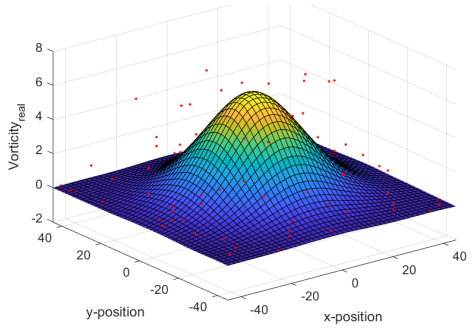

(d) Analytical Vorticity

Figure A.61: Spline fit for 200 data points, Dataset Number 4, and Noise level 0.1

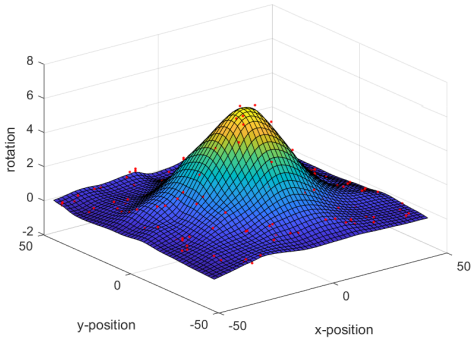

(a) Rotation Method 1

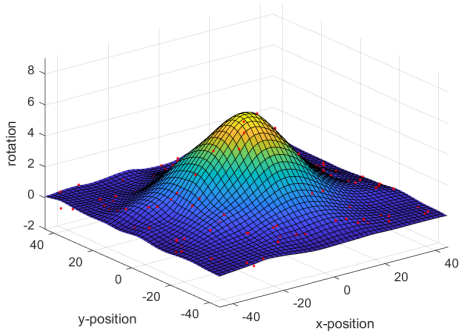

(b) Rotation Method 2

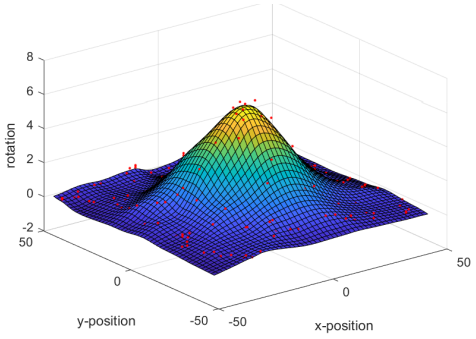

(c) Rotation Method 3

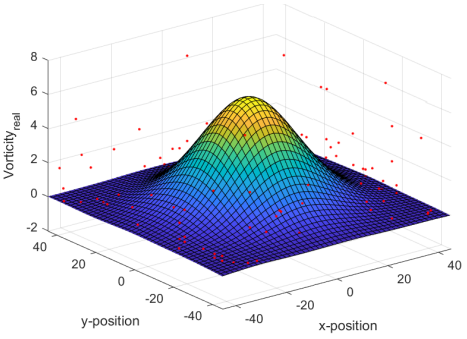

(d) Analytical Vorticity

Figure A.62: Spline fit for 200 data points, Dataset Number 7, and Noise level 0.1

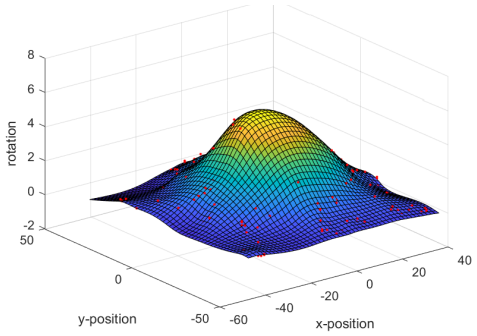

(a) Rotation Method 1

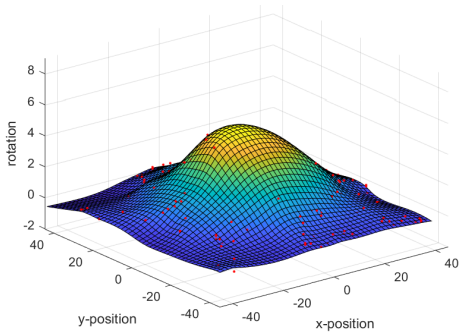

(b) Rotation Method 2

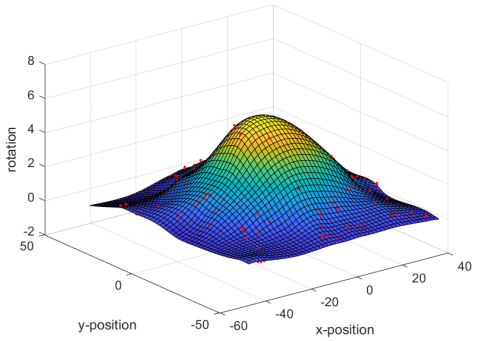

(c) Rotation Method 3

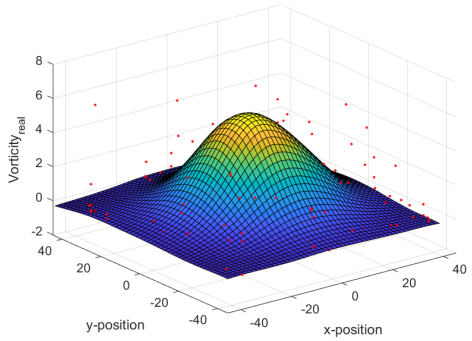

(d) Analytical Vorticity

Figure A.63: Spline fit for 200 data points, Dataset Number 10, and Noise level 0.1

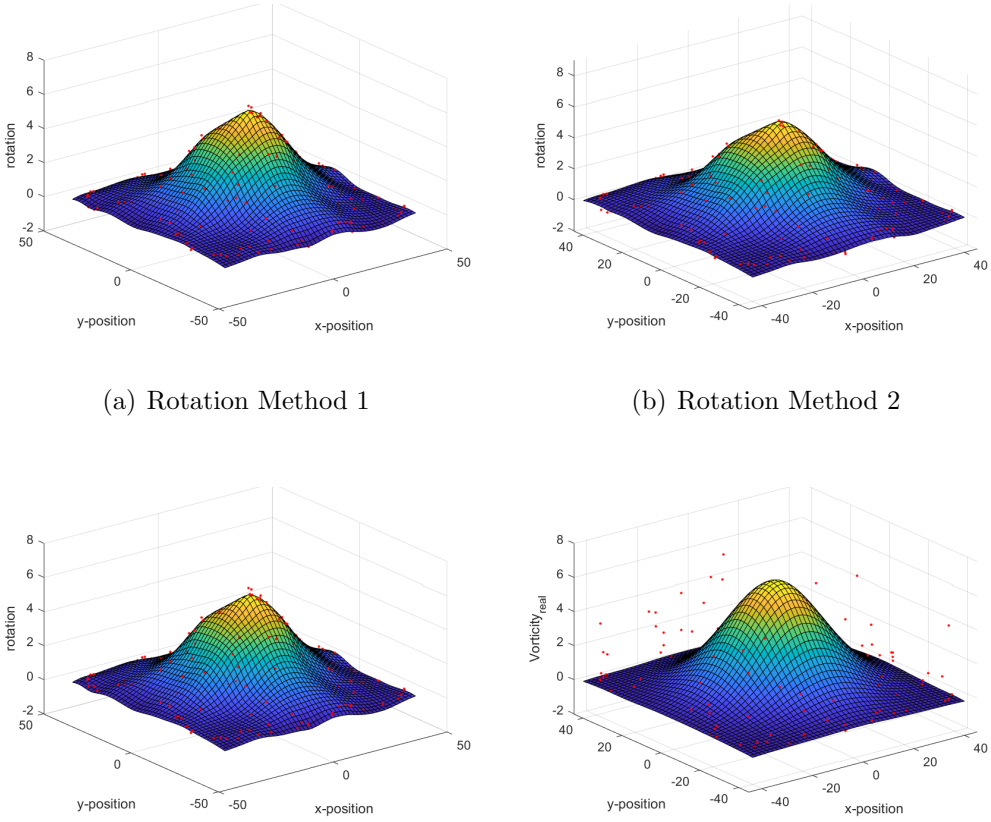

(a) Rotation Method 1

(b) Rotation Method 2

(c) Rotation Method 3

(d) Analytical Vorticity

Figure A.64: Spline fit for 200 data points, Dataset Number 13, and Noise level 0.1

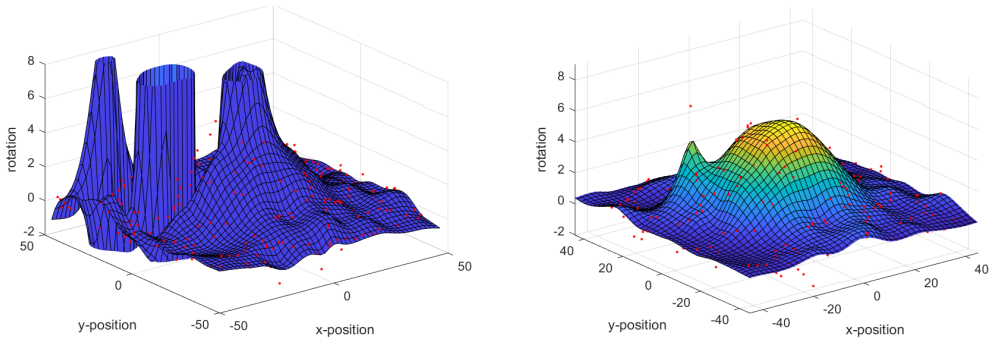

(a) Rotation Method 1

(b) Rotation Method 2

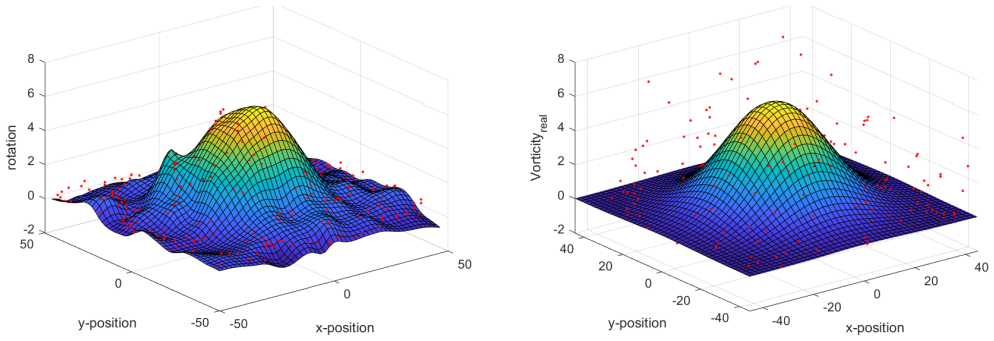

(c) Rotation Method 3

(d) Analytical Vorticity

Figure A.65: Spline fit for 400 data points, Dataset Number 4, and Noise level 0.1

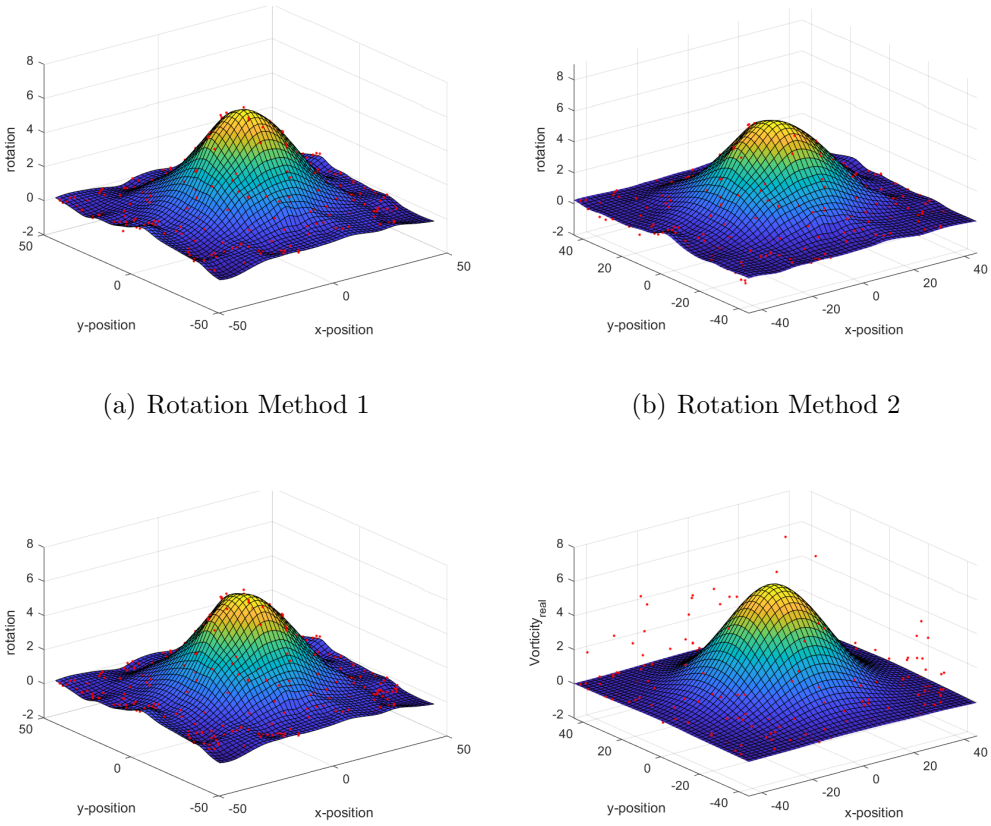

(a) Rotation Method 1

(b) Rotation Method 2

(c) Rotation Method 3

(d) Analytical Vorticity

Figure A.66: Spline fit for 400 data points, Dataset Number 7, and Noise level 0.1

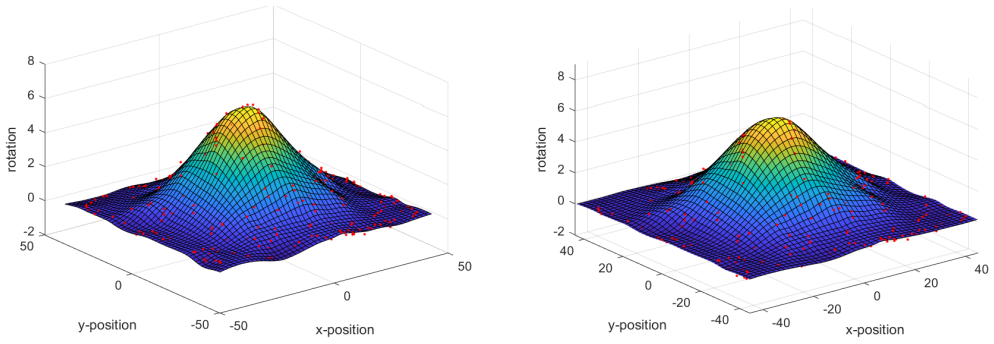

(a) Rotation Method 1

(b) Rotation Method 2

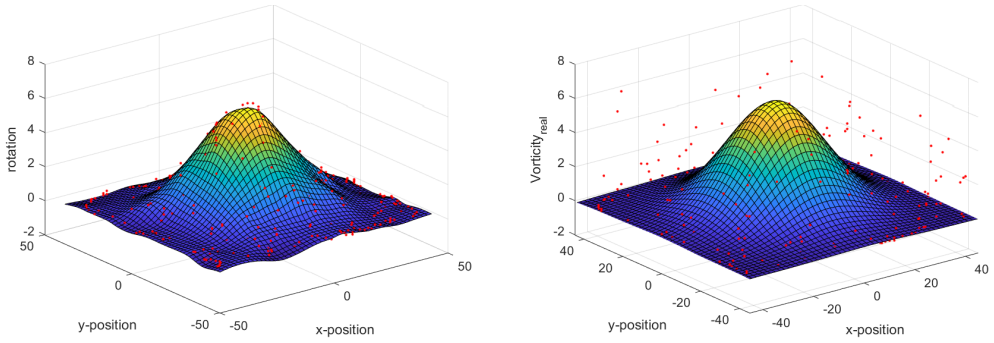

(c) Rotation Method 3

(d) Analytical Vorticity

Figure A.67: Spline fit for 400 data points, Dataset Number 10, and Noise level 0.1

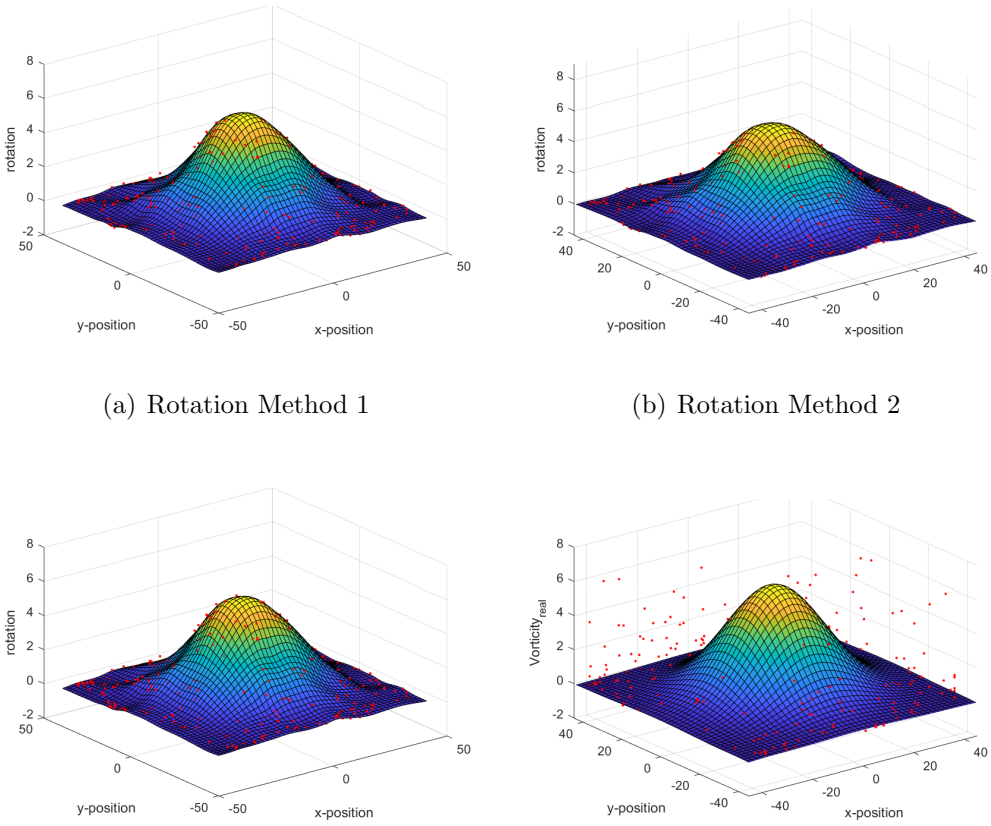

(a) Rotation Method 1

(b) Rotation Method 2

(c) Rotation Method 3

(d) Analytical Vorticity

Figure A.68: Spline fit for 400 data points, Dataset Number 13, and Noise level 0.1

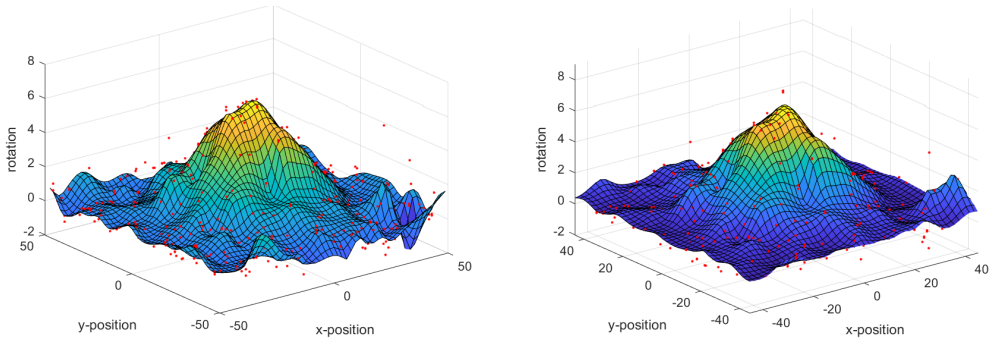

(a) Rotation Method 1

(b) Rotation Method 2

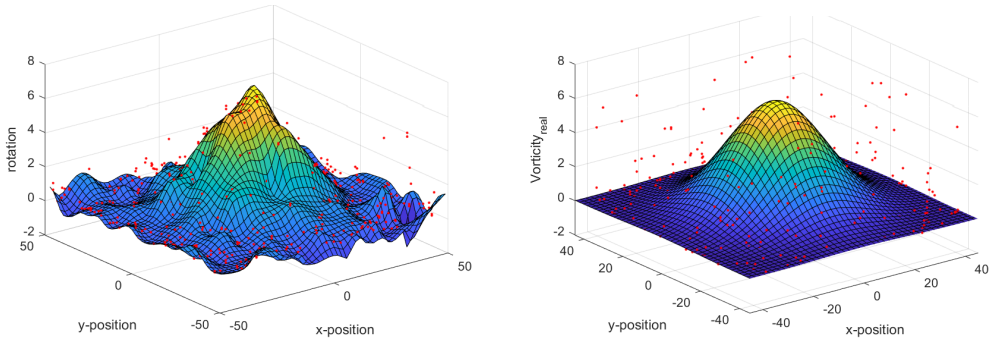

(c) Rotation Method 3

(d) Analytical Vorticity

Figure A.69: Spline fit for 600 data points, Dataset Number 4, and Noise level 0.1

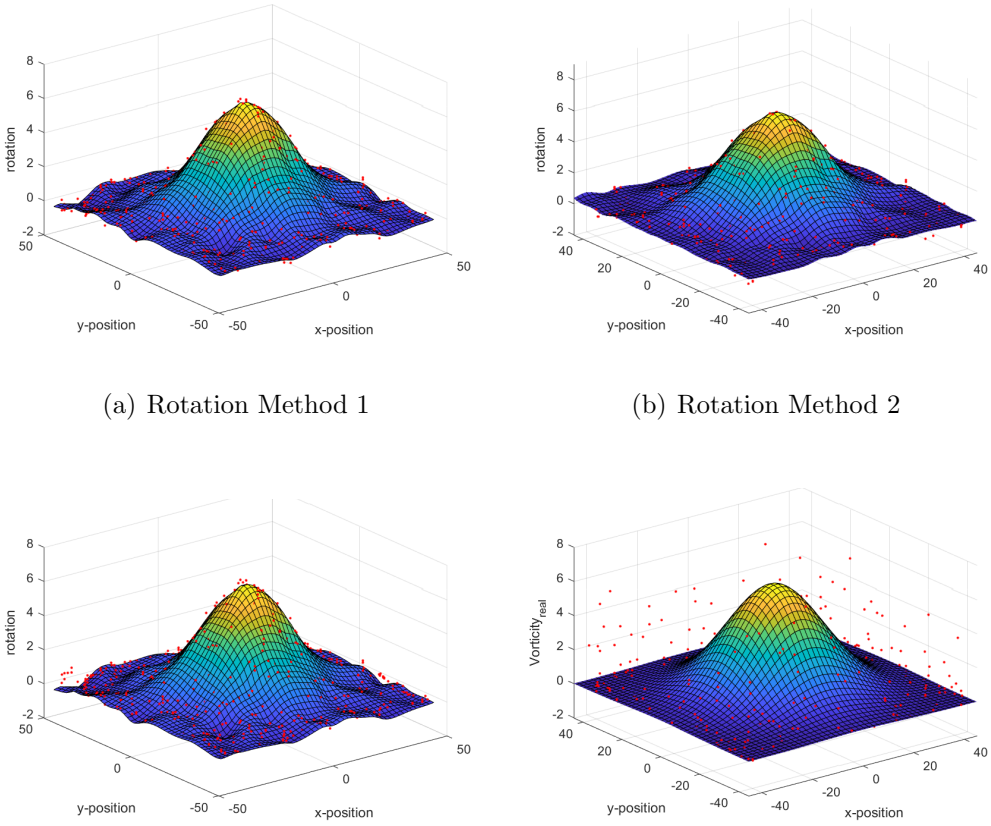

(a) Rotation Method 1

(b) Rotation Method 2

(c) Rotation Method 3

(d) Analytical Vorticity

Figure A.70: Spline fit for 600 data points, Dataset Number 7, and Noise level 0.1

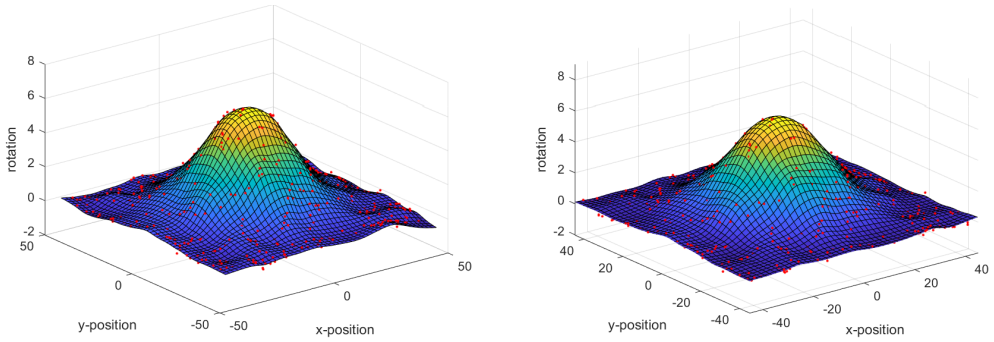

(a) Rotation Method 1

(b) Rotation Method 2

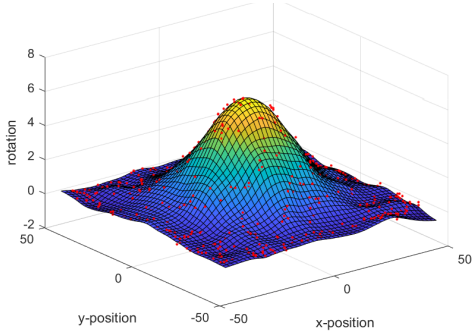

(c) Rotation Method 3

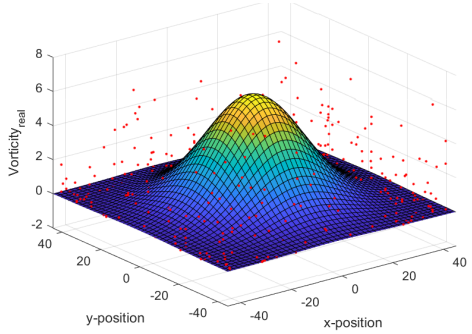

(d) Analytical Vorticity

Figure A.71: Spline fit for 600 data points, Dataset Number 10, and Noise level 0.1

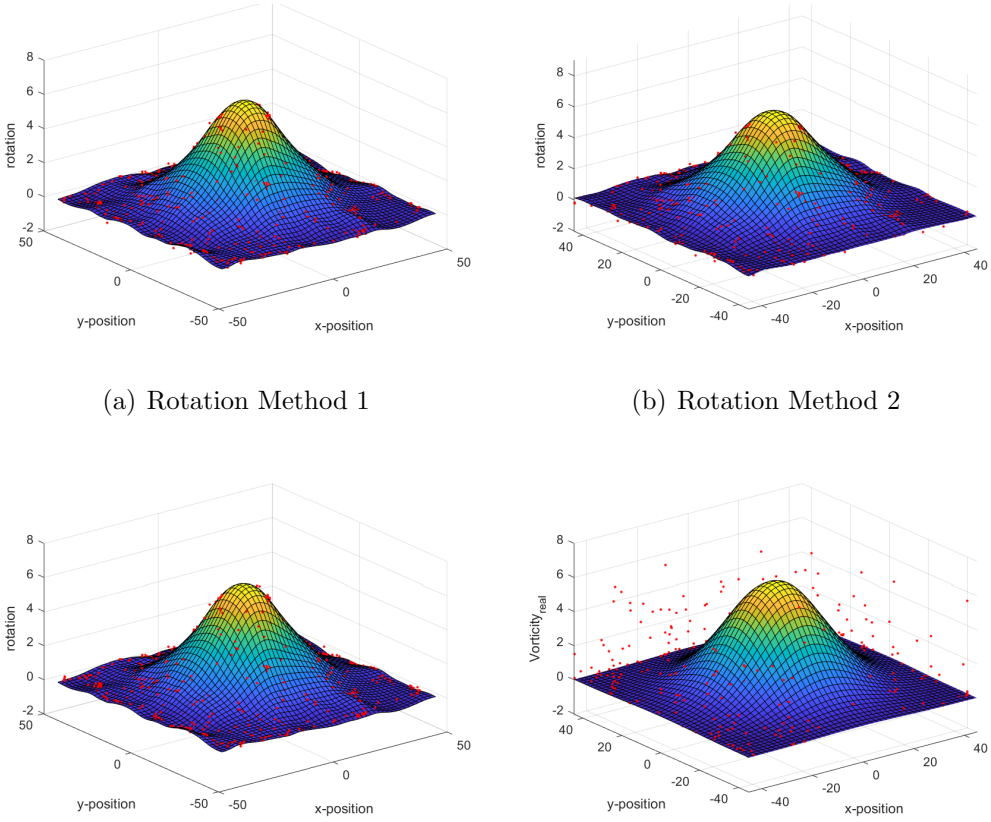

(a) Rotation Method 1

(b) Rotation Method 2

(c) Rotation Method 3

(d) Analytical Vorticity

Figure A.72: Spline fit for 600 data points, Dataset Number 13, and Noise level 0.1

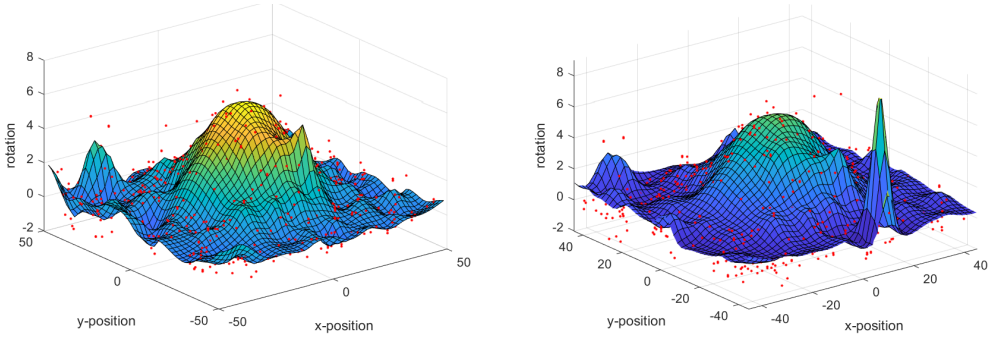

(a) Rotation Method 1

(b) Rotation Method 2

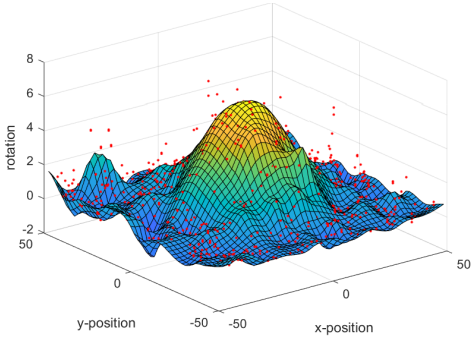

(c) Rotation Method 3

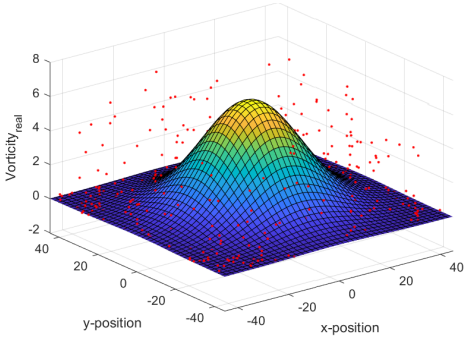

(d) Analytical Vorticity

Figure A.73: Spline fit for 800 data points, Dataset Number 4, and Noise level 0.1

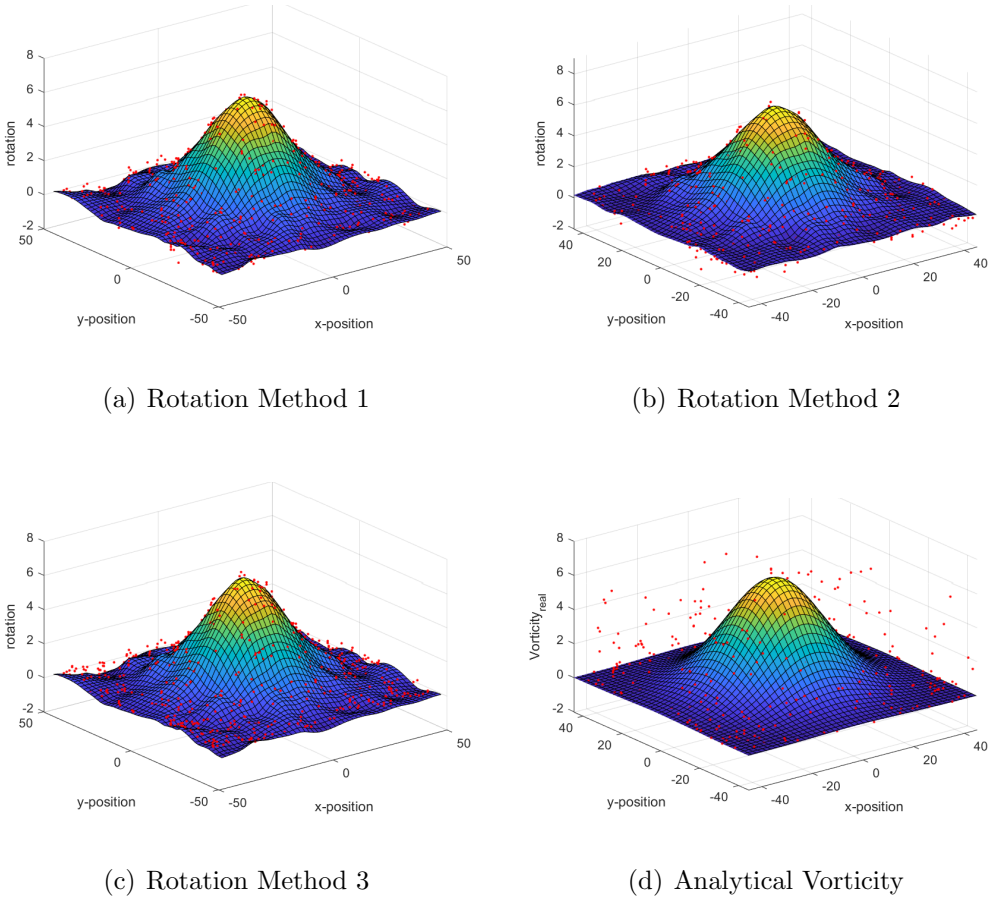

(a) Rotation Method 1

(b) Rotation Method 2

(c) Rotation Method 3

(d) Analytical Vorticity

Figure A.74: Spline fit for 800 data points, Dataset Number 7, and Noise level 0.1

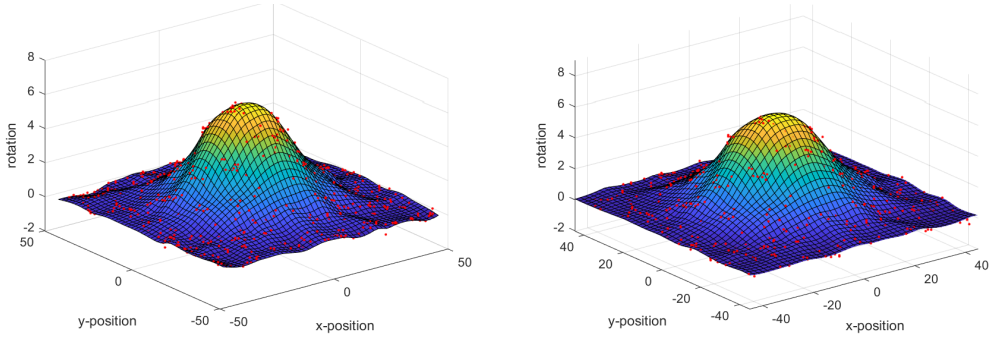

(a) Rotation Method 1

(b) Rotation Method 2

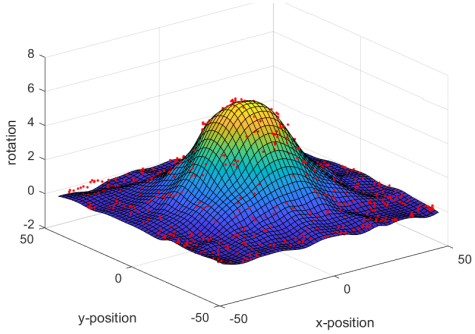

(c) Rotation Method 3

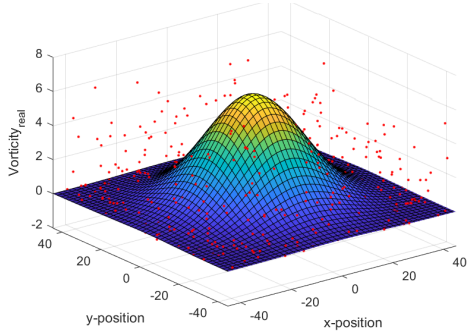

(d) Analytical Vorticity

Figure A.75: Spline fit for 800 data points, Dataset Number 10, and Noise level 0.1

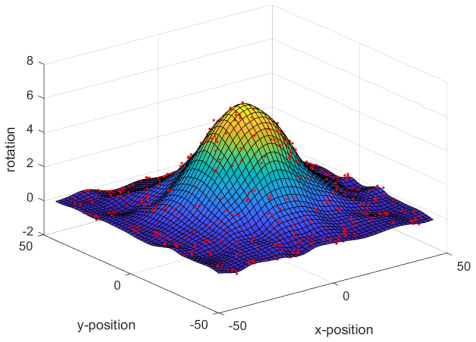

(a) Rotation Method 1

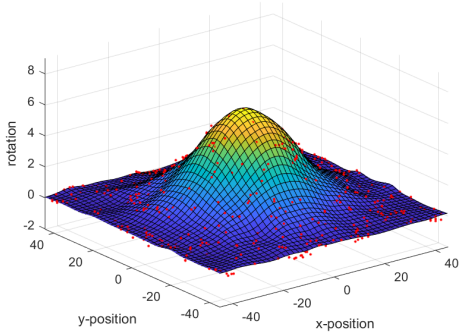

(b) Rotation Method 2

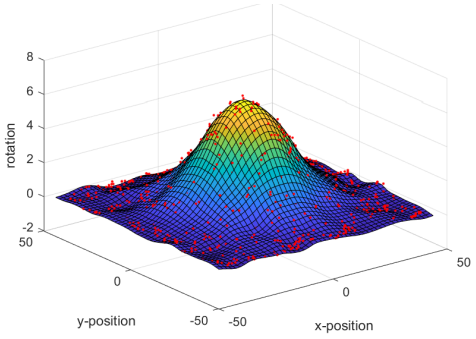

(c) Rotation Method 3

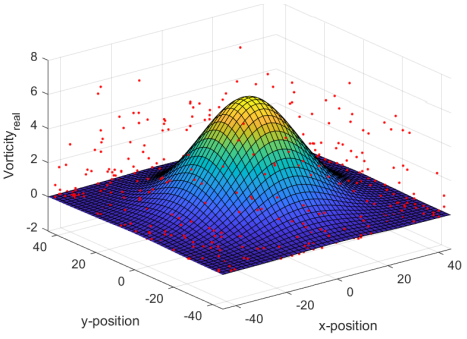

(d) Analytical Vorticity

Figure A.76: Spline fit for 800 data points, Dataset Number 13, and Noise level 0.1

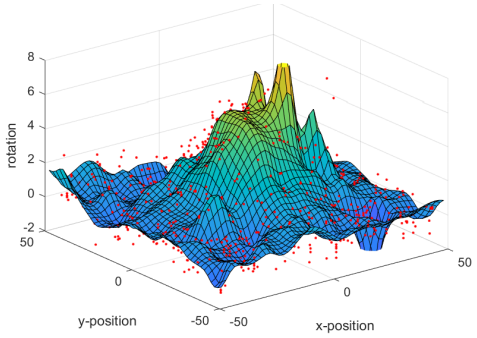

(a) Rotation Method 1

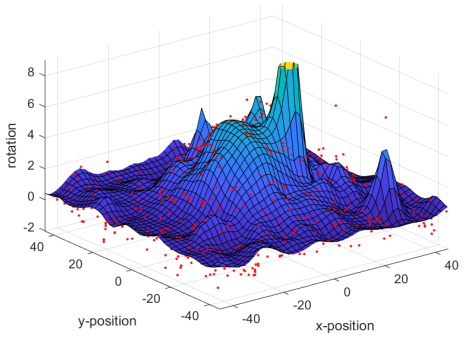

(b) Rotation Method 2

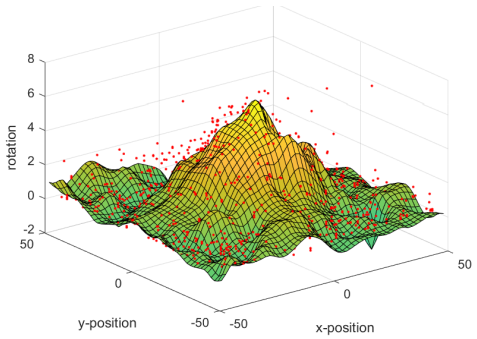

(c) Rotation Method 3

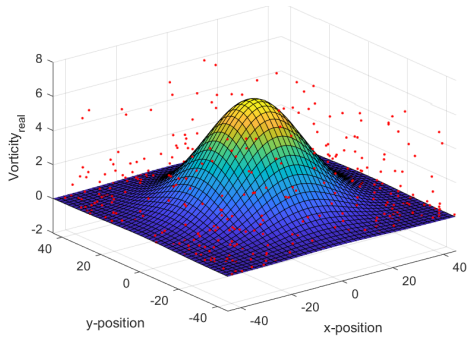

(d) Analytical Vorticity

Figure A.77: Spline fit for 1000 data points, Dataset Number 4, and Noise level 0.1

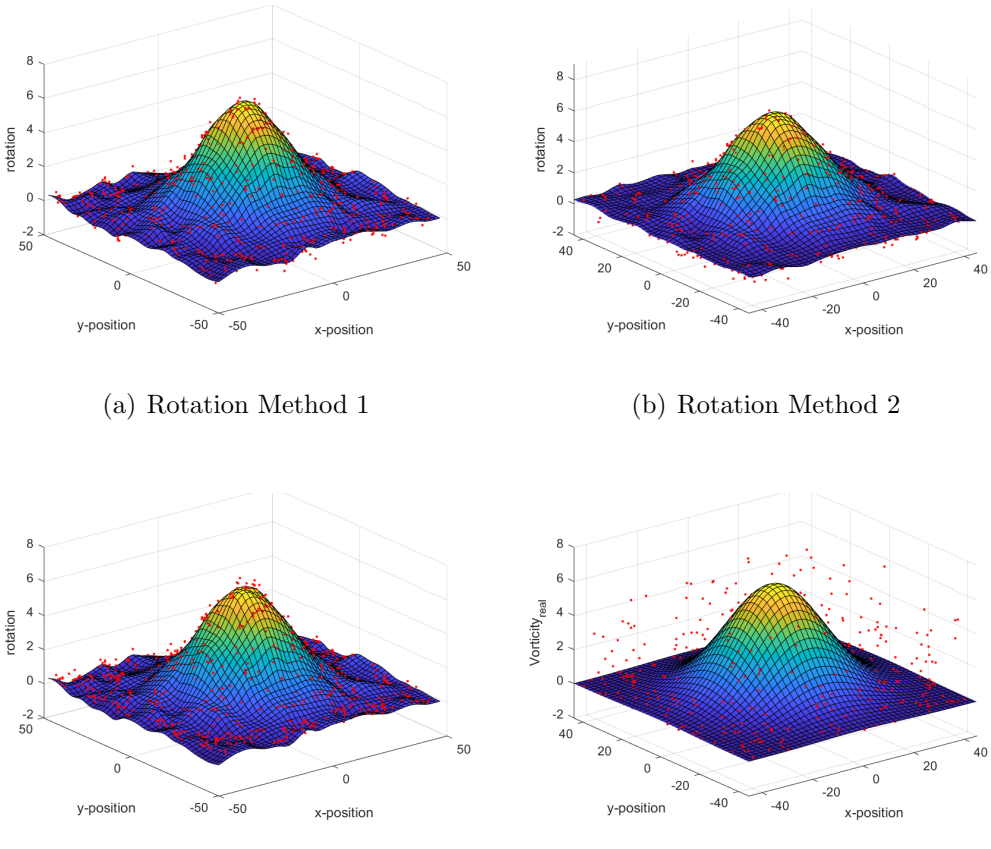

(a) Rotation Method 1

(b) Rotation Method 2

(c) Rotation Method 3

(d) Analytical Vorticity

Figure A.78: Spline fit for 1000 data points, Dataset Number 7, and Noise level 0.1

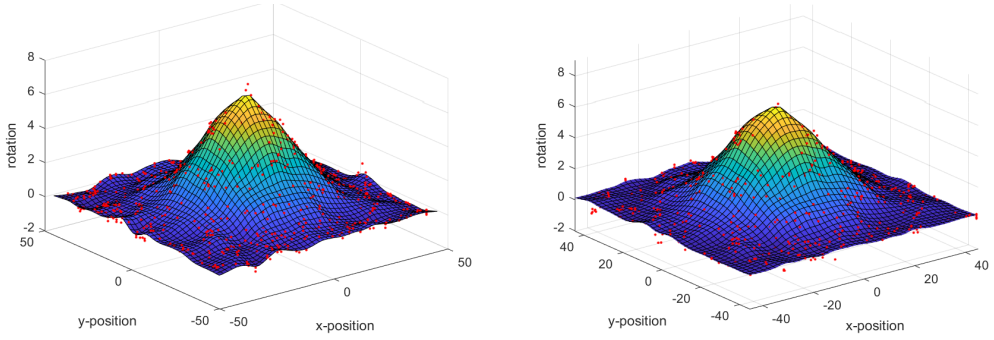

(a) Rotation Method 1

(b) Rotation Method 2

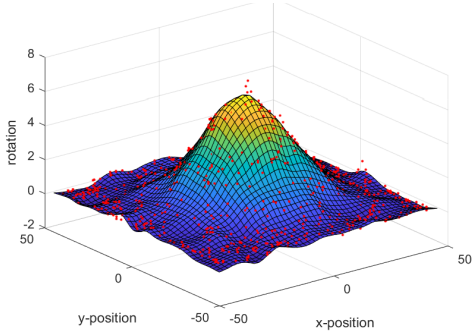

(c) Rotation Method 3

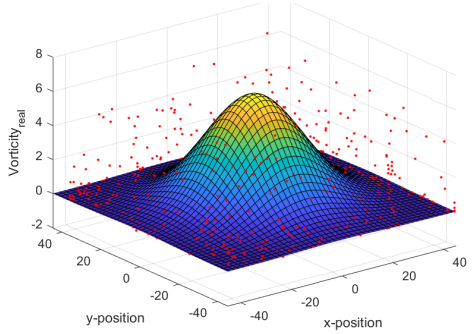

(d) Analytical Vorticity

Figure A.79: Spline fit for 1000 data points, Dataset Number 10, and Noise level 0.1

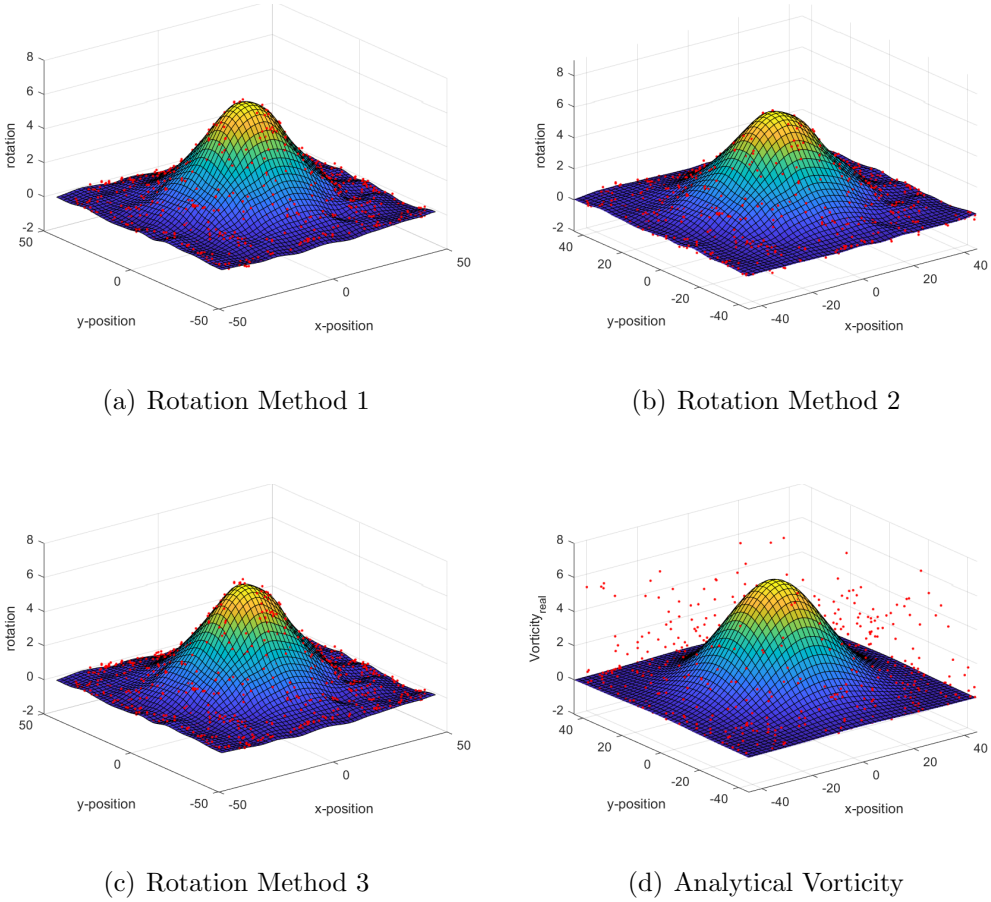

(a) Rotation Method 1

(b) Rotation Method 2

(c) Rotation Method 3

(d) Analytical Vorticity

Figure A.80: Spline fit for 1000 data points, Dataset Number 13, and Noise level 0.1